

Advanced Statistical Physics:

2. Phase Transitions

Leticia F. Cugliandolo

`leticia@lpthe.jussieu.fr`

Sorbonne Université

Laboratoire de Physique Théorique et Hautes Energies

Institut Universitaire de France

October 16, 2022

Contents

2	Phase transitions	1
2.1	The phenomenon	1
2.2	Some standard models of magnetism	3
2.3	Concepts	5
2.3.1	Symmetries	5
2.3.2	Order parameters	5
2.3.3	Thermodynamic limit	6
2.3.4	Pinning field	6
2.3.5	Broken ergodicity	7
2.3.6	Spontaneous broken symmetry	7
2.3.7	Phenomenology	8
2.3.8	Energy <i>vs.</i> entropy - the Peierls argument	9
2.4	Some celebrated methods	14
2.4.1	Low temperature expansion	14
2.4.2	High temperature expansion	14
2.4.3	Duality	15
2.4.4	The transfer matrix	15
2.4.5	One dimensional models	16
2.5	Mean field theory	17
2.5.1	Ignoring correlations	17
2.5.2	The “naive” mean-field approximation	21
2.5.3	The order parameter equation & mean-field criticality	22
2.5.4	Range of validity	27
2.5.5	The fully-connected Curie Weiss p -spin model	27
2.5.6	The Bethe-Peierls or cavity method	32
2.5.7	Universality	36
2.6	Ginzburg-Landau field theory	37
2.6.1	The Landau scheme	37
2.6.2	Correlation	42
2.6.3	Ginzburg criterium	45
2.6.4	First order phase transitions	47
2.6.5	Two applications	47
2.6.6	Summary	47
2.7	Critical phenomena	50
2.7.1	Some general definitions	50
2.7.2	Critical exponents & universality	52
2.7.3	The correlation length	54
2.7.4	Droplet theory	57
2.8	Scaling and the renormalisation group	58
2.8.1	Homogeneity & scaling	58

2.8.2	Relation between exponents	61
2.8.3	Scale invariance	62
2.8.4	Finite size scaling	63
2.8.5	The renormalisation group	69
2.8.6	Decimation in the one dimensional Ising chain	70
2.8.7	Kadanoff's block spins, renormalisation & re-scaling	76
2.9	Geometric description of 2nd order phase transitions	85
2.9.1	Geometric and FK clusters	85
2.9.2	Percolation	87
2.9.3	Mapping to the Potts model	95
2.10	Models with continuous symmetry	97
2.10.1	Spin waves	98
2.10.2	High temperature expansions	102
2.10.3	Vortices and the Kosterlitz-Thouless transition	103
2.10.4	The Villain model	110
2.10.5	Numerical evaluation	111
2.10.6	Applications	111
2.10.7	The Mermin-Wagner theorem	112
2.10.8	About universality	112
2.10.9	On interface energies	113
2.10.10	O(n) model: Goldstone modes	113
2.10.11	The Higgs mechanism	115
2.11	Melting in two dimensions	116
2.11.1	Positional vs. orientational order	116
2.11.2	Melting scenarii	119
2.12	First order phase transitions	121
2.12.1	Stability of ordered phases	122
2.12.2	The Potts model	125
2.12.3	Finite size effects	125
2.13	Summary	125
2.13.1	First order phase transitions	125
2.13.2	Second order phase transitions	126
2.13.3	Infinite order phase transitions	126
2.A	Appendices	127
2.A.1	Polar coordinate system	127
2.A.2	Fourier transform	127
2.A.3	The angle correlation	128
2.B	Problems	130
2.B.1	The classical Potts model	130
2.B.2	A classical Ising chain with alternating couplings	131

2 Phase transitions

This Chapter is dedicated to the study of classical equilibrium phase transitions.

2.1 The phenomenon

Consider the most common experimental situation in which a piece of material is in contact with an *external reservoir*. The material will be characterised by certain *global observables*, like its energy, magnetisation, *etc.*, which, for convenience, are usually normalised by the quantity of matter. Densities of energy, magnetisation, *etc.* are then defined dividing the macroscopic values by the number of particles (or the volume) of the system. The external environment is characterised by some parameters, like the temperature, magnetic field, pressure, *etc.* In principle, one is able to tune the latter and measure dependence of the former on them.

Sharp changes in the behaviour of *macroscopic systems* at critical points (curves) in parameter space have been observed experimentally. These correspond to *phase transitions* [1, 2, 3, 4, 5, 6, 7, 8, 9, 10, 11], a non-trivial *collective phenomenon* arising in the thermodynamic, $N \rightarrow \infty$ and $V \rightarrow \infty$, limit [12].

Phase diagrams as the one in Fig. 2.1 help to visually identify the global behaviour of a system according to the values that the *order parameters* (relevant observables) take in different regions of variation of the *control parameters* that give the axes to the phase diagram.

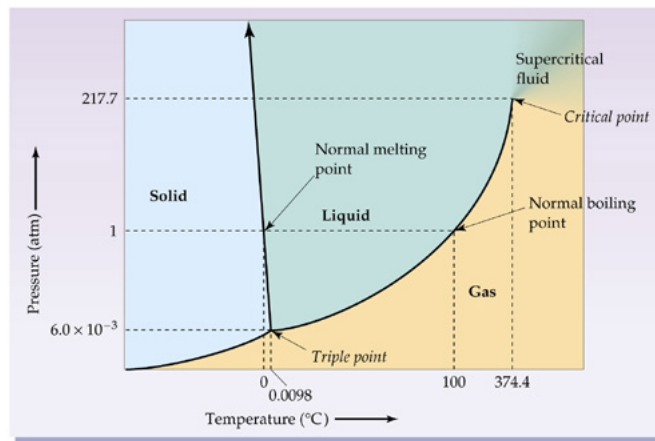


Figure 2.1: A quite generic phase diagram.

The phase diagram in Fig. 2.1 is bidimensional: the temperature-pressure plane and

both of these parameters can be externally controlled. In recent years, it has become popular, especially in cold atom experiments in atomic physics, to work in isolation. In these cases, one can monitor the conserved energy, and from it derive a temperature from the entropy-energy relation following the *microcanonical* prescription. Likewise, one can study the statistical properties of the systems for different values of the relevant *coupling constants* in the Hamiltonian, which can be tuned with smart experimental techniques.

Macroscopic models of agents in interaction may have *static* and *dynamic phase transitions*. The former are the usual ones studied with statistical physics methods. For example, in the canonical ensemble, one finds the phase transitions by looking for *non-analyticities* of the *free-energy density* (or another relevant thermodynamic potential) as a function of the control parameters, say just $\beta = 1/(k_B T)$,

$$-\beta f(\beta) = N^{-1} \ln \mathcal{Z}(\beta) \quad \text{with} \quad \mathcal{Z}(\beta) = \sum_{\mathcal{C}} e^{-\beta \mathcal{H}(\mathcal{C})} \quad (2.1)$$

where \mathcal{Z} is the partition function, \mathcal{C} represents all the system configurations, and $\mathcal{H}(\mathcal{C})$ is the Hamiltonian. In particular, one is interested in identifying the *order parameters* (in some cases this is easy, in others it is not) that characterise the various *equilibrium phases*, finding the *critical curves* of the control parameters in the phase diagram, and studying the *critical phenomenon* that is to say the behaviour of the order parameter and other properties close to the phase transition.

Mean-field theories have been notably successful in capturing much of the global behaviour of macroscopic systems. Nevertheless, they cannot reproduce details such as the functional form of the order parameters or the peculiarities of the critical phenomena. Still, they are notably useful to understand what is going on and get a feeling of the quantitative behaviour of real systems. Beyond mean-field theory, the *scaling theory* has been very successful in describing the phenomenology of phase transitions. It was later justified with the development of the *renormalisation group* ideas which gave a concrete means to calculate, for instance, critical exponents.

However, not all phase transitions conform to the picture described in the previous paragraph. Some transitions are not characterised by order parameters: it is the case of *topological phase transitions*. Other transitions are not accompanied by critical phenomena but show, instead, *discontinuities* of the order parameters and other peculiar features such as *metastability* and *hysteresis*.

In Fig. 2.1 we show a phase diagram of a particle system with the usual gas, liquid and solid phases. For the sake of simplicity, it is better to discuss phase transitions in the context of *magnetic systems*. This is what we shall do in the rest of this Chapter. The second part of the Lectures will deal with quantum statistical physics and we will then discuss *quantum phase transitions*.

Finally, we note that *dynamic phase transitions* are sharp changes in the dynamic evolution of a macroscopic system. We will not discuss them in these notes.

2.2 Some standard models of magnetism

Let us analyse a magnetic system. The Hamiltonian describing all microscopic details is a rather complicated one. It depends on the electrons' magnetic moments giving rise to the macroscopic magnetisation of the sample but also on the vibrations of the atomic crystal, the presence of structural defects, *etc.* If we call α a *microstate*, in the canonical ensemble its probability is $P_\alpha = e^{-\beta H_\alpha} / \mathcal{Z}$ with \mathcal{Z} the partition function, $\mathcal{Z} = \sum_\alpha e^{-\beta H_\alpha}$. It is, however, impossible and not necessarily interesting, to keep all details and work with all possible physical phenomena simultaneously. Imagine that we are only interested on the magnetic properties, characterised by the electronic magnetic moments.

The *Ising model* is a simplified mathematical representation of a magnetic system. It describes the magnetic moments as *classical spins*, s_i , taking values ± 1 , lying on the vertices of a cubic lattice in d dimensional space, and interacting via nearest-neighbour couplings, $J > 0$. The energy is then

$$\mathcal{H}(\{s_i\}) = -\frac{J}{2} \sum_{\langle ij \rangle} s_i s_j - \sum_i h_i s_i \quad (2.2)$$

where h_i is a local external magnetic field. Most typically one works with a uniform field, $h_i = h$ for all sites. The justification for working with an Ising variable taking only two values is that in many cases the magnetic moment is forced to point along an *easy axis* selected by crystalline fields. We then need a model that focuses just on these.

There are two external parameters in H , the coupling strength J and the external field h . $J > 0$ favours the alignment of the spin in the same direction (*ferromagnetism*) while $J < 0$ favours the anti-alignment of the spins (*antiferromagnetism*). The magnetic field tends to align the spins in its direction.

In *finite dimensional* cases, the spins lie on a d dimensional *lattice* that can have different geometries. For instance, a cubic lattice is such that each vertex has *coordination number*, or number of neighbours, $z = 2d$. Triangular, honeycomb, *etc.* lattices are also familiar. One can also consider the sum running over connected sites on a generic *graph*. The Ising model is specially attractive for a number of reasons:

- (i) It is probably the simplest example of modelling to which a student is confronted.
- (ii) It can be solved in some cases: $d = 1$, $d = 2$, $d \rightarrow \infty$. The solutions have been the source of new and powerful techniques later applied to a variety of different problems in physics and interdisciplinary fields.
- (iii) It has not been solved analytically in the most natural case, $d = 3$!
- (iv) In $d \geq 2$, for $h = 0$ and $J > 0$, it has a phase transition at a finite value of the control parameter T/J , an interesting collective phenomenon, separating two phases that are well-understood and behave, at least qualitatively, as real magnets with paramagnetic disorder at high T/J and ferromagnetic order at low T/J .
- (v) There is an *upper*, d_u , and a *lower*, d_l , *critical dimension*. Above d_u mean-field theory correctly describes the critical phenomenon. At and below d_l there is no

finite T phase transition. Below d_u mean-field theory fails to capture the critical properties.

- (vi) One can see at work generic tools to describe the critical phenomenon like *scaling* and the *renormalisation group*.
- (vii) The phenomenon of *frustration* is illustrated by the antiferromagnetic Ising model on the triangular lattice.
- (viii) Generalisations in which the interactions and/or the fields are frozen random variables taken from a probability distribution are typical examples of problems with *quenched disorder*. One then finds the *random bond Ising model* in which $h_i = 0$ and J_{ij} are taken from a pdf with positive support, the *random field Ising model* in which $J_{ij} = J$ and the h_i are chosen from a pdf with zero mean and finite variance, and the *spin-glass* problem in which J_{ij} are drawn from a pdf with positive and negative support.
- (ix) Generalisations in which spins are not just Ising variables but *n -component vectors* with a local constraint on their modulus are also interesting. Their energy is proposed to respect rotational symmetry in the $n \geq 2$ dimensional space,

$$\mathcal{H}(\{\vec{s}_i\}) = -\frac{J}{2} \sum_{\langle ij \rangle} \vec{s}_i \cdot \vec{s}_j - \sum_i \vec{h}_i \cdot \vec{s}_i, \quad (2.3)$$

with $n = 1$ (Ising), $n = 2$ (XY), $n = 3$ (Heisenberg), ..., $n \rightarrow \infty$ ($O(n)$) as particular cases. The *local constraint* on the length of the spin is

$$s_i^2 \equiv \sum_{a=1}^n (s_i^a)^2 = n. \quad (2.4)$$

Note that each component is now a continuous variable bounded in a finite interval, $-\sqrt{n} \leq s_i^a \leq \sqrt{n}$, that actually diverges in the $n \rightarrow \infty$ limit. When $n \rightarrow \infty$ it is sometimes necessary to redefine the coupling constants including factors of n that yield a sensible $n \rightarrow \infty$ limit of thermodynamic quantities.

- (x) One can add a dynamic rule to update the spins. We are then confronted to the *kinetic Ising model* (or its multi-component extensions) and more generally to the new World of stochastic processes.
- (xi) *Dynamic phase transitions* occur in the properties of the system's evolution. We will not discuss them in these Lectures.
- (xii) In the low temperature phase of clean models or even weakly frustrated/disordered ones, the progressive order is reached via *domain growth*, the simplest example of *phase ordering kinetics*.
- (xiii) Last but not least, it has been a paradigmatic model describing many problems beyond physics like *neural networks*, *social ensembles*, etc.

Note the difference between the two parameters, N and n . N is the number of spins in the system. n is the number of components that each spin vector has. There is still another dimension, the one of real space, that we call d .

2.3 Concepts

Let us now discuss some important concepts, *symmetries*, *order parameters*, *pinning fields*, *broken ergodicity* and *broken symmetry* [1, 2, 3, 4, 5, 6, 7, 8, 9, 10, 11], with the help of the concrete example of the Ising model. The discussion applies, though, in greater generality.

2.3.1 Symmetries

Let us treat separately the case of continuous and discrete symmetries.

Continuous

In the absence of an applied magnetic field the Hamiltonian (2.3) remains invariant under the simultaneous *rotation* of all spins:

$$\begin{aligned}\mathcal{H}(\{\vec{s}_i'\}) &= -\frac{J}{2} \sum_{\langle ij \rangle} \vec{s}_i' \cdot \vec{s}_j' = -\frac{J}{2} \sum_{\langle ij \rangle} R^{ab} s_i^b R^{ac} s_j^c = -\frac{J}{2} \sum_{\langle ij \rangle} R^{Tba} R^{ac} s_i^b s_j^c \\ &= -\frac{J}{2} \sum_{\langle ij \rangle} s_i^b s_j^b = -\frac{J}{2} \sum_{\langle ij \rangle} \vec{s}_i \cdot \vec{s}_j = \mathcal{H}(\{\vec{s}_i\})\end{aligned}\quad (2.5)$$

since R is an orthogonal transformation, such that $R^T R = I$, with R^T the transpose of R . The model is $O(n)$ symmetric. This symmetry is explicitly broken by the external field. (Summation over repeated a, b indices is assumed.)

Discrete

The Ising model with no applied field is invariant under the simultaneous *reversal* of all spins, $s_i \rightarrow s_i' = -s_i$, for all i , a discrete Z_2 symmetry.

2.3.2 Order parameters

An *order parameter* is generically defined as a quantity – the statistical average of an observable – that typically vanishes in one phase and is different from zero in another one (or other ones). One must notice though that the order parameter is *not unique* (e.g., any power of an order parameter is itself an order parameter) and that there can exist transitions without an order parameter as the *topological* Kosterlitz-Thouless transition in the 2d XY model that we will study later.

In the ferromagnetic Ising model the order parameter is the global magnetisation density¹

$$m = \frac{1}{N} \sum_{i=1}^N \langle s_i \rangle \quad \text{and} \quad \langle s_i \rangle = \mathcal{Z}^{-1} \sum_{\mathcal{C}} s_i e^{-\beta H(\mathcal{C})} \quad (2.6)$$

¹We will discuss the issues raised by the symmetries of Sec. 2.3.1 in Sec. 2.3.4.

where N is the total number of spins and the angular brackets represent the thermal average in the canonical ensemble (that we adopt henceforth unless otherwise stated) as indicated in the second equation. The sum over configurations \mathcal{C} is just a sum over all $s_i = \pm 1$ in this example.

In Ising antiferromagnetic models one can define *staggered magnetisations* that take into account the periodicity between two possible orientations of the local spins. Generalisations to systems with different internal dimension of the spins ($n > 1$) are straightforward.

2.3.3 Thermodynamic limit

The abrupt change in the order parameter at particular values of the external parameters, say the adimensional control parameters built with the temperature and magnetic field $(\beta J, \beta h)$, is associated to the divergence of some derivative of the free-energy (we use the canonical ensemble) with respect to one of these parameters. The partition function is a sum of positive terms. In a system with a finite number of degrees of freedom (as, for instance, in an Ising spin model where the sum has 2^N terms with N the number of spins) such a sum is an analytic function of the parameters. Thus, no derivative can diverge. One can then have a phase transition only in the *thermodynamic limit* in which the number of degrees of freedom diverges.

2.3.4 Pinning field

In the absence of a magnetic field, and for pairwise (two-body) interactions, the energy of an Ising model is an even function of the spins, $\mathcal{H}(\{s_i\}) = \mathcal{H}(\{-s_i\})$ and, consequently, the equilibrium magnetisation density computed as an average over *all* spin configurations with their canonical weight, $e^{-\beta \mathcal{H}(\mathcal{C})}$, vanishes at all temperatures:

$$\langle s_i \rangle = 0 \quad \forall i \quad \text{if} \quad h_i = 0 \quad \forall i. \quad (2.7)$$

At high temperatures, $m = 0$ (see Eq. (2.6)) characterises completely the equilibrium properties of the system since there is a unique paramagnetic state with vanishing magnetisation density. At low temperatures instead if we perform an experiment in a, say, ferromagnetic sample, we *do observe* a net magnetisation density. In practice, what happens is that when the experimenter takes the system through the transition he/she cannot avoid the application of tiny external fields – the experimental set-up, the Earth... – and there is always a small *pinning field* that actually selects one of the two possible equilibrium states, with positive or negative magnetisation density, allowed by symmetry. In the course of time, the experimentalist should see the full magnetisation density reverse, to ensure $m = 0$ in equilibrium (see Fig. 2.2). However, this is not seen in practice since astronomical time-scales would be needed for these reversals to take place.

We shall see the following statement at work when solving mean-field models exactly. To see $\langle s_i \rangle \neq 0$ one needs to compute

$$\lim_{h \rightarrow 0} \lim_{N \rightarrow \infty} \langle s_i \rangle_h = m \neq 0, \quad (2.8)$$

that is to say, the average under an applied field that is taken to zero only after the infinite size limit. This is the pinning field, which selects one out of two fully degenerate equilibrium states.²

2.3.5 Broken ergodicity

Introducing dynamics into the problem,³ *ergodicity breaking* can be stated as the fact that the temporal average over a long (but finite) time window

$$\bar{A}_t = \lim_{t_0 \ll \tau \ll t} \frac{1}{2\tau} \int_{t-\tau}^{t+\tau} dt' A(t') \quad (2.9)$$

is different from the static statistical one, with the sum running over all configurations with their associated Gibbs-Boltzmann weight:

$$\bar{A}_t \neq \langle A \rangle. \quad (2.10)$$

In practice, the temporal average is done in a long but finite interval $\tau < \infty$. During this time, the system is positively or negatively magnetised depending on whether it is in “one or the other degenerate equilibrium states” (see Fig. 2.2). Thus, the temporal average of the orientation of the spins, for instance, yields a non-vanishing result $\bar{A}_t = m_t \neq 0$. If, instead, one computes the statistical average summing over *all* configurations of the spins, the result is zero, as one can see using the symmetry arguments explained in Sec. 2.3.4. The reason for the discrepancy is that with the time average we are actually summing over half of the available configurations of the system: if the averaging time-window controlled by τ is not as large as a function of N , the trajectory does not have enough time to visit all configurations in phase space. One can reconcile the two results by summing only over the configurations with positive (or negative) magnetisation density in the statistical average, and recovering in this way a non-vanishing result.

Note that ergodicity breaking is a statement about the dynamics of a system.

2.3.6 Spontaneous broken symmetry

In the absence of an external field the Hamiltonian is symmetric with respect to the simultaneous reversal of all spins, $s_i \rightarrow -s_i$ for all i . The phase transition corresponds to a *spontaneous symmetry breaking* between the states of positive and negative magnetization. One can determine the one that is chosen when going through T_c either by applying a small *pinning field* that is taken to zero only after the thermodynamic limit, or by imposing

²In the ferromagnetic Ising model is very easy to identify the pinning field to be used. In problems with quenched random interactions in competition, like spin-glasses, it is not obvious a priori which are the pinning fields which have to be used.

³Note that Ising model does not have a natural dynamics associated to it. Convenient dynamic rules can be attributed to the evolution of the spins ensuring the system’s approach to canonical equilibrium.

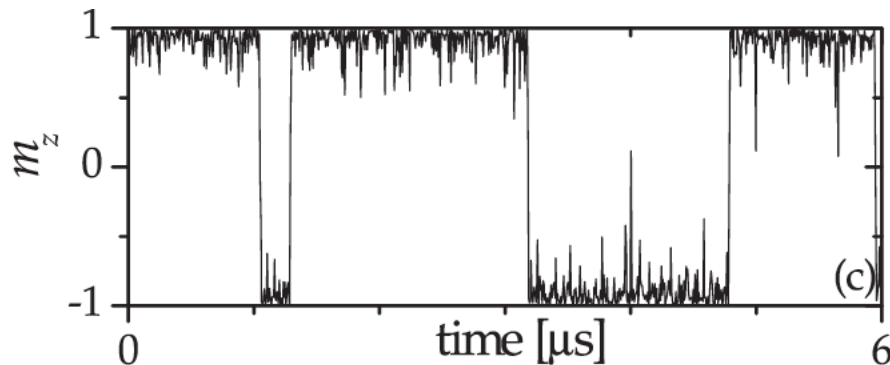


Figure 2.2: Time dependence of the global magnetisation in a magnetic system, with sudden switches from one state to the other. Image taken from [13].

adequate *boundary conditions* like, for instance, all spins pointing up on the borders of the sample. Once a system sets into one of the equilibrium states this is completely stable in the $N \rightarrow \infty$ limit. The mathematical statement of spontaneous symmetry breaking is then

$$\lim_{h \rightarrow 0^+} \lim_{N \rightarrow \infty} \langle s_i \rangle = - \lim_{h \rightarrow 0^-} \lim_{N \rightarrow \infty} \langle s_i \rangle \neq 0. \quad (2.11)$$

Ergodicity breaking necessarily accompanies spontaneous symmetry breaking but the reverse is not true; an example is provided by systems with quenched disorder. Indeed, spontaneous symmetry breaking generates disjoint ergodic regions in phase space, related by the broken symmetry, but one cannot prove that these are the only ergodic components in total generality. Mean-field spin-glass models provide a counterexample of this implication, in which many ergodic components not related by symmetry exist.

2.3.7 Phenomenology

Before launching the discussion our theoretical analysis, let us spend 5 minutes looking at typical equilibrium configurations of the two-dimensional Ising Model, the paradigmatic model with a finite temperature phase transition. Figure 2.3 shows three snapshots of this system in equilibrium above, at and below the critical temperature.

At infinite temperature, each spin has equal probability (a half) of pointing up and down. The snapshot on the left does not show any structure and it is completely disordered. The magnetisation density vanishes. At all *temperatures above the critical one*, which are not too close to it, one will see similar features.

At the critical temperature one sees *domains*, that is, regions in which the spins tend to point in one of the two directions, but these domains have reversed domains within. These domains seems to have all possible *length-scales*. There are still as many spins up as spins down and if one were to sum them up, the result would zero (apart from fluctuations). If one were to pick another configuration also in equilibrium at the critical temperature the

position and form of the domains will be totally different. There is nothing special about one region of the samples or another.

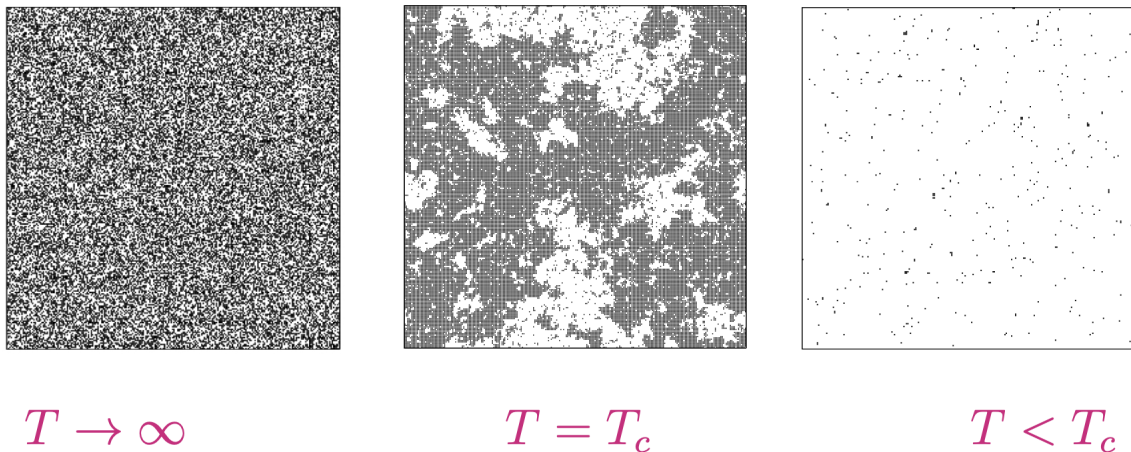


Figure 2.3: Three typical equilibrium configurations of the two-dimensional Ising model.

Finally, *below the critical temperature*, the configuration is mostly ordered in the, say, down direction. However, there are some isolated single spins, or even small *clusters* of spins, which are reversed with respect to the background. In a sense, there is a single domains with fluctuations within. This makes the global magnetisation density of this configuration be not completely saturated and hence slightly smaller than one. At a later time, during the equilibrium evolution of the sample, the location of the reversed spins or clusters will be different but, statistically, they will behave in the same way (same size distribution, same number of reverse spins, etc. apart from fluctuations). This snapshot demonstrates the spontaneous symmetry breaking mechanism whereby the negatively magnetised state has been selected in this experiment. Another experiment may give a positively magnetised equilibrium state. The two appear with equal probability of a half if no external magnetic field is applied.

2.3.8 Energy *vs.* entropy - the Peierls argument

Let us use a thermodynamic argument to describe the high and low temperature phases of a magnetic system and argue that for short-range interactions a one dimensional system with short-range interactions cannot sustain an order phase at non-zero temperature while one with sufficiently long-range interactions can.

The *free-energy* of a system is given by $F = U - TS$ where U is the internal energy, $U = \langle \mathcal{H} \rangle$, and S is the entropy. The equilibrium state may depend on temperature and it is

such that it minimises its free-energy F . A competition between the energetic contribution and the entropic one may then lead to a change in phase at a definite temperature, *i.e.* a different group of micro-configurations, constituting a state, with different macroscopic properties dominate the thermodynamics at one side and another of the transition.

At zero temperature the free-energy is identical to the internal energy U . In a system with nearest-neighbour ferromagnetic couplings between magnetic moments, the magnetic interaction is such that the energy is minimised when neighbouring moments are parallel.

Switching on temperature thermal agitation provokes the reorientation of the moments and, consequently, misalignments. Let us then investigate the opposite, infinite temperature case, in which the entropic term dominates and the chosen configurations are such that entropy is maximised. This is achieved by the magnetic moments pointing in random independent directions.

The competition between these two limits indicates whether a finite temperature transition is possible or not.

Short-range interactions in $d = 1$

At zero temperature the preferred configuration is such that all moments are parallel, the system is fully ordered, and for nearest-neighbour couplings $U = -J\#$ pairs.

For a model with N Ising spins, the entropy at infinite temperature is $S \sim k_B N \ln 2$.

Decreasing temperature magnetic disorder becomes less favourable. The existence or not of a finite temperature phase transitions depends on whether long-range order, as the one observed in the low-temperature phase, can remain stable with respect to *fluctuations*, or the reversal of some moments, induced by temperature. Up to this point, the discussion has been general and independent of the dimension d .

The competition argument made more precise allows one to conclude that there is no finite temperature phase transition in $d = 1$ while it suggests there is one in $d > 1$. Take a one dimensional ferromagnetic Ising model with closed boundary conditions (the case of open boundary conditions can be treated in a similar way),

$$\mathcal{H}(\{s_i\}) = -J \sum_{i=1}^N s_i s_{i+1} , \quad (2.12)$$

and $s_{N+1} = s_1$. At zero temperature it is ordered and its internal energy is just

$$U_o = -JN \quad (2.13)$$

with N the number of links and spins. Since there are two degenerate ordered configurations (all spins up and all spins down) the entropy is

$$S_o = k_B \ln 2 \quad (2.14)$$

The internal energy is extensive while the entropy is just a finite number. At temperature T the free-energy of the completely ordered state is then

$$F_o = U_o - TS_o = -JN - k_B T \ln 2 . \quad (2.15)$$

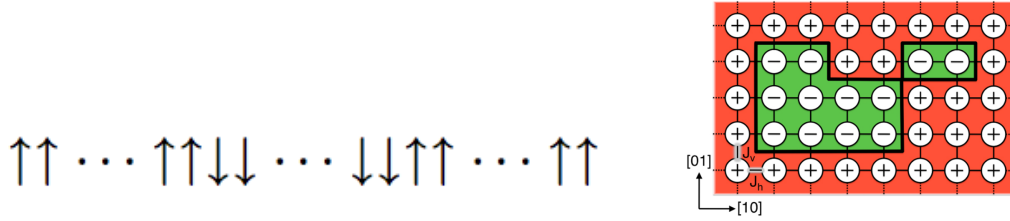


Figure 2.4: Left, a domain wall in a one dimensional Ising system and right, two bidimensional domains in a planar Ising system.

This is the *ground state* at finite temperature or global configuration that minimises the free-energy of the system.

Adding a *domain* of the opposite order in the system, *i.e.* reversing n spins, two bonds are unsatisfied and the internal energy becomes

$$U_2 = -J(N - 2) + 2J = -J(N - 4) , \quad (2.16)$$

for any n . Since one can place the misaligned spins anywhere in the lattice, there are N equivalent configurations with this internal energy. The entropy of this state is then

$$S_2 = k_B \ln(2N) . \quad (2.17)$$

The factor of 2 inside the logarithm arises due to the fact that we consider a reversed domain in each one of the two ordered states. At temperature T the free-energy of a state with *two domain walls* is

$$F_2 = U_2 - TS_2 = -J(N - 4) - k_B T \ln(2N) . \quad (2.18)$$

The variation in free-energy between the ordered state and the one with one reversed domain is

$$\Delta F = F_2 - F_o = 4J - k_B T \ln N . \quad (2.19)$$

Thus, even if the internal energy increases due to the presence of the domain walls, the increase in entropy is such that the free-energy of the state with a droplet in it is much lower, and therefore the state much more favourable, at any finite temperature T . One can repeat this argument reversing domains within domains and progressively disorder the sample. We conclude that spin flips are favourable and order is destroyed at any non-vanishing temperature. The ferromagnetic Ising chain does not support a non-zero temperature ordered phase and therefore does not have a finite temperature phase transition.

Note that this argument explicitly uses the fact that the interactions are short-ranged (actually, they extend to first neighbours on the lattice only in the example). Systems with sufficiently long-range interactions can have finite temperature phase transitions even in one dimension, as shown below.

Exercise 2.1 Solve the one dimensional Ising chain and confirm that it only orders at zero temperature. Identify the correlation length, $\xi(T)$, from the decay of the connected correlation function, $C(r) \equiv \langle (s_i - \langle s_i \rangle)(s_j - \langle s_j \rangle) \rangle |_{|\vec{r}_i - \vec{r}_j| = r} \sim e^{-r/\xi(T)}$, and its temperature dependence.

Power-law decaying interactions in $d = 1$

Take now a one dimensional Ising model

$$\mathcal{H}(\{s_i\}) = -\frac{J}{2} \sum_{i \neq j} J_{ij} s_i s_j = -J \sum_{i=0}^{N-1} \sum_{k=1}^{N-i} J_{i+i+k} s_i s_{i+k} \quad (2.20)$$

with open boundary conditions and algebraically decaying ferromagnetic interactions

$$J_{i+i+k} \sim J r_{i+i+k}^{-\alpha} \equiv J r_{i+i+k}^{-(1+\sigma)} = J (ak)^{-(1+\sigma)}, \quad (2.21)$$

where $r_{i+i+k} = |\vec{r}_i - \vec{r}_{i+k}| = ak$, a is the lattice spacing, and we used here the notation in [66] that compared to the one of the Introductory chapter is $\alpha = \sigma + 1$. From the arguments put forward in that chapter, we expect a change in behaviour at $\sigma = 0$ or $\alpha = d = 1$.

In a perfect ferromagnetic configuration the energy is $U_0 = -J \sum_{i=0}^{N-1} \sum_{k=1}^{N-i} (ak)^{-(1+\sigma)}$ that in a continuous limit, $ak \mapsto y$, $a \sum_k \mapsto \int dy$, and $a \sum_i \mapsto \int dx$ reads

$$\begin{aligned} U_0 &\mapsto -\frac{J}{a^2} \int_0^{L-a} dx \int_a^{L-x} dy \frac{1}{y^{1+\sigma}} = \frac{J}{a^2} \frac{1}{\sigma} \int_0^{L-a} dx [(L-x)^{-\sigma} - a^{-\sigma}] \\ &= \frac{J}{a^2} \frac{1}{\sigma} \frac{1}{1-\sigma} [-a^{1-\sigma} + L^{1-\sigma} - a^{-\sigma}(L-a)]. \end{aligned} \quad (2.22)$$

We see that for $\sigma < 0$ the energy is superextensive, $U_0 \propto -L^{1-\sigma}$. One can cure this problem by re-scaling J , $J \mapsto JL^{\sigma-1}$, that is, considering a much weaker interaction strength, scaling with system size. Instead, for $\sigma > 0$ the large system size limit is controlled by the last term and the (still negative) ground state energy is extensive.

We now make an explicit calculation to check whether this system can have long-range order in the cases $\sigma > 0$ (equivalent to $\alpha > d = 1$).

Consider an excitation over the ferromagnetically order state in which n spins on the left point down and $N-n$ spins on the right point up, that is to say, a configuration with a single sharp domain wall (possible because of the open boundary conditions). The excess energy of this excitation with respect to the perfectly ordered ground state in which all spins point up is:

$$\Delta U = 2J \sum_{i=0}^n \sum_{j=n-i+1}^{N-i} \frac{1}{(aj)^{1+\sigma}}. \quad (2.23)$$

Clearly, if $n = 0$ or $n = N - 1$, $\Delta U = 0$. In the continuous space limit, $a \rightarrow 0$, the sums

can be transformed into integrals

$$\begin{aligned}
\Delta U &\mapsto \frac{2J}{a^2} \int_0^z dx \int_{z-x+a}^{L-x} dy \frac{1}{y^{1+\sigma}} \\
&= -\frac{2J}{a^2\sigma} \int_0^z dx [(L-x)^{-\sigma} - (z-x+a)^{-\sigma}] \\
&= \frac{2J}{a^2\sigma(1-\sigma)} [(L-z)^{1-\sigma} - L^{1-\sigma} - a^{1-\sigma} + (z+a)^{1-\sigma}] \quad (2.24)
\end{aligned}$$

where we called $L = Na$ the length of the chain and z the placement of the domain wall. We now study this expression in the case $L \gg z \gg a$, that is to say, when the domain wall is placed at a finite distance from the origin compared to the infinite size limit. The contribution of the first two terms in the square brackets is proportional to z/L^σ for $z \ll L$ and negligible for $\sigma > 0$. The third term is just a short-length regularisation depending on the lattice size. The last term is the important one that we approximate as

$$\approx \frac{2J}{a^2\sigma(1-\sigma)} z^{1-\sigma} \quad (2.25)$$

using $z \gg a$. Therefore, the excitation energy increases with the length to the reversed domain for $0 < \sigma < 1$ (while in the first-neighbour interaction case it was independent of it). The reversal of large domains is not favourable energetically and this is an indication that long-range order can exist in such a model with $0 < \sigma < 1$. In the case $\sigma < 0$ interactions are strongly long-ranged and order should be even more favorable. (Many mathematical papers from the 60s-80s, by the most celebrated statistical physicists of the time, derived conditions on the decay of the power law interaction to inhibit magnetic order at any non-vanishing temperature.) In contrast, for $\sigma > 1$ the energy of a large droplet is bounded and the entropic term at finite temperature will end up destroying the ferromagnetic order.

Two dimensional case with short-range interactions

A similar argument in $d > 1$ suggests that one can have, as indeed happens, a finite temperature transition in these cases [3]. Look at the right picture in Fig. 2.16 and focus on the domain in the left-down location. It has 14 broken bonds and therefore a boundary with length $L_b = 14$. Fix one internal spin, say the only one which is not at the interface, and consider all possible domains which contain this spin and with the same boundary length $L_b = 14$. An estimate of the number of such domains is μ^{L_b} with μ a number independent of L_b . The difference of the free-energy with and without the reversed domain goes as

$$\Delta F = 2JL_b - k_B T L_b \ln \mu \quad (2.26)$$

and it can be positive at low T and negative at high T . Therefore, this argument does not rule out an ordered phase at low but non-vanishing temperature. The crucial difference

with the one dimensional case is that in the $2d$ case the energy difference scales with L_b and it is not finite.

2.4 Some celebrated methods

Lattice models can be studied by series expansions which start with some exactly solvable limits and develop perturbations around them. For instance, in ferromagnetic models one expands around the perfectly ordered configuration at $T = 0$ (Subsubsec. 2.4.1) or the totally disordered one at $T \rightarrow \infty$ (Subsubsec. 2.4.2). Dualities between models of interest in the hard phase and simpler models to solve in the easy phase have been very useful since the work of Kramers & Wannier on the Ising model (Subsubsec. 2.4.3). Finally, the transfer matrix allows one to solve low dimensional statistical physics models (Subsubsec. 2.4.4).

2.4.1 Low temperature expansion

At zero temperature, $\beta \rightarrow \infty$, and the Boltzmann factor is dominated by the configurations that minimise the energy. For a ferromagnetic Ising model, these are the two perfectly magnetised states, and a series expansion for the partition function is obtained by including low energy excitations around this state. The lowest energy excitation is a single reversed spin, which costs $(2J)(2d)$ energy on a hypercubic lattice, and has multiplicity N . The next lowest energy excitation is a dimer of overturned spins with energy cost $2J(4d - 2)$, and a multiplicity of Nd . Going on in this way one notices that the excitations are in one to one correspondence with graphs on the lattice. With an enumeration technique one then includes as many terms as possible in the partition sum and cuts it at a given order.

In a compact notation, as in a saddle-point approximation,

$$\mathcal{Z} = \sum_{\mathcal{C}} e^{-\beta \mathcal{H}(\mathcal{C})} \sim e^{-\beta \mathcal{H}(\mathcal{C}_{\min})} \sum_{\mathcal{C}} e^{-\frac{\beta}{2} \mathcal{H}''(\mathcal{C}_{\min})(\mathcal{C} - \mathcal{C}_{\min})^2 + \dots}, \quad (2.27)$$

The exponential of the higher order terms collected in the dots can then be expanded (assuming they are small) and, typically, their averages computed taking the average of the Gaussian weight and using Wick's theorem. In field theory this corresponds to the *weak coupling expansion*. For continuously varying fields, this gives the standard *perturbation theory*.

2.4.2 High temperature expansion

The partition function of the Ising ferromagnet reads

$$\mathcal{Z} = \sum_{s_i = \pm 1} e^{\beta J \sum_{\langle ij \rangle} s_i s_j} = \sum_{s_i = \pm 1} \prod_{\langle ij \rangle} e^{\beta J s_i s_j} \quad (2.28)$$

Using the identity $e^{\beta J s_i s_j} = a(1 + b s_i s_j)$ with $a = \cosh(\beta J)$ and $b = \tanh(\beta J)$ and the fact that b is order β , an expansion in powers of b can be established. The average of products of the spins that remains can be non-zero only if each spin appears an even number of times. The expansion can then be represented as graphs on the lattice, a representation that makes the enumeration of terms easier, and it is a particular case of a *cluster expansion* [14].

Quite generally, the high temperature expansions are power series expansion of the partition function around a model that is a union of non-interacting ones and converges in some non-trivial regions of parameters, in particular when the interaction is small [15].

2.4.3 Duality

Dualities are symmetries that relate the free energy of a model at, say, high temperature or weak coupling, to another at low temperature or strong coupling. The relation is used to solve the simple model (typically the one at high T or weak coupling) and infer the behaviour of the other one. Moreover, since the two models should coincide at the critical point, the relation also allows to find the critical parameter as well. This idea was applied by Kramers and Wannier to the $2d$ ferromagnetic Ising model on the square lattice [16], it was later used in many other statistical physics models, and more recently became popular in the field theoretical context.

2.4.4 The transfer matrix

The transfer matrix allows one to obtain the equilibrium properties of Ising chains with periodic boundary conditions and generic interaction strengths and random fields. Take the Ising chain

$$\mathcal{H}(\{s_i\}) = - \sum_{i=1}^N (J_i s_i s_{i+1} + h_i s_i) \quad (2.29)$$

with J_i and h_i link and site dependent exchanges and fields, respectively. Impose periodic boundary conditions such that $s_{N+1} = s_1$. The partition function can be evaluated with the *transfer matrix* method introduced by Kramers and Wannier [17] and Onsager [18]. Indeed,

$$\mathcal{Z}_N = \sum_{\{s_i=\pm 1\}} T_{1s_1s_2} T_{2s_2s_3} \dots T_{Ns_Ns_1} = \text{Tr} \prod_{i=1}^N T_i \quad (2.30)$$

where T_i are 2×2 matrices in which one takes the two row and column indices to take the values ± 1 . Then

$$T_i = \begin{pmatrix} e^{\beta(J_i+h_i)} & e^{\beta(-J_i+h_i)} \\ e^{\beta(-J_i-h_i)} & e^{\beta(J_i-h_i)} \end{pmatrix} \quad (2.31)$$

Note that, for random exchanges and/or fields, that is to say, for J_i and h_i taken from probability distributions, Eq. (2.30) is a product of random matrices. Methods from random matrix theory can then be used to study disordered spin chains [19].

The free-energy per spin is given by

$$-\beta f_N = -\frac{1}{N} \ln \mathcal{Z}_N = -\frac{1}{N} \ln \text{Tr} \prod_{i=1}^N T_i \quad (2.32)$$

The thermodynamic quantities such as the energy per spin, the magnetic susceptibility and others can be computed from this expression. The local quantities, such as the local averaged magnetisation or the correlation functions are evaluated with the help of the *spin operator*

$$\Sigma = \begin{pmatrix} 1 & 0 \\ 0 & -1 \end{pmatrix} \quad (2.33)$$

as

$$\begin{aligned} \langle s_i \rangle &= \frac{1}{\mathcal{Z}_N} \text{Tr} T_1 T_2 \dots T_{i-1} \Sigma T_i \dots T_N, \\ \langle s_i s_j \rangle &= \frac{1}{\mathcal{Z}_N} \text{Tr} T_1 \dots T_{i-1} \Sigma T_i \dots T_{j-1} \Sigma T_j \dots T_N. \end{aligned} \quad (2.34)$$

Disordered exchanges and no magnetic fields

This problem was solved in an exercise with the change of variables $\sigma_i = s_i s_{i+1}$. Let us see now how one can solve it with the transfer matrix method. For $h_i = 0$, all matrices can be diagonalized with the change of basis, $P U_i P^{-1} = T_i$ with

$$P = \begin{pmatrix} 1 & 1 \\ 1 & -1 \end{pmatrix} \quad U_i = \begin{pmatrix} 2 \cosh \beta J_i & 0 \\ 0 & 2 \sinh \beta J_i \end{pmatrix} \quad (2.35)$$

and $P^{-1} = P/2$. One then has

$$\mathcal{Z}_N = \left(\prod_{i=1}^N (2 \cosh \beta J_i) \right) \left(\prod_{i=1}^N (1 + \tanh \beta J_i) \right) \approx \prod_{i=1}^N (2 \cosh \beta J_i) \quad (2.36)$$

More details on the analysis of this kind of chains with the transfer matrix method can be found in [19].

2.4.5 One dimensional models

In one dimension the partition function of a number of magnetic models can be computed exactly and the absence of a finite temperature phase transition corroborated from the absence of non-analyticities in the free-energy. In the two following exercises this fact is made explicit in the one dimensional Ising chain and XY model.

Exercise 2.2 Calculate the free-energy of the one dimensional ferromagnetic Ising chain (no external field applied) $\mathcal{H} = -J \sum_{i=1}^N s_i s_{i+1}$. Discuss free and periodic ($s_1 = s_{N+1}$) boundary conditions separately. Calculate the correlation function between two spins s_i and s_k . Trick: use the fact that $s_j^2 = 1$ for all j to introduce identities on all sites in between i and k . Prove that $C_{ik} \equiv \langle s_i s_k \rangle = \langle \eta_i \rangle \langle \eta_{i+1} \rangle \dots \langle \eta_{k-1} \rangle \langle \eta_k \rangle = \tanh(\beta J)^{|k-i|} = e^{(k-i) \ln \tanh(\beta J)}$ with $\eta_i = s_i s_{i+1}$.

Exercise 2.3 Calculate the free-energy of the one dimensional ferromagnetic XY chain (no external field applied) $\mathcal{H} = -J \sum_{i=1}^N \vec{s}_i \cdot \vec{s}_{i+1}$. Discuss free and periodic ($\vec{s}_1 = \vec{s}_{N+1}$) boundary conditions separately.

Exercise 2.4 Study the equilibrium properties of the nearest-neighbour Ising model in one dimension with the addition of a fully connected term: $\mathcal{H} = -J_{\text{nn}} \sum_{i=1}^N \vec{s}_i \cdot \vec{s}_{i+1} + J_{\text{fc}} (\sum_i s_i^2)^2$ with J_{fc} conveniently rescaled with N so as to make the energy extensive. This model can be studied in the canonical and microcanonical ensembles and for certain values of the parameters inequivalence of results are found. See, *e.g.* [66] and references therein for a discussion.

2.5 Mean field theory

In spite of their apparent simplicity, the statics of ferromagnetic Ising models has been solved analytically only in one and two dimensions. The mean-field approximation allows one to solve the Ising model in *any* spatial dimensionality. Even though the qualitative results obtained are correct, the quantitative comparison to experimental and numerical data shows that the approximation fails below an *upper critical dimension* d_u . It is however very instructive to see the mean-field approximation at work.

We will first present the standard mean-field approximation to a finite dimensional Ising model.

Next we will study a generic Ising spin Hamiltonian

$$\mathcal{H}(\{s_i\}) = - \sum_{i_1 \dots i_p} J_{i_1 \dots i_p} s_{i_1} \dots s_{i_p} - \sum_i h_i s_i$$

with p -spin interactions which we do not specify for the moment and under local external magnetic fields. The usual two-body model is recovered with $p = 2$ but larger values of p will be interesting since they allow to see first-order phase transitions within the same framework. We will scale the coupling constants $J_{i_1 \dots i_p}$ with the number of spins in the sample so as to ensure the extensive property of the energy, $\mathcal{H} = O(N)$. For the moment we do not restrict the sum over the spins, it will be determined by the type of interaction, and we will make it explicit later.

2.5.1 Ignoring correlations

The usual way of deriving the mean-field approximation is to write

$$s_i = m_i + \delta s_i \tag{2.37}$$

with $\delta s_i = s_i - m_i$, and $m_i = \langle s_i \rangle$ the local magnetisation density which are the guessed *local order parameters*. (We remark here that these do not have to be identical, nor take the same sign at this stage. Indeed, in problems in which the coupling strengths are not all equal, and may even have sign variations, the m_i will depend on the index i and even have different signs. It is the case of *random ferromagnets* or *spin-glasses*.) The next step is to replace this expression in each term contributing to the sum over spins in the

Hamiltonian that, for concreteness, we take to have pair interaction⁴

$$\sum_{i_1 \dots i_p} \dots \mapsto \sum_{ij} \dots \quad p = 2 \quad (2.38)$$

and keep only first order terms in powers of δs_i , which are assumed to be small. Then,

$$s_i s_j \simeq m_i m_j + m_i \delta s_j + m_j \delta s_i = m_i s_j + m_j s_i - m_i m_j. \quad (2.39)$$

The extension to p -spin interactions is straightforward. This leads to a model with N non-interacting Ising spins coupled to m_i -dependent local fields:

$$\sum_{ij} J_{ij} s_i s_j \approx - \sum_{ij} J_{ij} m_i m_j + 2 \sum_{ij} J_{ij} s_i m_j. \quad (2.40)$$

This way of presenting the approximation makes its “mean field” character transparent. The fact that correlations between different spins are neglected will soon become clear, from the calculation of the connected correlations. This approximation cannot be accurate when the correlations are strong, *i.e.* close to the critical point.

Having truncated the Hamiltonian we are now able to compute the partition sum. The first term in (2.40) is just independent of the spins and can be taken out of the partition sum, and the model just became one of independent spins in an effective local field⁵

$$h_i^{\text{eff}} = \sum_{\partial i} J_{ij} m_j \quad \text{and} \quad h_i^{\text{loc}} = h_i^{\text{eff}} + h_i \quad (2.41)$$

which add up to the external ones, h_i , to make a total local field h_i^{loc} . The notation ∂i indicates the first neighbours of the site i on the lattice or graph on which the model is defined. Thus the sum $\sum_{\partial i}$ runs over the spins j that interact with the selected spin i . One has

$$\mathcal{Z} \approx e^{-\beta \sum_{ij} J_{ij} m_i m_j} \sum_{\{s_i = \pm 1\}} e^{\beta \sum_{i=1}^N s_i (\sum_{\partial i} J_{ij} m_j + h_i)} \quad (2.42)$$

$$= e^{-\beta \sum_{ij} J_{ij} m_i m_j} \prod_{i=1}^N 2 \cosh \left[\beta \left(\sum_{\partial i} J_{ij} m_j + h_i \right) \right] \quad (2.43)$$

The external local fields h_i may act as *pinning fields* or as *sources* to compute spin averages and correlation functions (see below). Therefore, the *free-energy density* $-\beta f = N^{-1} \ln \mathcal{Z}$, that is the thermodynamic potential from which we can derive the macroscopic properties of the model, is now written as a function of the $\{m_i\}$ local order parameters:

$$f(\{m_i\}) \approx \frac{1}{N} \sum_{ij} J_{ij} m_i m_j - \frac{k_B T}{N} \sum_{i=1}^N \ln \left\{ 2 \cosh \left[\beta \left(\sum_{\partial i} J_{ij} m_j + h_i \right) \right] \right\}. \quad (2.44)$$

⁴In many cases the sum is introduced with $1/2$ in front of it which corresponds to a redefinition of the coupling constants $J_{ij} \mapsto J_{ij}/2$.

⁵The reason for the factor $1/2$ in front of the sum $\sum_{\partial i}$ is that $\sum_{i \neq j} = \frac{1}{2} \sum_i \sum_{\partial i}$.

How many are the terms in the sum $\sum_{\partial i}$ and where are situated the corresponding spins in the sample, depend on the range of the interactions.

Exercise 2.5 Study the scaling, with N , of the two terms contributing to f for different kinds of interaction ranges.

Going back to (2.42), one can extract the probability of the now independent spins,

$$P_i(s_i) = \frac{e^{\beta h_i^{\text{loc}}(\{m_j\})s_i}}{e^{-\beta h_i^{\text{loc}}(\{m_j\})s_i} + e^{\beta h_i^{\text{loc}}(\{m_j\})s_i}} , \quad (2.45)$$

with the $\{m_j, j = \partial i\}$, and still having to be determined self-consistently.

The free-energy density (2.44) is a function of the parameters $\{m_i\}$ that are not fixed yet. However, we recall that we introduced them by requiring $\langle s_i \rangle = m_i$. Therefore, one must have

$$m_i = \sum_{\{s_k = \pm 1\}} s_i P_i(s_i) \quad \text{or, equivalently,} \quad m_i = \frac{\partial \ln \mathcal{Z}}{\partial (\beta h_i)} = \frac{\partial (-\beta F)}{\partial (\beta h_i)} \quad (2.46)$$

and these conditions lead to the generic *mean-field equations*

$$m_i = \tanh[\beta h_i^{\text{loc}}(\{m_j\})] = \tanh\left[\beta \sum_{\partial i} J_{ij} m_j + \beta h_i\right] . \quad (2.47)$$

Another way to fix the local order parameters $\{m_i\}$ is to ask them to be the extreme values of $f(\{m_i\})$. We will carry out this analysis after presenting alternative ways to derive the mean-field free-energy density in terms of the $\{m_i\}$ s.

Uniform interactions and fields

If we now take all interactions to be equal, $J_{ij} = J$, and all magnetic fields to be the same, $h_i = h$, all spins see the same environment. In consequence, we can assume that all the m_i are equal, $m_i = m$. Then,

$$f(m) \approx \frac{J}{N} \sum_{ij} m^2 - k_B T \ln \left\{ 2 \cosh \left[\beta \left(J \sum_{\partial i} m + h \right) \right] \right\} . \quad (2.48)$$

The result of the two sums depends of the range of the interactions in the Hamiltonian. One can easily see that for the fully-connected model, the free-energy density will be order one only if we scale $J \mapsto J/N$. Instead, for models with finite range interactions the sum over j has a finite number of terms, f is $O(1)$, and on a lattice with coordination z

$$f(m) \approx \frac{1}{2} J z m^2 - k_B T \ln \{ 2 \cosh [\beta (J z m + h)] \} \quad (2.49)$$

One can see that the more spins interact with the chosen one the closer the spin sees an average field, *i.e.* the *mean-field*. The number of interacting spins increases with

the range of interaction and the dimension of space in a problem with nearest neighbour interactions on a lattice.

The equation of state is now

$$m = \tanh[\beta(Jzm + h)] , \quad (2.50)$$

and, for $h = 0$, it has only one solution $m = 0$ at temperatures $T \geq T_c = Jz$, and three solutions $m = 0$ and $m = \pm|m_1|$ at $T < T_c$. Other properties of this equation will be discussed below.

Exercise 2.6 Take the limit $k_B T \rightarrow 0$ in Eq. (2.49) evaluated at $h = 0$ and show that the minima of the free-energy density are located at $m = \pm 1$ as they should. This kind of calculation can be used as a check to verify the factors in Eq. (2.49).

The mean-field approximation neglects spin-spin correlations. What does this mean? The *connected correlation function* of two spins s_k and s_l is defined as

$$\langle s_k s_l \rangle_c \equiv \langle s_k s_l \rangle - \langle s_k \rangle \langle s_l \rangle = \langle (s_k - \langle s_k \rangle)(s_l - \langle s_l \rangle) \rangle . \quad (2.51)$$

In the problem with $J_{ij} = J$, in the absence of an applied field, it is given by

$$\begin{aligned} \langle s_k s_l \rangle_c &= \frac{1}{\mathcal{Z}} \sum_{\{s_n = \pm 1\}} s_k s_l e^{-\beta J \sum_{ij} (m_i m_j - 2s_i m_j)} \\ &\quad - \frac{1}{\mathcal{Z}} \sum_{\{s_n = \pm 1\}} s_k e^{-\beta J \sum_{ij} (m_i m_j - 2s_i m_j)} \frac{1}{\mathcal{Z}} \sum_{\{s_n = \pm 1\}} s_l e^{-\beta J \sum_{ij} (m_i m_j - 2s_i m_j)} . \end{aligned} \quad (2.52)$$

We could have set all m_j to be equal to m here but we keep the generic notation. The first remark is that the sum over $\{s_n\}$ indicates N sums over the states of each spin. The sums that are not the ones associated to s_k and s_l are identical in the numerators and denominators (\mathcal{Z}) and therefore cancel. The factors $e^{-\beta J \sum_{ij} m_i m_j}$ also cancel since they appear in identical form in numerators and denominators. If the spins k and l are different, and not close to each other so that no spin is shared by the two terms in the exponential, the first sum factorises

$$\begin{aligned} \langle s_k s_l \rangle_c &= \frac{\sum_{s_k = \pm 1} s_k e^{\beta J \sum_{\partial k} s_k m_j} \sum_{s_l = \pm 1} s_l e^{\beta J \sum_{\partial l} s_l m_j}}{\sum_{s_k = \pm 1, s_l = \pm 1} e^{\beta J \sum_{\partial k} s_k m_j - \beta J \sum_{\partial l} s_l m_l}} \\ &\quad - \frac{\sum_{s_k = \pm 1} s_k e^{\beta J \sum_{\partial k} s_k m_j}}{\sum_{s_k = \pm 1} e^{\beta J \sum_{\partial k} s_k m_j}} \frac{\sum_{s_l = \pm 1} s_l e^{\beta J \sum_{\partial l} s_l m_j}}{\sum_{s_l = \pm 1} e^{\beta J \sum_{\partial l} s_l m_j}} \end{aligned} \quad (2.53)$$

and this result is identical to zero. We thus confirm the *absence of correlations* within this approximation.

Exercise 2.7 Prove that the connected correlation can be evaluated as

$$\langle s_k s_l \rangle_c = \frac{\partial^2(-\beta F)}{\partial(\beta h_i) \partial(\beta h_j)} . \quad (2.54)$$

2.5.2 The “naive” mean-field approximation

Take an Ising model on any lattice or graph. The naive mean-field approximation consists in assuming that the probability density of the system’s spin configuration can be written as a product of independent factors [6]

$$P(\{s_i\}) = \prod_{i=1}^N P_i(s_i) \quad \text{with} \quad P_i(s_i) = \frac{1+m_i}{2} \delta_{s_i,1} + \frac{1-m_i}{2} \delta_{s_i,-1} \quad (2.55)$$

and $m_i = \langle s_i \rangle$, where the thermal average has to be interpreted in the restricted sense, *i.e.* taken over one ergodic component, in a way that $m_i \neq 0$. Note that one introduces an order-parameter dependence in the probabilities.

Exercise 2.8 Prove that P is correctly normalised and $m_i = \langle s_i \rangle$ where $\langle \dots \rangle$ is now computed with the weight P . Compute $\langle s_i s_j \rangle$ and discuss the result.

The free-energy density

Using this assumption one can compute the total free-energy

$$F = U - TS \quad (2.56)$$

where the average is taken with the factorized probability distribution (2.55) and the entropy S is given by

$$S = -k_B \sum_{\{s_i=\pm 1\}} P(\{s_i\}) \ln P(\{s_i\}) . \quad (2.57)$$

The entropy of such Ising spins is

$$\begin{aligned} S &= -k_B \sum_{s_i=\pm 1} \prod_{k=1}^N P_k(s_k) \ln \prod_{l=1}^N P_l(s_l) = -k_B \sum_{l=1}^N \sum_{s_l=\pm 1} P_l(s_l) \ln P_l(s_l) \\ &= -k_B \sum_i \left(\frac{1+m_i}{2} \ln \frac{1+m_i}{2} + \frac{1-m_i}{2} \ln \frac{1-m_i}{2} \right) . \end{aligned} \quad (2.58)$$

In general one finds the internal energy

$$U = - \sum_{ij} J_{ij} \langle s_i s_j \rangle - \sum_i h_i \langle s_i \rangle = - \sum_{ij} J_{ij} m_i m_j - \sum_i h_i m_i . \quad (2.59)$$

Comparing to the previous derivation

One can easily show that the two expressions for the configuration probability are equivalent. In both cases they are factorised in local terms which depend on the parameters $\{m_i\}$. A simple calculation, proposed in the following exercise, makes the two expressions coincide.

Exercise 2.9 Using the mean-field eqs. (2.47), show that (2.45) and (2.55) coincide.

Uniform interactions and fields

One can also use this approximation to treat pure ferromagnetic Ising model, $J_{ij} = J$. The internal energy is

$$U = -J \sum_{ij} m_i m_j - h \sum_i m_i . \quad (2.60)$$

For a uniformly applied magnetic field, $h_i = h$, all local magnetisations equal the total density one, $m_i = m$, and the “order-parameter dependent” free-energy density reads

$$f(m) = -\frac{1}{2}Jzm^2 - hm + k_B T \left(\frac{1+m}{2} \ln \frac{1+m}{2} + \frac{1-m}{2} \ln \frac{1-m}{2} \right) \quad (2.61)$$

with z the coordination of the lattice on which the model is defined (we used $\sum_{\langle ij \rangle} \cdot = \frac{1}{2} \sum_i \sum_{\partial i} \cdot = Nz/2 \cdot$). Although this equation looks different from eq. (2.49) it is just a rewriting of it and it leads to the same extremes, as we show below.

2.5.3 The order parameter equation & mean-field criticality

The equation of state fixes the order parameter, m_{sp} , and it is given by the extrema of $f(m)$, determined⁶ by $df(m)/dm = 0$

$$m_{\text{sp}} = \tanh(\beta z J m_{\text{sp}} + \beta h) . \quad (2.62)$$

The stable states are those that also satisfy $d^2 f/dm^2|_{m_{\text{sp}}} > 0$. The sub-script sp stands for *saddle-point* and we will see the reason for this name later on.

Exercise 2.10 Prove that the equation that fixes the extrema of eq. (2.61) and (2.49) is indeed eq. (2.62).

This *equation of state* predicts a *second order phase transition*⁷ at $k_B T_c = zJ$ when $h = 0$. This transition is seen as the value of the parameters at which the equation passes from having just one solution at $m_{\text{sp}} = 0$ to having three solutions, one still at $m_{\text{sp}} = 0$, and the other two at $m_{\text{sp}} \neq 0$, symmetrically placed around 0, always at $h = 0$. Since

⁶Note that this approximation amounts to replacing the exact equation $m_i = \langle \tanh \beta(h_i + \sum_j J_{ij} s_j) \rangle$ by $m_i = \tanh \beta(h_i + \sum_j J_{ij} m_j)$.

⁷Ehrenfest classified phase transitions based on the lowest derivative of the free energy that is discontinuous. In second order ones, the linear susceptibility of the order parameter diverges, and this can be calculated as the second derivative of the free-energy with respect to the field $\chi = \partial^2(-\beta F)/\partial(\beta h)^2|_{h=0}$, hence their name.

the way in which the non-vanishing solutions appear is continuous, the transition is also called *continuous*.

The relation $k_B T_c = zJ$ correctly captures the fact that T_c is proportional to J and that it depends on the lattice geometry. For a cubic lattice $z = 2d$, and the dependence on d is qualitatively correct in the sense that T_c increases with increasing d . However, the actual value is incorrect in all finite dimensions. In particular, this treatment predicts a *finite T_c in $d = 1$* which is clearly wrong. The growth of T_c with z for general lattices is fine.

The equilibrium states are not single configurations but are in almost all cases, ensembles of many microscopic configurations with the same global properties. This can be discussed at sub-critical temperatures. At $T = 0$, there is only one spin configuration with $m = 1$ and another one with $m = -1$. These are the only cases in which the equilibrium states are made by a unique microscopic configuration. At $T = \epsilon$, thermal fluctuations will at least turn round a single spin and $m = 1 - 2/N$ (or $m = -1 + 2/N$). There are N such configurations. And so on and so forth.

Having an expression for the free-energy density as a function of the order parameter, which is determined by eq. (2.62), one can compute all observables and, in particular, their *critical behaviour*. Expanding this mean-field equation, at $h = 0$ and $T = T_c = zJ$, close to $m_{\text{sp}} \simeq 0$ one deduces

$$m_{\text{sp}}(k_B T - k_B T_c)\beta_c \sim -\frac{1}{3}m_{\text{sp}}^3 \quad \Rightarrow \quad m_{\text{sp}} \sim \left(1 - \frac{T}{T_c}\right)^{1/2} \quad (2.63)$$

or $m_{\text{sp}} = 0$ close to T_c . The $m_{\text{sp}} = 0$ solution is the high temperature one, while the other two are the symmetric low temperature ones (we ignored an irrelevant numerical factor). The *critical exponent* is $\beta = 1/2$ independently of d . This behaviour is sketched in the left panel in Fig. 2.5.

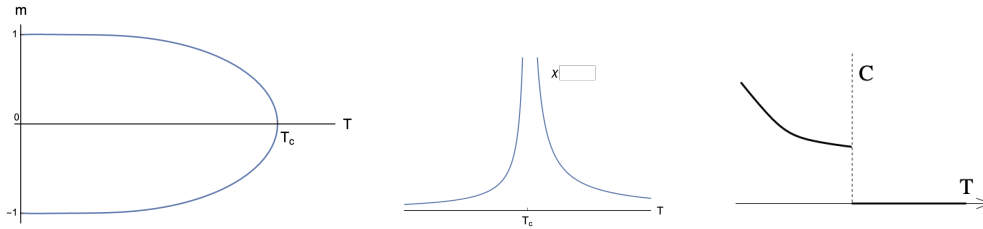


Figure 2.5: The magnetisation density, linear susceptibility and heat capacity of the Ising model in its mean-field approximation.

Let us now consider the solution in the presence of a very weak field and compute the *linear magnetic susceptibility*

$$\chi \equiv \left. \frac{\partial m_{\text{sp}}^{(h)}}{\partial h} \right|_{h \sim 0}. \quad (2.64)$$

Take the variation of the mean-field equation itself to write

$$\frac{\partial m_{\text{sp}}^{(h)}}{\partial h} = \frac{\beta}{\cosh^2[\beta(Jzm_{\text{sp}}^{(h)} + h)] - \beta T_c}. \quad (2.65)$$

At zero field, and slightly above the zero field critical temperature, $m_{\text{sp}} = 0$, and

$$\chi_+ = \frac{\beta}{\cosh^2[\beta(Jzm_{\text{sp}})] - \beta T_c} \sim \frac{1}{k_B T - k_B T_c}. \quad (2.66)$$

Still at zero field, and slightly below the zero field critical temperature $m_{\text{sp}} \sim \pm(1 - T/T_c)^{1/2}$, and is also very small. Taylor expanding $\cosh^2 y \sim 1 + y^2/2$,

$$\begin{aligned} \chi_- &= \frac{\beta}{\cosh^2[\beta(Jzm_{\text{sp}})] - \beta T_c} \sim \frac{\beta_c}{1 + [\beta_c(Jzm_{\text{sp}})]^2/2 - \beta_c T_c} \\ &= \frac{2\beta_c}{m_{\text{sp}}^2} \propto \frac{1}{k_B T_c - k_B T}. \end{aligned} \quad (2.67)$$

Thus, on both sides of the transition χ diverges as $|T - T_c|^{-1}$ and its *critical exponent* $\gamma = 1$ also for all d . Note that the prefactors are different. This behaviour is sketched in the middle panel in Fig. 2.5.

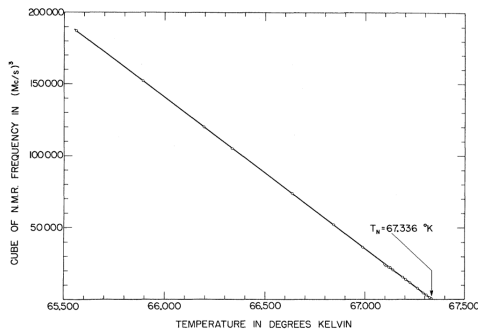


FIG. 1. Temperature dependence of the cube of the F^{19} nuclear resonance frequency for the first 1.8 degrees below T_N . The points lie on the straight line shown to within the experimental uncertainty of about 5 milli-degrees.

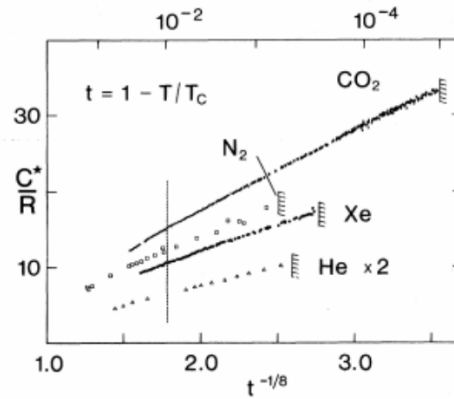


Figure 2.6: Experimental measurement of the order parameter in a magnetic system [22]. The cubic power of m against temperature, suggests for the exponent $\beta \sim 1/3$, differently from $\beta = 1/2$ in mean-field (the actual value is slightly different from $1/3$). Experimental measurement of the heat capacity in terms of the reduced temperature $t \propto T_c - T$ to the power $-1/8$ [23]. The is value is close to the now accepted $\alpha \sim 0.11$.

Experiments (and more recently very careful numerical simulations) measured exponents which are not equal to these integer values, see Fig. 2.6, and do depend on d . Therefore, the mean-field critical behaviour is incorrect in all finite d , with exponents

that do not depend on dimensionality. The mean-field values are summarised in Tables 1, and in Table 2 where there are also compared to the analytic ones in $d = 2$ and numerical estimates in $d = 3$. Still, the nature of the *qualitative* paramagnetic-ferromagnetic transition at $h = 0$ in $d > 1$ is correctly captured.

The Taylor expansion of the free-energy in power of m , close to the critical point where $m \sim 0$, yields the familiar cross over from a function with a single minima at m to the *double well* form tilted by the external field:

$$f(m) \sim -k_B T \ln 2 + \frac{1}{2}(k_B T - zJ)m^2 + \frac{k_B T}{12}m^4 - hm. \quad (2.68)$$

Indeed, below $k_B T = zJ = T_c$ the sign of the quadratic term becomes negative and the function develops two minima away from $m = 0$.

	exponent	definition	conditions	mean-field
Specific heat	α	$C_v \propto t ^{-\alpha}$	$t \rightarrow 0, \quad h = 0$	0
Order parameter	β	$m \propto (-t)^\beta$	$t \rightarrow 0^-, \quad h = 0$	1/2
Susceptibility	γ	$\chi \propto t ^{-\gamma}$	$t \rightarrow 0, \quad h = 0$	1
Critical isotherm	δ	$h \propto m ^\delta \text{sign}(m)$	$h \rightarrow 0, \quad t = 0$	3
Correlation length	ν	$\xi \propto t ^{-\nu}$	$t \rightarrow 0, \quad h = 0$	1/2
Correlation function	η	$G(\mathbf{r}) \propto \mathbf{r} ^{-d+2-\eta}$	$r = 0, \quad h = 0$	0

Table 1: Definitions of the commonly used critical exponents. m is the *scalar* order parameter, *e.g.* the magnetisation, h is an external field conjugate to the order parameter, *e.g.* a magnetic field, t denotes the distance from the critical point, *e.g.* $|T - T_c|/T_c$, and d is the space dimensionality. The mean-field values are given in the last column.

This form allows one to confirm that continuous phase transitions do not have *latent heat*, $L = T\Delta S$, since the *entropy* is continuous,

$$S = -\frac{\partial F}{\partial T} = \ln 2 \quad \text{for} \quad T \rightarrow T^\pm, \quad (2.69)$$

though with a *kink* at T_c , since the *specific heat*

$$C = \frac{\partial \langle \mathcal{H} \rangle}{\partial T} = \beta^2 \frac{\partial^2 \ln \mathcal{Z}}{\partial T^2} \quad (2.70)$$

is discontinuous at the transition. Above T_c , the free-energy density is linear in $k_B T$ and the specific heat vanishes. Below T_c and close to the transition it is a quadratic function of the distance to criticality,

$$\begin{aligned} f(m_{\text{sp}}) &= -k_B T \ln 2 + \frac{1}{2}(k_B T - k_B T_c)m_{\text{sp}}^2 + \frac{k_B T}{12}m_{\text{sp}}^4 \\ &\sim -k_B T \ln 2 + a(k_B T - k_B T_c)^2. \end{aligned} \quad (2.71)$$

Then

$$C \propto \beta_c^2 \frac{\partial^2(T - T_c)^2}{\partial T^2} \propto \text{ct} > 0 \quad (2.72)$$

and the heat capacity jumps discontinuously from zero to a finite value at T_c , see the third panel in Fig. 2.5.

Exercise 2.11 Plot the full $f(m)$ and the approximate one and discuss the similarities and differences.

Exercise 2.12 Study the small m behaviour of $f(m)$ in eq. (2.49) and compare.

Exercise 2.13 Obtain these and all other mean-field exponents.

Finally, one can study the problem under a *finite magnetic field*. It is then easy to see that for all finite temperature and non-zero fields the solution to the equation of state is different from zero. Its sign depends on the sign of h . At the limits $h \pm \infty$ the magnetisation saturates at $m \pm 1$. Decreasing the field amplitude the magnetisation amplitude decreases as well. At fixed $|h|$, the absolute value of the magnetisation, $|m|$, continuously decreases with temperature approaching zero at $T \rightarrow \infty$ only.

One can wonder what happens at fixed temperature if the field is varied from, say, positive to negative values. At temperatures below the critical one at zero field, when approaching the zero field limit from above, the magnetisation approaches a non-zero positive value and then jumps, *discontinuously*, to a negative non-zero value to keep increasing, in absolute value, for increasingly negative field.

In practice, if one were to do this experiment and change the field with some finite velocity protocol, the magnetisation would continue on the initial, say positive, magnetisation branch even for negative external fields. This is a *metastable state* which will disappear at a *spinodal point*, given by $|h_s|$. The metastable state is a local, but not global, stable minimum of the free-energy density. The systems leave such metastable states helped by thermal fluctuations with a *nucleation process* which we will discuss later. Looping the external field around its zero value, at fixed temperature below the zero-field T_c , allows to see *hysteresis*.

The aim is, finally, to find the way in which the magnetisation vanishes with h right at the critical temperature at zero field. Going back to the equation of state and expanding the $\tanh y$ to $\mathcal{O}(y^3)$,

$$m_{\text{sp}}^{(h)} \sim \beta z J m_{\text{sp}}^{(h)} + \beta h - \frac{1}{3}(\beta z J m_{\text{sp}}^{(h)} + \beta h)^3 \quad \Rightarrow \quad \beta h \sim \frac{1}{3}(m_{\text{sp}}^{(h)} + \beta_c h)^3 \quad (2.73)$$

at $T_c(h = 0)$. Assuming that $m_{\text{sp}}^{(h)} \sim h^{1/\delta}$ and $\delta > 1$, then the second term in the cubic power is negligible with respect to the first one, and

$$m_{\text{sp}}^{(h)} \sim (3\beta_c h)^{1/3} \sim h^{1/3} \quad (2.74)$$

consistently with the assumption made.

The evolution of the free-energy density with the field is sketched in Fig. 2.7. The right panel shows the experimental measurement of hysteresis loops.

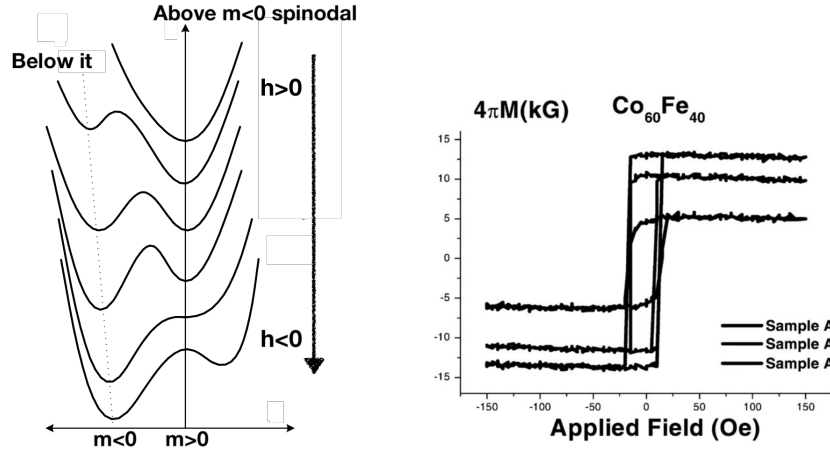


Figure 2.7: (a) The order parameter dependence of the free-energy density for different values of an external magnetic field h going from $h > 0$ to $h < 0$. (b) Several hysteresis loops. Image taken from [21].

2.5.4 Range of validity

The structure of the phase diagram followed from some fairly basic properties of the Taylor expansion of the free energy and the equation for the order parameter and can be expected to be correct in many respects but wrong in others.

The validity of mean field theory depends strongly on the spatial dimension d :

- In $d = 1$ mean field theory fails since there is no phase transition at non zero T_c while it predicts one. $d_l = 1$ for this model.
- In $d = 2$ and $d = 3$ the basic structure of the phase diagram is correct, but the critical behaviour is wrong, in the sense that the exponents do not take the correct values.
- In $d > 4 = d_u$, the upper critical dimension, mean field theory gives the right exponents.

The range of correctness of this approach also depends on the dimension of the order parameter (n), which plays a role in the value taken by the lower critical dimension, at and below which mean-field theory totally fails.

2.5.5 The fully-connected Curie Weiss p -spin model

A set of models for which the mean-field approximation is exact are those defined on a the complete graph, also called fully-connected. We discuss here the generic p -spin model and we later specialise to the ferromagnetic class.

Naive mean-field

Using the factorization of the joint probability density that defines the mean-field approximation, we have already found

$$F(\{m_i\}) = - \sum_{i_1 \neq \dots \neq i_p} J_{i_1 \dots i_p} m_{i_1} \dots m_{i_p} - \sum_i h_i m_i + k_B T \sum_{i=1}^N \left(\frac{1+m_i}{2} \ln \frac{1+m_i}{2} + \frac{1-m_i}{2} \ln \frac{1-m_i}{2} \right) \quad (2.75)$$

where in the first sum we wrote explicitly that there are no self interactions. Recall that a Taylor expansion of the entropic contribution around $m_i = 0$ leads to a polynomial expression that is the starting point in the Landau theory of second order phase transitions.

The local magnetizations, m_i , are then determined by requiring that they minimize the free-energy density and a positive definite Hessian,

$$\frac{\partial f(\{m_j\})}{\partial m_i} = 0 \quad \frac{\partial^2 f(\{m_j\})}{\partial m_i \partial m_j} \quad (2.76)$$

(i.e. with all eigenvalues being positive at the extremal value). The first equation yields

$$m_i = \tanh \left(p\beta \sum_{i_2 \neq \dots \neq i_p} J_{ii_2 \dots i_p} m_{i_2} \dots m_{i_p} + \beta h_i \right). \quad (2.77)$$

If $J_{i_1 \dots i_p} = J/(p!N^{p-1})$ for all p uplets and the applied field is uniform, $h_i = h$, one can take $m_i = m$ for all i and these expressions become (2.79) and (2.82) below, respectively. (Note that a factor $p!$ has been added to the denominator in order to normalise the interactions in such a way that each p -uplet is counted only once in the sum. This is especially useful if one wants to study the $p \rightarrow \infty$ limit.) The mean-field approximation is exact for the fully-connected pure Ising ferromagnet, as we shall show below. [Note that the fully-connected limit of the model with pair interactions ($p = 2$) is correctly attained by taking $J \rightarrow J/(2N)$ and $z = 2d \rightarrow N$ in (2.62) leading to $T_c = J$.]

Exact solution

Let us solve the ferromagnetic model exactly. The sum over spin configurations in the partition function can be traded for a sum over the variable, $x = N^{-1} \sum_{i=1}^N s_i$, that takes values $x = -1, -1 + 2/N, -1 + 4/N, \dots, 1 - 4/N, 1 - 2/N, 1$. Neglecting subdominant terms in N , one then writes

$$\mathcal{Z} = \sum_x e^{-N\beta f(x)} \quad (2.78)$$

with the x -parameter dependent ‘free-energy density’

$$f(x) = -\frac{J}{p!} x^p - hx + k_B T \left(\frac{1+x}{2} \ln \frac{1+x}{2} + \frac{1-x}{2} \ln \frac{1-x}{2} \right). \quad (2.79)$$

The first two terms are the energetic contribution while the third one is of entropic origin since $N!/(N(1+x)/2)!(N(1-x)/2)!$ spin configurations have the same magnetization density. The average of the parameter x is simply the averaged magnetization density:

$$\langle x \rangle = \frac{1}{N} \sum_{i=1}^N \langle s_i \rangle = m . \quad (2.80)$$

Exercise 2.14 Prove this statement.

In the large N limit, the partition function – and all averages of x – can be evaluated in the saddle-point approximation

$$\mathcal{Z} \approx \sum_{\alpha} e^{-N\beta f(x_{\text{sp}}^{\alpha})} , \quad (2.81)$$

where x_{sp}^{α} are the absolute minima of $f(x)$ given by the solutions to $\partial f(x)/\partial x|_{x_{\text{sp}}} = 0$,

$$x_{\text{sp}} = \tanh \left(\frac{\beta J}{(p-1)!} x_{\text{sp}}^{p-1} + \beta h \right) , \quad (2.82)$$

together with the conditions $d^2 f(x)/dx^2|_{x_{\text{sp}}} > 0$. Note that the contributing saddle-points should be degenerate, *i.e.* have the same $f(x_{\text{sp}}^{\alpha})$ for all α , otherwise their contribution is exponentially suppressed. The sum over α then just provides a numerical factor of two in the case $h = 0$. Now, since

$$x_{\text{sp}} = -\partial f(x)/\partial h|_{x_{\text{sp}}} = \langle x \rangle = m , \quad (2.83)$$

as we shall show in Eq. (2.84), the solutions to the saddle-point equations determine the order parameter. We shall next describe the phases and phase transition qualitatively and we will later justify this description analytically.

Model in a finite field

In a finite magnetic field, eq. (2.82) has a unique positive – negative – solution for positive – negative – h at all temperatures. The model is ferromagnetic at all temperatures and there is no phase transition in this parameter.

2nd order transition for $p = 2$

In the absence of a magnetic field this model has a paramagnetic-ferromagnetic phase transition at a finite T_c . The order of the phase transition depends on the value of p . This can be seen from the temperature dependence of the free-energy density (2.79). Figure 2.8 displays $f(x)$ in the absence of a magnetic field at three values of T for the $p = 2$ (left), $p = 3$ (center) and $p = 4$ (right) models (we call the independent variable m since the stationary points of $f(x)$ are located at the magnetisation density of the equilibrium and metastable states, as we shall show below). At high temperature the unique minimum is

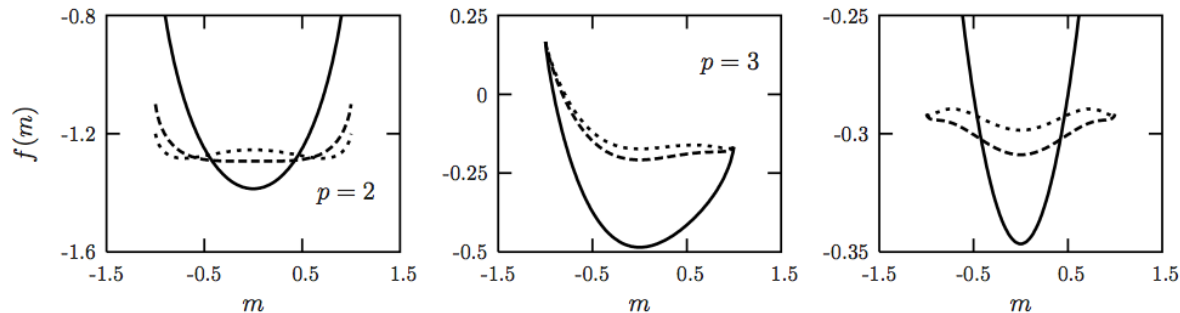


Figure 2.8: The free-energy density $f(m)$ of the $p = 2$ (left), $p = 3$ (center) and $p = 4$ (right) models at three values of the temperature $T < T_c$ (light dashed line), $T = T_c$ (dark dashed line) and $T > T_c$ (solid line) and with no applied field. (The curves have been translated vertically.)

$m = 0$ in all cases. For $p = 2$, when one reaches T_c , the $m = 0$ minimum splits in two that slowly separate and move towards higher values of $|m|$ when T decreases until reaching $|m| = 1$ at $T = 0$ (see Fig. 2.8-left). The transition occurs at $T_c = J$ as can be easily seen from a graphical solution to eq. (2.82), see Fig. 2.9-left. Close but below T_c , the magnetisation increases as $m \sim (T_c - T)^{1/2}$. The linear magnetic susceptibility has the usual Curie behaviour at very high temperature, $\chi \approx \beta$, and it diverges as $\chi \sim |T - T_c|^{-1}$ on both sides of the critical point. The order parameter is continuous at T_c and the transition is of second-order thermodynamically.

1st order transition for $p > 2$

For $p > 2$ the situation changes. For even values of p , at T^* two minima (and two maxima) at $|m| \neq 0$ appear. These coexist as metastable states with the stable minimum at $m = 0$ until a temperature T_c at which the three free-energy densities coincide, see Fig. 2.8-right. Below T_c the $m = 0$ minimum continues to exist but the $|m| \neq 0$ ones are favoured since they have a lower free-energy density. For odd values of p the free-energy density is not symmetric with respect to $m = 0$. A single minimum at $m^* > 0$ appears at T^* and at T_c it reaches the free-energy density of the paramagnetic one, $f(m^*) = f(0)$, see Fig. 2.8-center. Below T_c the equilibrium state is the ferromagnetic minimum. For all $p > 2$ the order parameter is discontinuous at T_c , it jumps from zero at T_c^+ to a finite value at T_c^- . The linear magnetic susceptibility also jumps at T_c . While it equals β on the paramagnetic side, it takes a finite value given by eq. (2.85) evaluated at m^* on the ferromagnetic one. In consequence, the transition is of first-order.

Pinning field, broken ergodicity and spontaneous broken symmetry

The saddle-point equation (2.82) for $p = 2$ [or the mean-field equation (2.62)] admits two equivalent solutions in no field. What do they correspond to? They are the magnetisation density of the equilibrium ferromagnetic states with positive and negative value.

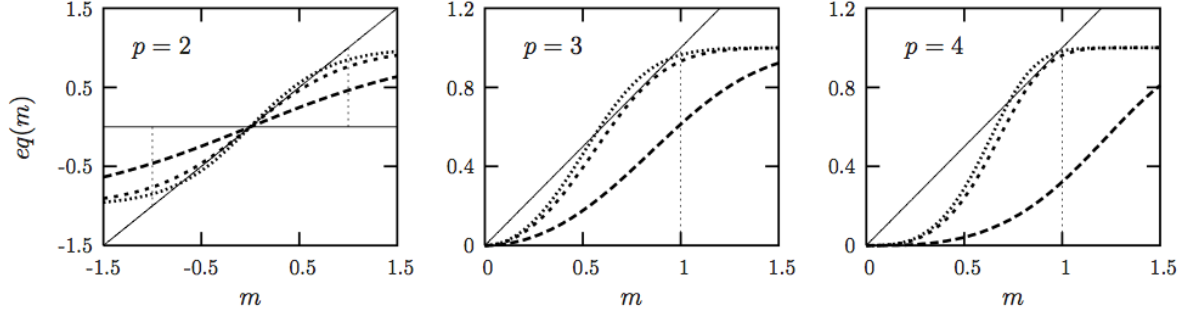


Figure 2.9: Graphical solution to the equation fixing the order parameter x for $p = 2$ (left), $p = 3$ (center) and $p = 4$ (right) ferromagnetic models at three values of the temperature $T < T^*$, $T = T^*$ and $T > T^*$ and with no applied field. The curves represent the sigmoid function on one side of the equation to be solved. Note that the rhs of this equation is antisymmetric with respect to $m \rightarrow -m$ for odd values of p while it is symmetric under the same transformation for even values of p . We show the positive quadrant only to enlarge the figure. T^* is the temperature at which a second minimum appears in the cases $p = 3$ and $p = 4$.

At $T < T_c$ if one computes $m = N^{-1} \sum_{i=1}^N \langle s_i \rangle = \sum_x e^{-\beta N f(x)} x$ summing over the two minima of the free-energy density one finds $m = 0$ as expected by symmetry. Instead, if one computes the averaged magnetisation density with the partition sum restricted to the configurations with positive (or negative) x one finds $m = |m_{\text{sp}}|$ (or $m = -|m_{\text{sp}}|$).

In practice, the restricted sum is performed by applying a small magnetic field, computing the statistical properties in the $N \rightarrow \infty$ limit, and then setting the field to zero. In other words,

$$m_{\pm} \equiv \frac{1}{N} \sum_{i=1}^N \langle s_i \rangle_{\pm} = \left(\frac{1}{\beta N} \frac{\partial \ln \mathcal{Z}}{\partial h} \right) \Big|_{h \rightarrow 0^{\pm}} = - \frac{\partial f(x_{\text{sp}})}{\partial h} \Big|_{h \rightarrow 0^{\pm}} = \pm |x_{\text{sp}}|. \quad (2.84)$$

By taking the $N \rightarrow \infty$ limit in a field one selects the positive (or negatively) magnetised states.

For all odd values of p the phase transition is not associated to symmetry breaking, since there is only one non-degenerate minimum of the free-energy density that corresponds to the equilibrium state at low temperature. The application of a pinning field is then superfluous.

For any even value of p and at all temperatures the free-energy density in the absence of the field is symmetric with respect to $m \rightarrow -m$, see the left and right panels in Fig. 2.8. The phase transition corresponds to a *spontaneous symmetry breaking* between the states of positive and negative magnetisation. One can determine the one that is chosen when going through T_c either by applying a small *pinning field* that is taken to zero only after the thermodynamic limit, or by imposing adequate boundary conditions. Once a system

sets into one of the equilibrium states this is completely stable in the $N \rightarrow \infty$ limit. In pure static terms this means that one can separate the sum over all spin configurations into independent sums over different sectors of phase space that correspond to each equilibrium state. In dynamic terms it means that temporal and statistical averages (taken over all configurations) in an infinite system do not coincide.

The magnetic linear susceptibility for generic p is given by

$$\chi \equiv \left. \frac{\partial m}{\partial h} \right|_{h \rightarrow 0^\pm} = \left. \frac{\partial x_{\text{sp}}}{\partial h} \right|_{h \rightarrow 0^\pm} = \frac{\beta}{\cosh^2\left(\frac{\beta J}{(p-1)!} x_{\text{sp}}^{p-1}\right) - \frac{\beta J}{(p-2)!} x_{\text{sp}}^{p-2}}. \quad (2.85)$$

For $p = 2$, at $T > T_c$, $x_{\text{sp}} = 0$ the susceptibility is given by $(T - J)^{-1}$ predicting the second order phase transition with a divergent susceptibility at $T_c = J$. Approaching T_c from below the two magnetized states have the same divergent susceptibility, $\chi \sim (T_c - T)^{-1}$.

For $p > 2$, at $T > T_c$, $x_{\text{sp}} = 0$ and the susceptibility takes the Curie form $\chi = \beta$. The Curie law, $\chi = \beta$, jumps to a different value at the critical temperature due to the fact that x_{sp} jumps.

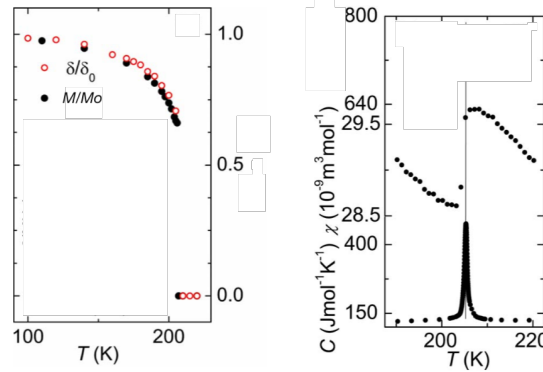


Figure 2.10: Evidence for a thermal first order phase transition in SrFe_2As_2 at $T_c = 205\text{K}$. Temperature dependence of the lattice distortion and the magnetisation normalised to their saturation values at low T . Magnetic susceptibility and specific heat near the transition. Figures from [24].

2.5.6 The Bethe-Peierls or cavity method

Recursive structures like the Cayley tree and the Bethe lattice [11] provide a pedagogical environment for the study of physical problems; in this setting the models can be treated with a direct analytic approach without resorting to approximate methods.

A *Cayley tree* is a tree in which each non-*leaf* graph vertex has a constant number of *branches* c . An example with connectivity $c = 3$ is shown in Fig. 2.11 and one with connectivity $c = 2$ in Fig. 2.12. The *Bethe lattice* is an infinite Cayley tree. It is therefore a connected dendritic structure with constant coordination, c , and *no loops*.

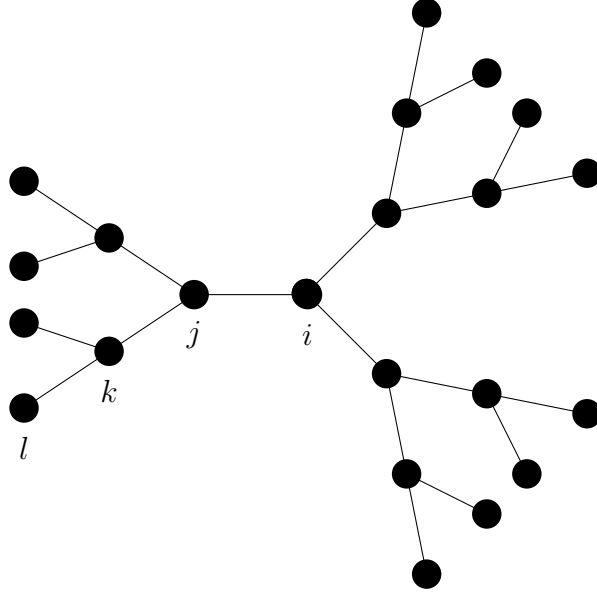


Figure 2.11: A Cayley tree with $c = 3$. Three branches span from the central site. The outbound sites are the leafs.

A Cayley tree is recursively constructed as follows. A central, *seed* or *root* site (i in Fig. 2.11) is placed and it is the zeroth *generation* of the lattice. c sites which are first neighbours of the seed site constitute the first generation of the lattice. Each first-generation site also has c nearest neighbours: one already present in the zeroth generation and $c - 1$ new sites added in the second generation. The n th generation of sites consists of the $c - 1$ new sites neighbouring to the $c(n - 1)$ -generation sites. There are thus $c(c - 1)^{n-1}$ sites in the n -th generation. This can be checked in the example in Fig. 2.11 focusing on the first $n = 1$ generation (site j and similar) for which the formula yields $c = 3$, which is correct. Another particular case is the second $n = 2$ generation for which the formula yields $c(c - 1) = 6$, as also verified in the figure.

The number of sites accessible in n steps from a given site increases exponentially with n , much faster than the power n^d of a d -dimensional lattice. Thus, the Bethe lattice is often considered to represent a sort of $d \rightarrow \infty$ limit. They provide a setting in which the geometrical properties of space lose importance and mean-field treatments can become exact.

The number of sites, N , and the number of sites on the surface, N_s , in a tree with n generations are

$$N = 1 + c + c(c - 1) + \cdots + c(c - 1)^{n-1} = 1 + c \frac{(c - 1)^n - 1}{c - 2} = \frac{c(c - 1)^n - 2}{c - 2}, \quad (2.86)$$

$$N_s = c(c - 1)^{n-1},$$

so, for large n ,

$$\lim_{n \gg 1} \frac{N_s}{N} = \frac{c-2}{c-1}. \quad (2.87)$$

On the Cayley tree, the surface contains a finite fraction of its total number of sites as long as $c > 2$. In a finite dimensional lattice, on the contrary, the surface to volume ratio is $N_s/N \rightarrow N^{-1/d} \rightarrow 0$. This is also the case in the one dimensional lattice, see Fig. 2.12 which is also a Cayley tree with $c = 2$.

Having a recursive spatial structure allows one to build recursive relations for the partition functions and then derive exact solutions. For instance, Domb showed that the Bethe-Peierls (BP) approximation to the nearest-neighbour (NN) ferromagnetic (FM) Ising problem is exact on this structure [25, 2].

A modern presentation of the procedure goes as follow [26, 27]. First, one defines

- ∂j as the set of vertices adjacent to j , that is to say, those sites which are connected to j .
- $\partial j \setminus i$ for those vertices linked to j but distinct from i .

and then

- $\mathcal{Z}_{j \rightarrow i}(s_j)$, the partial partition function for the sub-tree rooted at j , excluding the branch directed towards i , with a fixed value of the spin variable on the site j , that is taken to be s_j .
- $\mathcal{Z}_j(s_j)$, the partition function of the whole tree, also keeping the value of the spin variable on the site j fixed to s_j .

The meaning of ∂j and $\partial j \setminus i$ in a one dimensional lattice ($c = 2$) is displayed in Fig. 2.12.

For a generic tree structure (not necessarily with fixed connectivity) and a model with nearest-neighbour two body interactions. the recursion rules are

$$\begin{aligned} \mathcal{Z}_{j \rightarrow i}(s_j) &= e^{\beta h_j s_j} \prod_{k \in \partial j \setminus i} \sum_{\{s_k = \pm 1\}} \mathcal{Z}_{k \rightarrow j}(s_k) e^{\beta J_{jk} s_j s_k}, \\ \mathcal{Z}_j(s_j) &= e^{\beta h_j s_j} \prod_{l \in \partial j} \sum_{\{s_l = \pm 1\}} \mathcal{Z}_{l \rightarrow j}(s_l) e^{\beta J_{jl} s_j s_l}. \end{aligned} \quad (2.88)$$

It is useful to normalise these quantities, $\eta_{j \rightarrow i}(s_j) \equiv \mathcal{Z}_{j \rightarrow i}(s_j) / \sum_{\{s' = \pm 1\}} \mathcal{Z}_{j \rightarrow i}(s')$ and $\eta_j(s_j) \equiv \mathcal{Z}_j(s_j) / \sum_{\{s' = \pm 1\}} \mathcal{Z}_j(s')$, and re-write the recursion equations as

$$\begin{aligned} \eta_{j \rightarrow i}(s_j) &= \frac{1}{z_{j \rightarrow i}} e^{\beta h_j s_j} \prod_{k \in \partial j \setminus i} \sum_{\{s_k = \pm 1\}} \eta_{k \rightarrow j}(s_k) e^{\beta J_{jk} s_j s_k}, \\ \eta_j(s_j) &= \frac{1}{z_j} e^{\beta h_j s_j} \prod_{l \in \partial j} \sum_{\{s_l = \pm 1\}} \eta_{l \rightarrow j}(s_l) e^{\beta J_{jl} s_j s_l}, \end{aligned} \quad (2.89)$$

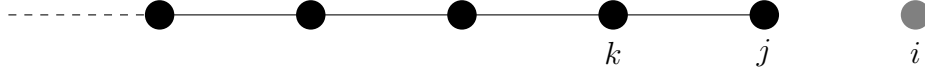


Figure 2.12: A one dimensional lattice or a Cayley tree with $c = 2$. The sketch in the figure does not connect site j to site i and the boundary of j excluding i , $\partial j \setminus i$ is just k . Instead, the full boundary ∂j in the complete lattice in which the link between j and i is also present, consists of the sites k and i . (Note that we are changing notation with respect to [27], the i and j).

where $z_{j \rightarrow i}$ and z_i are normalization constants. These η s can now be interpreted as probability laws for the random variable s_i .

On a given tree the recursion equations (2.89) for all directed edges of the graph have a single solution, easily found by propagating the recursion from the leaves of the graph. Moreover, $\eta_i(s_i)$ is the marginal probability of the full Gibbs-Boltzmann distribution $P(\{s_i\})$ and with it one can compute, for example, the average magnetization $\langle s_i \rangle$.

For constant couplings $J_{ij} = J$ and magnetic fields $h_i = h$, and on the Bethe lattice, where all vertices have the same connectivity c , the probabilities $\eta_{j \rightarrow i}$ should be translational invariant and do not depend on the sites j and i . Calling η_{cav} their common value, and replacing in eqs. (2.89):

$$\begin{aligned} \eta_{\text{cav}}(s) &= \frac{1}{z_{\text{cav}}} e^{\beta h s} \sum_{s_1, \dots, s_{c-1}} \eta_{\text{cav}}(s_1) \dots \eta_{\text{cav}}(s_{c-1}) e^{\beta J s(s_1 + \dots + s_{c-1})}, \\ \eta(s) &= \frac{1}{z} e^{\beta h s} \sum_{s_1, \dots, s_c} \eta_{\text{cav}}(s_1) \dots \eta_{\text{cav}}(s_c) e^{\beta J s(s_1 + \dots + s_c)}, \end{aligned} \quad (2.90)$$

with new normalisation constants z and z_{cav} . The term cavity comes from the fact that one site has been removed from the neighbourhood of the considered vertex.

The Ising variable s can only take two values and, therefore, each of the probability distributions η_{cav} and η can be parametrised by a single real number, a cavity or effective magnetic field,

$$\eta_{\text{cav}}(s) = \frac{e^{\beta h_{\text{cav}} s}}{2 \cosh(\beta h_{\text{cav}})}, \quad \eta(s) = \frac{e^{\beta h_{\text{eff}} s}}{2 \cosh(\beta h_{\text{eff}})}, \quad (2.91)$$

solutions of

$$\begin{aligned} h_{\text{cav}} &= h + \frac{c-1}{\beta} \text{arctanh}[\tanh(\beta J) \tanh(\beta h_{\text{cav}})], \\ h_{\text{eff}} &= h + \frac{c}{\beta} \text{arctanh}[\tanh(\beta J) \tanh(\beta h_{\text{cav}})]. \end{aligned} \quad (2.92)$$

thus making the resolution of (2.90) extremely simple.

At zero external field $h = 0$, there is a phase transition at $\beta = \beta_c$, separating a high temperature paramagnetic phase ($h_{\text{cav}} = h_{\text{eff}} = 0$) from a low temperature ferromagnetic phase ($h_{\text{cav}}, h_{\text{eff}} \neq 0$). The critical temperature is easily obtained linearising the equation for h_{cav} around $h_{\text{cav}} = 0$ and is the solution of $(c - 1) \tanh(\beta_c J) = 1$.

It is worth noting that the spin-spin correlation function can be explicitly calculated. It is given in the paramagnetic phase by $C_{ij} = \langle s_i s_j \rangle = [\tanh(\beta J)]^{d(i,j)}$, where $d(i, j)$ is the distance between sites i and j , defined as the length of the shortest path connecting sites i and j . The associated correlation length, $\xi = -\ln \tanh(\beta J)$, is finite at the transition point $\beta = \beta_c$. Nevertheless, the associated magnetic linear susceptibility $\chi = N^{-1} \sum_i d\langle s_i \rangle / dh|_{h=0}$ diverges. This can be shown using the fluctuation-dissipation theorem, $\chi = \beta N^{-1} \sum_{ij} C_{ij} = \beta \sum_{d=0}^{\infty} \mathcal{N}_d C_d$, where \mathcal{N}_d is the number of points at distance d from a given reference point and scales as $(c - 1)^d$ for large d . Therefore, if C_d decays slower than $(c - 1)^{-d}$, the corresponding susceptibility is divergent. Phase transitions on Bethe lattices are special since they have *diverging susceptibilities and finite correlations lengths*. For finite dimensional lattices, \mathcal{N}_d grows as a power of d , and one needs a diverging correlation length to obtain a diverging susceptibility.

2.5.7 First hints on universality

The phase diagram of the Ising model in $d \geq 2$ shows great similarity with the one of the liquid-gas transition, if one identifies $T \Leftrightarrow T$ and $h \Leftrightarrow P$. In both cases there is a line of first order phase transitions which ends at a critical point, Fig. 2.13. In the particle problem, an appropriate treatment with, e.g., the van der Waals equation, shows that going across the transition curve at constant pressure, the volume V of the liquid/gas jumps discontinuously, and its density behaves and the one of the magnetisation in the Ising model, when crossing the zero field line below T_c .

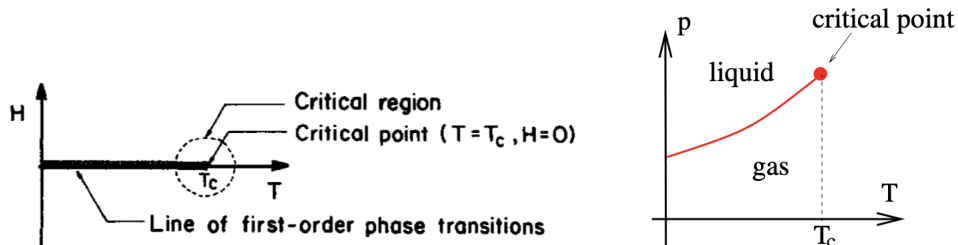


Figure 2.13: The magnetic phase diagram and the pressure-temperature phase diagram for the liquid-gas transition in $d \geq 2$.

The connection between the two problem can be made explicit with the mapping from Ising to occupation variables, $s_i = 2n_i - 1$, with $n_i = 0, 1$, and the creation of a *lattice gas model*.

2.6 Ginzburg-Landau field theory

Landau proposed an extension of Weiss mean-field theory for ferromagnets (Sect. 2.5.5) that has a much wider range of applicability, includes space, and allows to predict when it applies and when it fails with the application of the Ginzburg criterium. Not only that, it also yields critical exponents which depends on the spatial dimension.

2.6.1 The Landau scheme

In a few words, in Landau theory one first identifies the order parameter for the phase transition, that is to say, a quantity with zero average in the disordered phase and non-zero average on the ordered side. Next, one proposes a *field theory* for a *coarse-grained field* that represents the averaged relevant variable – giving rise to the order parameter – over a *mesoscopic scale* ℓ that is, by definition, much larger than the interatomic distance a , $\ell \gg a$, and much shorter than the system size, $L \gg \ell$. In the case of an Ising spin system, the field in each coarse-graining volume $v = \ell^d$ is defined as

$$\phi(\vec{x}) \equiv \frac{1}{\ell^d} \sum_{j \in v_{\vec{x}}} s_j, \quad (2.93)$$

see Fig. 2.14, where \vec{x} is the center of the coarse-graining volume $v_{\vec{x}}$. The *field* ϕ is a discrete variable taking real values in $[-1, 1]$, by steps $\propto \ell^{-d}$, which in the limit $\ell \gg a$ approaches a continuous limit. One can construct a field ϕ that takes a different value per lattice site (using overlapping coarse-graining volumes) in which case the coordinates of the space variable \vec{x} vary by steps of a , the lattice spacing. Instead, one can use non-overlapping coarse-graining volumes in which case the coordinates of the space variable \vec{x} vary by steps of ℓ , the coarse-graining linear size. This is the case shown in Fig. 2.14.

The next step consists in constructing (or proposing) an effective free-energy of the interacting system. One can proceed as for the fully-connected Ising model, where we transformed the sum over the N spin variables into a sum over possible values of an auxiliary variable (which at the saddle-point level becomes the averaged magnetisation) taking into account the associated degeneracy (entropy). In this vein

$$\mathcal{Z} = \sum_{\{s_i = \pm\}} e^{-\beta \mathcal{H}(\{s_i\})} = \sum_{\alpha} e^{-\beta \mathcal{H}_{\alpha}(\{s_i\})} = \int \mathcal{D}\phi \sum_{\alpha/\phi} e^{-\beta \mathcal{H}_{\alpha}(\{s_i\})}. \quad (2.94)$$

The first sum is the partition function definition. The second one runs over all microscopic spin configurations, the *microstates* which we labeled α . The third constrained sum runs over all microstates which are compatible with a certain field value ϕ . The integral is a *functional integral* over all possible realisations of the field:

$$\mathcal{D}\phi = \prod_{\vec{x}} d\phi(\vec{x}). \quad (2.95)$$

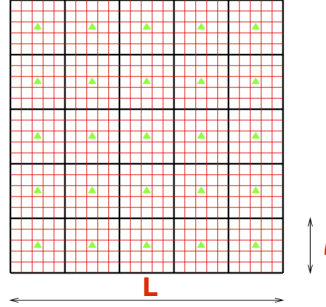


Figure 2.14: Coarse-graining of a square lattice model. In this representation we placed the spins at the centres of the white boxes delimited by the red squares. The black boxes are then the regions over which the spins are averaged to calculate the scalar field. The positions at which the scalar fields are evaluated are the centers of the black boxes, represented by the green dots.

In other words, all values that the field can take at each point in space (it is easier to think about the product as discrete one though in the end we work in continuous space). The factor $\sum_{\alpha/\phi} e^{-\beta \mathcal{H}_\alpha(\{s_i\})}$ is a positive definite function of ϕ . We can then define a *free-energy at fixed field*, $F(\phi)$, using

$$e^{-\beta F(\phi)} \equiv \sum_{\alpha/\phi} e^{-\beta \mathcal{H}_\alpha(\{s_i\})} \quad (2.96)$$

where

$$F(\phi) = -k_B T \ln \sum_{\alpha/\phi} e^{-\beta \mathcal{H}_\alpha(\{s_i\})} . \quad (2.97)$$

The partition function (2.94) becomes

$$\mathcal{Z} = \int \mathcal{D}\phi e^{-\beta F(\phi)} \quad (2.98)$$

and we now have a *statistical field theory* which is described by a functional $F(\phi)$ that plays the rôle of a generalised Hamiltonian.

In general, we do not know how to compute $F(\phi)$. Landau's proposal is to expand $F(\phi)$ in powers of ϕ and its gradients $\vec{\nabla}\phi$ and then determine, depending on the problem at hand, which terms vanish and which among the non-vanishing ones are the most relevant. The first question is answered using *symmetry arguments*. Let us illustrate the argument in the magnetic problem modelled by the Ising model.

- The Hamiltonian under no applied field is *invariant* under simultaneous *reversal of all spins* $s_i \rightarrow -s_i$. The free-energy $F(\phi)$ should then be such that $F(\phi) = F(-\phi)$.
- The Hamiltonian is *local*, in the sense of having only nearest-neighbour interactions. Correlations can only be built through intermediate spins. The same should be true

of the field $\phi(\vec{x})$. In consequence, the free-energy should be local

$$F(\phi) = \int d^d x f[\phi(\vec{x})] \quad (2.99)$$

with $f[\phi(\vec{x})]$ a local function of the field and its spatial derivatives. These gradient terms control how the field at one point affects the field at a neighbouring point.

- The original lattice has a *discrete translation symmetry*. For certain lattices (e.g. a square one) there can also be *discrete rotation symmetries*. At distances much larger than the lattice scale, where the field theory applies, both these symmetries should be preserved.
- One further assumes that the free energy density is an *analytic function* of $\phi(\vec{x})$ and its derivatives, and *Taylor expands* it, for small fields and close to T_c , where the order parameter vanishes for a second order phase transition.
- As already said, the expansion is expected to be valid close to T_c where $\langle \phi \rangle \sim 0$ and then $\phi \sim 0$ too (if ℓ is sufficiently large to avoid large local fluctuations). In this case, one keeps only the *first terms in the power expansion*.
- One restricts attention to situations where $\phi(\vec{x})$ varies rather slowly in space, that it varies appreciably only over distances that are much larger than the distance between boxes. This means that we can also consider a *gradient expansion* of $f[\phi(\vec{x})]$. The terms with high order derivatives, $c'(\nabla^2 \phi)^2$, should then be negligible with respect to the first one, $c\nabla^2 \phi$. Indeed, writing $\phi(\vec{x})$ using a Fourier expansion

$$\phi(\vec{x}) = \sum_{\vec{q}} e^{i\vec{q}\vec{x}} \phi(\vec{q}) \quad (2.100)$$

where the sum runs over wave-vectors that satisfy $q \ll \ell^{-1}$ due to the cut-off introduced by the size of the coarse-graining box (we are here considering non-overlapping boxes, otherwise the condition is $q \ll a^{-1}$). Since $(c'/c)^{1/2}$ is usually of the order of the microscopic interactions, $c'/c \ll \ell^2$, for each q such that $q \ll \ell^{-1}$ one has

$$c'q^4 |\phi(\vec{q})|^2 \ll cq^2 |\phi(\vec{q})|^2. \quad (2.101)$$

Based on the arguments itemised above, for a second order phase transition in the Ising universality class, the Landau free-energy reads

$$F(\phi) = \int d^d x \left[\frac{c}{2} (\nabla \phi(\vec{x}))^2 + \frac{\lambda}{4} \phi^4(\vec{x}) + \frac{a}{2} \frac{T - T_c}{T_c} \phi^2(\vec{x}) \right]. \quad (2.102)$$

The coefficients are hard to compute from first principles and one just uses an intuitive reasoning to fix them. More precisely, the coefficients are *chosen* in such a way to reproduce the continuous transition when going through T_c . The first term mimics an *elastic*

energy related to the ferromagnetic interactions and the condition is $c > 0$. It is clear that it contributes only when the field ϕ varies in space, that is, mostly where there are *domain walls* or *interfaces*. The second term can also be estimated as an expansion, up to fourth order, of the *entropic contribution* in powers of $T - T_c$ that is expected to be valid only close to T_c . The entropic contribution in the fully connected Curie-Weiss model with $p = 2$, see eq. (2.79) combined with the energetic term proportional to J (that is equal to T_c for $p = 2$) leads to exactly this expansion. The prefactor $a/2$ can be added for convenience, to arrange the dimensions of the constants so that

$$\frac{[c][\phi^2]}{[x^2]} = [a][\phi^2] = [\lambda][\phi^4] . \quad (2.103)$$

Note that this ‘order-parameter dependent’ free-energy is not quadratic, and hence non-trivial, due to the term ϕ^4 . The averages can be computed by introducing an applied field and adding the following *source term* to the free-energy,

$$- \int d^d x \, h(\vec{x}) \phi(\vec{x}) , \quad (2.104)$$

and taking the corresponding functional derivatives. The actual values of the parameters in the expansion of the free-energy are not known in general. They are determined by comparison to experiments or from first-principle computations.

The saddle-point equation

If one realises that the free-energy in the exponential is proportional to the volume of the system, the integral over all ϕ configurations in the partition function can be evaluated with a *saddle-point approximation* (expected to be accurate in the limit $V \rightarrow \infty$). This evaluation is what is usually called the *Landau approximation* or *mean-field approximation*. Let us call $\phi_{\text{sp}}(\vec{x})$ the value of the field that renders the exponent minimum, *i.e.* the *state of the system*. Since the elastic term is positive definite, it is simply minimised by a constant field configuration, $\phi_{\text{sp}}(\vec{x}) = \phi_{\text{sp}}$. The parameter dependence of ϕ_{sp} is next determined by the requirement that the ‘*potential energy*’ contribution $V(\phi) = \frac{\lambda}{4}\phi^4 + \frac{a}{2} \frac{(T-T_c)}{T_c} \phi^2$ be minimised (we set $h = 0$). For the *$\lambda\phi^4$ scalar field theory* one finds

$$\lambda\phi_{\text{sp}}^3 + a \frac{T - T_c}{T_c} \phi_{\text{sp}} = 0 \quad (2.105)$$

with solutions $\phi_{\text{sp}} = 0$ (the symmetric or disordered phase) and

$$\phi_{\text{sp}} = \pm \sqrt{\frac{a}{\lambda} \frac{T_c - T}{T_c}} \quad \beta = 1/2 . \quad (2.106)$$

Finally, at this ‘zero-th’ order level, the partition function is

$$\mathcal{Z} \sim e^{-\beta F(\phi_{\text{sp}})} = e^{-\beta L^d v(\phi_{\text{sp}})} \quad (2.107)$$

with

$$V(\phi_{\text{sp}}) = L^d v(\phi_{\text{sp}}) = L^d \left[\frac{\lambda}{4} \phi_{\text{sp}}^4 + \frac{a}{2} \frac{T - T_c}{T_c} \phi_{\text{sp}}^2 \right] = -L^d \frac{a^2}{4\lambda} \left(\frac{T_c - T}{T_c} \right)^2. \quad (2.108)$$

Next we will evaluate the effect of the Gaussian fluctuations and how they can limit the validity of this simple treatment.

The domain walls

The effective free-energy formalism we have just developed includes information about the spatial variation of the order parameter as well. Since there are two degenerate low states below the critical temperature, one can have low lying excitations with *domain walls* between large spatial regions dominated by one and the other of these.

Imagine there is half space with one equilibrium state and the other half with the other, in a system with open boundary conditions, and that the spatial direction along which the field changes is x . Such a configuration is represented by a field that varies from $\phi(-L) = -\phi_{\text{sp}}$ to $\phi(L) = \phi_{\text{sp}}$, where we simplified the notation and we focused on the spatial direction of change, without writing the field dependence on the other ones. Presumably, the variation is continuous and somehow smooth.

The saddle-point equations that keep a possible space variation of the field differs from eq. (2.105) only by the presence of a gradient term:

$$c \frac{d^2 \phi(x)}{dx^2} - \lambda \phi^3(x) - a \frac{T - T_c}{T_c} \phi(x) = 0 \quad (2.109)$$

and the solution is

$$\phi(x) = \phi_{\text{sp}} \tanh \left(\frac{x - x_{\text{dw}}}{W} \right), \quad (2.110)$$

where ϕ_{sp} is given in eq. (2.106), x_{dw} is the position of the domain wall and W its width, fully determined by the field theory parameters,

$$W = \sqrt{\frac{c}{a} \frac{T_c}{T_c - T}}. \quad (2.111)$$

These expressions have the following properties.

- The position of the domain wall is not fixed and it can be anywhere in the sample (recall Peierls argument).
- The approach to the asymptotic values is exponential: the order parameter relaxes exponentially quickly back to the ground state values ϕ_{sp} .
- At $T = 0$ the width W is only determined by the square root of the ratio between the elasticity coefficient c and a , which has dimensions of length as it should, and the larger its value the harder it is to make *sharp* walls.

- at $T \rightarrow T_c$ the width diverges, giving a hint that something different happens at T_c with, actually, a proliferation of interfaces.
- The width of the domain wall is related to the correlation length, ξ , which we will define and calculate below.

Substituting the expression (2.110) in the free-energy one obtains the *cost* of a domain wall. A simple evaluation proves that the cost of a domain wall is not proportional to the volume of the system, but to the area of the domain wall. More precisely, in a system with linear size L , the free energy of the ground state scales as L^d while the additional free energy required by the wall scales only as L^{d-1} :

$$\Delta F = F_{\text{dw}} - F_{\text{sp}} \sim L^{d-1} \sqrt{\frac{c}{a\lambda^4} \left(1 - \frac{T}{T_c}\right)^3}. \quad (2.112)$$

We note that the excess free-energy due to the presence of the domain vanishes at the transition. The free-energy per unit area is called the *surface tension*. This result, together with the fact that the domain walls get thicker and thicker as one approaches the critical point, indicates that large order-parameter fluctuations emerge near the critical point.

These configurations are usually called *topological solutions*. They are determined by the boundary conditions (we imposed different constant saddle points at the ends of the system) and their energy is concentrated in a finite region of space, where the field changes.

Exercise 2.15 Write the saddle-point equation in the form $\ddot{\phi}(x) = V'(\phi)$ with the double dot representing double space derivation, $\ddot{\phi}(x) = d^2\phi(x)/dx^2$. Interpret x as time, and ϕ as the position of a particle. Solve now the differential equation as a mechanical problem in an inverted potential from the one in the Landau theory. Hint: use energy conservation and fix the energy of the particle using the boundary conditions $\phi(x) \rightarrow \pm\phi_{\text{sp}}$ at $x \rightarrow \infty$. Find in this way the domain wall configuration (2.110).

2.6.2 The spatial correlation function

The essential ingredient of the Landau-Ginzburg theory which was lacking in the earlier approach is the existence of spatial structure and correlations. The *connected correlation function* (or cumulant) measures the spatial extent over which a local fluctuation will influence another one. It is defined as

$$C_{\text{conn}}(\vec{x}, \vec{y}) \equiv \langle (\phi(\vec{x}) - \langle \phi \rangle)(\phi(\vec{y}) - \langle \phi \rangle) \rangle = \langle \phi(\vec{x})\phi(\vec{y}) \rangle - \langle \phi \rangle^2 = C(r). \quad (2.113)$$

In statistically homogeneous systems as the ones we are treating here, without $C(\vec{x}, \vec{y})$ is an isotropic and translational invariant correlation, depends only $|\vec{x} - \vec{y}| = |\vec{r}| = r$ and can be computed within the same Landau theory.

Going back to the definition of the averages using the partition function,

$$C_{\text{conn}}(\vec{x}, \vec{y}) = \frac{1}{\beta^2} \frac{\delta^2 \ln \mathcal{Z}_h(\phi)}{\delta h(\vec{x}) \delta h(\vec{y})}. \quad (2.114)$$

where

$$\ln \mathcal{Z}_h = \ln \int \mathcal{D}\phi e^{-\beta F(\phi)} e^{\beta \int d^d x h(\vec{x})\phi(\vec{x})} \Big|_{h=0}, \quad (2.115)$$

with $F(\phi)$ the Landau free-energy functional in eq. (2.102) and the source term in eq. (2.104) having been added.

If one works close to the phase transition, the averaged field is close to zero and one neglects, for this calculation, the quartic term in F . The total free-energy is, then, a simpler quadratic functional of ϕ .

The only difficulty to calculate the functional sum over the field configurations is posed by the gradient term. To deal with it, one Fourier transforms the fields,

$$\phi(\vec{k}) = \int d^d x e^{i\vec{k}\cdot\vec{x}} \phi(\vec{x}) \quad (2.116)$$

where, to make the notation simpler, we do not add a tilde to the wave-vector dependent, Fourier transformed, field. Since the scalar field $\phi(\vec{x})$ is real, the field $\phi(\vec{k})$ is complex, with $\phi(-\vec{k}) = \phi^*(\vec{k})$, so there is no doubling of degrees of freedom.

After some straightforward manipulations,

$$\begin{aligned} F_h(\phi) &= \int \frac{d^d k}{(2\pi)^d} \left[\frac{c}{2} k^2 \phi(\vec{k}) \phi(-\vec{k}) + \frac{a}{2} \frac{T - T_c}{T_c} \phi(\vec{k}) \phi(-\vec{k}) - h(\vec{k}) \phi(-\vec{k}) \right] \\ &= \int \frac{d^d k}{(2\pi)^d} \left[\frac{c}{2} k^2 |\phi(\vec{k})|^2 + \frac{a}{2} \frac{T - T_c}{T_c} |\phi(\vec{k})|^2 - h(\vec{k}) \phi^*(\vec{k}) \right] \end{aligned} \quad (2.117)$$

and the function integral $\mathcal{D}\phi(\vec{x}) = \prod_{\vec{x}} d\phi(\vec{x})$ is transformed into another one over the complex functions $\phi(\vec{k})$,

$$\mathcal{D}\phi(\vec{k}) = \prod'_{\vec{k}} d\phi(\vec{k}) d\phi^*(\vec{k}), \quad (2.118)$$

where the prime indicates that $\phi(\vec{k})$ and $\phi^*(\vec{k})$ are related *via* $\phi(-\vec{k}) = \phi^*(\vec{k})$.

In order to separate the ϕ dependence from the h one, it is convenient to redefine the fields with a translation

$$\varphi(\vec{k}) \equiv \phi(\vec{k}) - \frac{h(\vec{k})}{ck^2 + a(T - T_c)/T_c}. \quad (2.119)$$

The Landau free-energy becomes

$$F_h(\varphi) = \int \frac{d^d k}{(2\pi)^d} \left[\frac{c}{2} k^2 |\varphi(\vec{k})|^2 + \frac{a}{2} \frac{T - T_c}{T_c} |\varphi(\vec{k})|^2 - \frac{1}{2} \frac{|h(\vec{k})|^2}{ck^2 + a(T - T_c)/T_c} \right] \quad (2.120)$$

and the partition function is

$$\mathcal{Z}_h = \int \mathcal{D}\varphi e^{-\beta F_h(\varphi)} = A \exp \left[\frac{\beta}{2} \int \frac{d^d k}{(2\pi)^d} \frac{|h(\vec{k})|^2}{ck^2 + a(T - T_c)/T_c} \right] \quad (2.121)$$

where A is a Gaussian integral which does not depend on the source h and will not contribute to the variations in eq. (2.114). By reverting the Fourier transform, this expression can be rewritten as

$$\mathcal{Z}_h = A \exp \left[\frac{\beta}{2} \int d^d \vec{x} d^d \vec{y} h(\vec{x}) G(\vec{x} - \vec{y}) h(\vec{y}) \right] \quad (2.122)$$

with

$$G(\vec{x} - \vec{y}) = \int \frac{d^d k}{(2\pi)^d} \frac{e^{-i\vec{k} \cdot \vec{x}}}{ck^2 + a(T - T_c)/T_c} = \frac{1}{c} \int \frac{d^d k}{(2\pi)^d} \frac{e^{-i\vec{k} \cdot \vec{x}}}{k^2 + \xi^{-2}} \quad (2.123)$$

with the *correlation length*

$$\xi^{-2} \equiv \frac{a(T - T_c)}{c T_c} . \quad (2.124)$$

Now, the direct calculation of the variations with respect to $h(\vec{x})$ and $h(\vec{y})$ yields

$$C^{\text{conn}}(\vec{x}, \vec{y}) = k_B T G(\vec{x} - \vec{y}) . \quad (2.125)$$

The calculation of the integral over Fourier modes proceeds with a trick:

$$\frac{1}{k^2 + \xi^{-2}} = \int_0^\infty du e^{-u(k^2 + \xi^{-2})} . \quad (2.126)$$

Thus,

$$\begin{aligned} G(\vec{x} - \vec{y}) &= \frac{1}{c} \int \frac{d^d k}{(2\pi)^d} e^{-i\vec{k} \cdot \vec{x}} \int_0^\infty du e^{-u(k^2 + \xi^{-2})} \\ &= \frac{1}{c} \int_0^\infty du e^{-r^2/(4u)} e^{-u/\xi^2} \int \frac{d^d k}{(2\pi)^d} e^{-u(\vec{k} + i\vec{x}/(2u))^2} \\ &\propto \frac{1}{c} \int_0^\infty du u^{-d/2} e^{-r^2/(4u)} e^{-u/\xi^2} \end{aligned} \quad (2.127)$$

with $r = |\vec{x}|$. The last integral to be performed can be put in the form of a Bessel function. More practically, one can estimate its long r behaviour by using a saddle-point evaluation,

$$I = \int_0^\infty du u^{-d/2} e^{-r^2/(4u)} e^{-u/\xi^2} = \int_0^\infty du e^{-r^2/(4u) - u/\xi^2 - (d/2) \ln u} = \int_0^\infty du e^{-S(u)} \quad (2.128)$$

with $S(u) = r^2/(4u) + u/\xi^2 + (d/2) \ln u$ and

$$I \sim e^{-S(u_{\text{sp}})} (S''(u_{\text{sp}}))^{-1/2} = e^{-S(u_{\text{sp}}) - \frac{1}{2} \ln S''(u_{\text{sp}})} . \quad (2.129)$$

The saddle point equation is

$$S'(u_{\text{sp}}) = -\frac{r^4}{4u_{\text{sp}}^2} + \frac{1}{\xi^2} + \frac{d}{2} \frac{1}{u_{\text{sp}}} = 0 \quad (2.130)$$

and its relevant solution

$$u_{\text{sp}} = \frac{\xi^2}{2} \left(-\frac{d}{2} + \sqrt{\frac{d^2}{4} + \frac{r^2}{\xi^2}} \right). \quad (2.131)$$

The second derivative of S which determines the stability of the saddle point and the Gaussian corrections is

$$S''(u) = \frac{r^2}{2u^3} - \frac{d}{2u^2}. \quad (2.132)$$

One can now distinguish two limits:

- For $r \gg \xi$, $u_{\text{sp}} \sim r\xi/2$, $S(u_{\text{sp}}) \sim -r/\xi$, $S''(u_{\text{sp}}) \sim 4/r\xi^3$ and

$$G(r) \sim e^{-r/\xi} \quad (2.133)$$

where we just kept the leading exponential decay (and neglect the Gaussian correction that contributes a power law correction).

- For $r \ll \xi$, $u_{\text{sp}} \sim r^2/(2d)$, $S(u_{\text{sp}}) = \frac{d}{2} + \frac{1}{2d} \frac{r^2}{\xi^2} + \frac{d}{2} \ln(r^2/2d) \sim d \ln r$, $S''(u_{\text{sp}}) = 2d^3/r^4$ and

$$G(r) \sim e^{-d \ln r - \frac{1}{2} \ln(2d^3/r^4)} \sim e^{-d \ln r + 2 \ln r} \sim r^{2-d}. \quad (2.134)$$

The crossover is controlled by the correlation length which behaves as

$$\xi \sim |T - T_c|^{-\nu} \quad \nu = 1/2. \quad (2.135)$$

Right at the critical point $\xi \rightarrow \infty$, $r \ll \xi$, and

$$G(r) \sim r^{2-d-\eta} \quad \eta = 0. \quad (2.136)$$

Within the quadratic treatment of the Landau theory, the exponent η vanishes but we will see that in improved treatments it will take a non-vanishing value.

Putting these results together,

$$\boxed{C_{\text{conn}}(r) \sim r^{2-d-\eta} e^{-r/\xi}, \quad \xi \sim |T_c - T|^{-\nu},} \quad (2.137)$$

which includes the $r \ll \xi$ power law behaviour and the $r \gg \xi$ exponential decay in a single formula.

2.6.3 Ginzburg criterium

Including the contribution of the *Gaussian fluctuations* to the saddle-point evaluation one can see when these become too important and render the saddle-point method invalid. This analysis is called the *Ginzburg criterion* [20] and tells us that there is an upper critical dimension,

$$d_u = 4 \quad (2.138)$$

above which the mean-field description of the ferromagnetic transition is *exact!* Below d_u mean-field theory fails. However, it does not fail everywhere in parameter space. It just fails when very close to the critical point, in a system-dependent *critical region*. The behaviour away from the critical region is still well-described by the Landau-Ginzburg phenomenological theory. A signature of the failure of the Landau-Ginzburg theory is that it predicts the mean-field exponents in (2.162) for all d which is clearly incorrect for small d .

In just a bit more detail, the Ginzburg criterium states that the Landau mean-field theory breaks down when

$$\langle \delta\phi_{coh}^2 \rangle \sim \langle \phi \rangle^2 \quad (2.139)$$

where

$$\delta\phi_{coh} \equiv V_{coh}^{-1} \int d^d x (\phi(\vec{x}) - \langle \phi \rangle), \quad (2.140)$$

$V_{coh} = \xi^d$ with ξ the coherence length, defined in the previous subsection, and $\langle \phi \rangle$ the equilibrium order parameter within the same approximation, that is

$$\langle \phi \rangle = \phi_{sp} \propto |T - T_c|^{1/2} \propto \xi^{-1}. \quad (2.141)$$

The left-hand-side in (2.139) is

$$\langle \delta\phi_{coh}^2 \rangle = V_{coh}^{-1} \int d^d r C_{conn}(r) \quad (2.142)$$

where C_{conn} is the connected correlation function

$$C_{conn}(\vec{x}, \vec{y}) \equiv \langle (\phi(\vec{x}) - \langle \phi \rangle)(\phi(\vec{y}) - \langle \phi \rangle) \rangle = \langle \phi(\vec{x})\phi(\vec{y}) \rangle - \langle \phi \rangle^2 = C_{conn}(r). \quad (2.143)$$

$C_{conn}(\vec{x}, \vec{y})$ is an isotropic and translational invariant correlation, depends only $|\vec{x} - \vec{y}| = |\vec{r}| = r$ and can be computed within the same Landau theory and compared to the right-hand-side of the same eq. (2.139), that is simply $\langle \phi \rangle^2 = \phi_{sp}^2 \sim \xi^{-2}$, a vanishing quantity. Using the critical scaling form of $C_{conn}(r)$ with $\eta = 0$ (derived in the previous subsection) one has

$$\langle \delta\phi_{coh}^2 \rangle \sim \frac{\Omega_d}{\xi^d} \int_a^\xi dr r^{d-1} r^{2-d-\eta} e^{-r/\xi} = \frac{\Omega_d}{\xi^{d-2}} \int_a^\xi d\left(\frac{r}{\xi}\right) \frac{r}{\xi} e^{-r/\xi} = \frac{\Omega_d}{\xi^{d-2}} A \quad (2.144)$$

with A a finite constant. Therefore, the condition becomes

$$\xi^{2-d} \ll \xi^{-2} \quad \implies \quad \boxed{\xi^{4-d} \ll 1} \quad (2.145)$$

which for $d > 4$ is verified while for $d \leq 4$ it is not and the approximation fails.

Landau theory, thus, establishes its own limits of validity: it is valid until the fluctuations of the order parameter become of the order of the order parameter itself when both are coarse-grained over a volume determined by the correlation length.

2.6.4 First order phase transitions

The Landau approach can be adapted to capture first order phase transitions too. The potential in the free energy functional is chosen in such a way to yield a discontinuous order parameter when a control parameter is changed. This can be achieved in a non-symmetric, or in a symmetric way, similarly to what we discussed in the context of the p -spin Ising model. We will discuss some aspects of first order phase transitions in Sec. 2.12.

2.6.5 Two applications

In the Ψ -theory of superconductivity that got Ginzburg the 2003 Nobel Prize a scalar complex field Ψ is the order parameter and it is coupled to a vector electromagnetic field potential \vec{A} . A link between Bardeen-Cooper-Schrieffer's microscopic theory of superconductivity and the Landau-Ginzburg phenomenological model can be established.

In high energy applications the field theory is usually postulated. The so-called $\lambda\phi^4$ theories are standard ones in which the field is a complex variable and the Lagrangian density reads

$$L(\phi) = \partial_\mu \phi^* \partial^\mu \phi - \alpha \phi^* \phi - \frac{1}{2} \lambda (\phi^* \phi)^2 \quad (2.146)$$

with $\alpha > 0$ or $\alpha < 0$ on the two sides of the transition. Many other field theories with more complex fields (vectorial, tensorial) are also possible.

2.6.6 Summary

A field for the magnetisation can be rather simply derived by coarse-graining the spins over a coarse-graining length ℓ . This simply amounts to computing the averaged spin on a box of linear size ℓ . In the limit $\ell \gg a$ where a is the lattice spacing many spins contribute to the sum. For instance, an Ising bimodal variable is thus transformed into a continuous real variable taking values in $[-1, 1]$. Studying the problem at long distances with respect to ℓ (or else taking a continuum spatial limit) the problem transforms into a *statistical field theory*, which one guesses based on symmetry and simplicity arguments. This is the route followed by Landau.

Figure 2.15 taken from [3] summarises the two scenarii corresponding to second order (the panels in the first row) and first order phase transitions (the next six panels). The figures show the evolution of the free-energy density as a function of the order parameter, called η here, when temperature (called T in the first three panels and t in the next six ones) is modified.

The order parameter is determined by a saddle-point equation which typically takes the form $x =$ a sigmoid function. The difference between *second order* and *first order* transitions is the way in which the sigmoid function changes when the control parameter is modified.

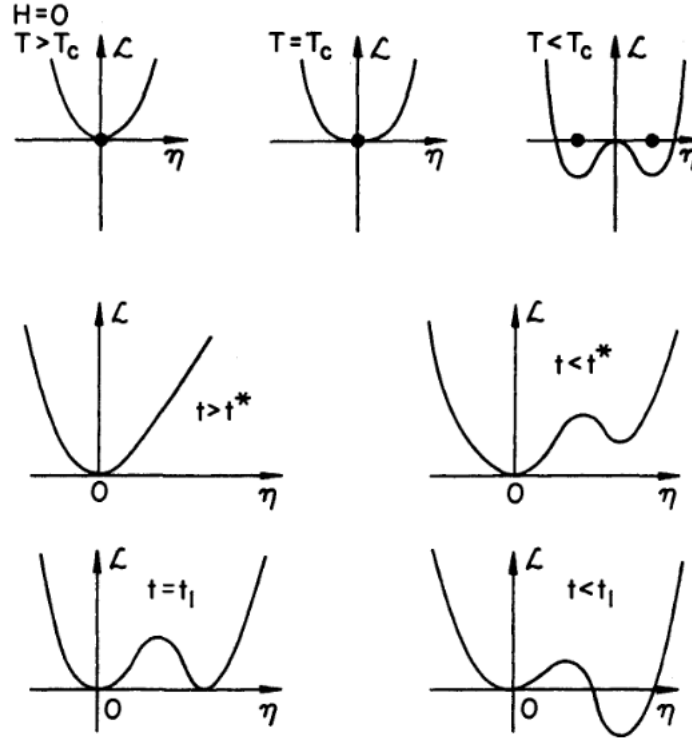


Figure 2.15: Second order (first line) and first order (second and third lines) phase transitions. Figures taken from [3].

- In a second order phase transition the non-vanishing solutions split from the vanishing one in a continuous way. A possible strategy to find the critical parameters is, then, to look for the values at which the slope of the sigmoid function close to zero equals one. The macroscopic order parameter describes the character and strength of the broken symmetry.
- In a first order phase transition the sigmoid function touches the diagonal axis at a non-vanishing value when the local minimum at $x \neq 0$ first appears. Further changing the parameters this point splits in two and the sigmoid function crosses the diagonal at three points, say $x = 0$, x_1 (a maximum of the free-energy density) and x_2 (the non-zero minimum of the free-energy function). Other two crossings are symmetrically placed on $x < 0$ values if the model is invariant under $x \mapsto -x$.

In a second order phase transition a new state of reduced symmetry, lower than the one of the Hamiltonian, develops continuously from the disordered (high temperature) phase. This is the phenomenon of spontaneously broken symmetry. There will therefore be a number (sometimes infinite) of equivalent (e.g. equal free energy) symmetry related states. These are macroscopically different, and thermal fluctuations will not connect one to another in the thermodynamic limit.

Landau (1962) and Ginzburg (2003) got Nobel Prizes in Physics for their work along these lines (Landau on superfluidity, Ginzburg on superconductors and superfluids). The strategy of Ginzburg and Landau proved to be very useful to describe phase transitions of very different type using, as a starting point, the identification of the order parameter and a proposal for the field theory describing the physical problem one is interested in. It is particularly well-suited for problems with *long-range interactions* such as superconductors and ferroelectrics since in these cases fluctuations are suppressed.

Field theories are the natural tool to describe *particle physics and cosmology*. For example, the *Big Bang* leaves a radiation-dominated universe at very high temperature close to the Planck scale. As the initial fireball expands, temperature falls precipitating a sequence of phase transitions. The exact number and nature of these transitions is not known. It is often considered that they are at the origin of the structures (galaxies, clusters, *etc.*) seen in the universe at present, the original seeds being due to density fluctuations left behind after the phase transition. The similarity between the treatment of *condensed matter* problems and *high energy physics* becomes apparent once both are expressed in terms of field theories. It is however often simpler to understand important concepts like spontaneous symmetry breaking in the language of statistical mechanics problems.

Some traditional examples

We have discussed the ferromagnetic Ising model and its scalar field theory representation. There are many physical examples in which the order parameters are not as simple. Examples are:

- Anti-ferromagnets, with the staggered magnetisation $\sum_i (-1)^i s_i$.
- Heisenberg ferromagnets, with vector order parameter $\sum_i \vec{s}_i$ (the XY case in two-dimensions is special and we will discuss it later).
- Solids in three dimensions have broken translational and rotational symmetries, and a convenient order parameter is the amplitude of the density wave. (The melting transition in two dimensions is highly non-trivial.)
- Nematic liquid crystal are formed by long molecules which align parallel to one another at low temperatures, although the position of the molecules remains disorder as in a liquid. The liquid becomes anisotropic, and a second rank tensor characterises the strength of the anisotropy and can be used as the order parameter.

Problems and remarks

The exponents in the mean-field approximation and Landau scalar field theory do not depend on the dimension d of space.

The development of *series expansions* in the 50s (and more recently with the help of computers) derived Ising model exponents which were consistent with independency from the lattice structure, but strong dependence on the spatial dimension. Evidence in favour

of the universal, though space-dimensional dependent, exponents also began to mount from experiments during the same period and later.

2.7 Critical phenomena and scaling

The notion of *universality* was originally introduced by experimentalists to describe the observation that several apparently unrelated physical systems were characterised by the same type of singular behaviour near a continuous phase transition. It implies that the emerging long-range correlations of fluctuations of the order parameter are fully specified by the symmetry properties and conservation laws and do not depend on the details of the microscopic interactions (or microscopic dynamics).

2.7.1 Some general definitions

Correlation functions yield a very useful way to characterise phases and phase transitions. The two-point spatial correlation measures how much the fluctuation of the local (say, scalar) order parameter $O(\vec{x})$ around its averaged value influences the same quantity at a given distance within the system:

$$C(\vec{x}, \vec{y}) = \langle (O(\vec{x}) - \langle O(\vec{x}) \rangle) (O(\vec{y}) - \langle O(\vec{y}) \rangle) \rangle . \quad (2.147)$$

The averages $\langle O(\vec{x}) \rangle$ and $\langle O(\vec{y}) \rangle$ are not expected to depend on the space points \vec{x} and \vec{y} in a homogeneous system but, for completeness, we keep this potential dependence in the notation used. These are also called *connected correlation functions*. In the disorder phase the order parameter vanishes and connected and normal correlation functions coincide. In the ordered phase this is not the case. In cases with *translational invariance* the correlation function can depend on the distance vector between the two measuring points $\vec{x} - \vec{y}$ only; if furthermore there is *isotropy*, the correlation function can only depend on the distance between the two measuring points $r \equiv |\vec{x} - \vec{y}|$. One can define higher order correlation functions with products involving more terms but, usually, it is not needed to study them to understand the global behaviour of the system.

(In models with no order parameter, such as the $2d$ XY model to be studied later, the correlation function of the would-be order parameter still yields relevant information about the systems behaviour.)

Close to a continuous phase transition, in an infinite size system, $L \rightarrow \infty$, a two-point correlation function should behave as

$$C(\vec{x}, \vec{y}) \simeq r^{2-d-\eta} f\left(\frac{r}{\xi}\right) \quad \text{with} \quad \begin{cases} f(0) = 1 , \\ f(x \rightarrow \infty) \sim x^\eta e^{-x} . \end{cases} , \quad (2.148)$$

with ξ the *correlation length*, and the only relevant length scale. This expression is integrable over the full volume unless the exponential factor disappears. This is indeed what happens at T_c where the correlation length ξ diverges, according to

$$\xi \simeq |T - T_c|^{-\nu} \quad (2\text{nd order}) , \quad \xi \simeq e^{c|T - T_c|^{-\nu}} \quad (\infty \text{ order}) . \quad (2.149)$$

We will discuss the meaning of the *anomalous exponent* η , and the infinite order case, later.

Time-delayed correlation functions characterise the temporal de-correlation of equilibrium fluctuations. The equal space, time delayed connected correlations are defined as

$$C(\vec{x}; t, t') = \langle (O(\vec{x}, t) - \langle O(\vec{x}, t) \rangle) (O(\vec{x}, t') - \langle O(\vec{x}, t') \rangle) \rangle. \quad (2.150)$$

In a *stationary state*, one-time quantities are independent of absolute time $\langle O(\vec{x}, t) \rangle \rightarrow \langle O(\vec{x}) \rangle$ and two-time quantities depend upon the time difference only. In an equilibrium homogeneous state the space point dependence should drop-off. Putting all this together, close to criticality one expects

$$C(\vec{x}; t, t') \simeq C(t - t') \simeq |t - t'|^{(2-d-\eta)/z} e^{-|t-t'|/\tau} \quad (2.151)$$

with z the dynamic critical exponent and τ the *correlation time*. In second order cases, the correlation length and correlation time are linked by

$$\xi \simeq \tau^{1/z}. \quad (2.152)$$

In infinite order cases the relation is expected to be exponential.

In experiments it is often easier to measure *linear response functions* instead of correlation functions. The linear response of the local observable $O(\vec{x})$ is defined as

$$\chi(\vec{x}, \vec{y}) = \left. \frac{\delta \langle O(\vec{x}) \rangle_h}{\delta h(\vec{y})} \right|_{h=0} \quad (2.153)$$

where the infinitesimal perturbation $h(\vec{y})$ is applied linearly to the same observable O in such a way that the Hamiltonian of the system is modified as $H \mapsto H - \int d^d x h(\vec{x}) O(\vec{x})$. The notation $\langle \dots \rangle_h$ indicates that the average has to be calculated in the presence of the field, that is to say, with the perturbed Hamiltonian.

A simple calculation yields the *fluctuation-dissipation theorem*

$$\chi(\vec{x}, \vec{y}) = \beta (\langle O(\vec{x}) O(\vec{y}) \rangle - \langle O(\vec{x}) \rangle \langle O(\vec{y}) \rangle) \quad (2.154)$$

where all averages in the right-hand-side are measured with no applied field. This is a model independent relation since it does not depend on the form of the Hamiltonian H and only relies on the assumption of equilibrium. β is the inverse temperature $\beta = 1/(k_B T)$.

Exercise 2.16 Prove eq. (2.154) assuming equilibrium in the canonical ensemble.

Exercise 2.17 Prove that for an Ising model the spin susceptibility of a single spin to a field coupled to itself is bounded from below and found its bound.

In a homogenous case one expects $\chi(\vec{x}, \vec{y}) = \tilde{\chi}(\vec{r})$ with $\vec{r} = \vec{x} - \vec{y}$. If the problem is furthermore isotropic then $\chi(\vec{x}, \vec{y}) = \tilde{\chi}(r)$ with $r = |\vec{x} - \vec{y}|$. In the following, we will not write the tilde keeping in mind that the two functions are different. Under these

assumptions, the integration of the susceptibility or linear response over the full space reads

$$\int d^d x \int d^d y' \chi(\vec{x}, \vec{y}) = V \Omega_d \int dr r^{d-1} \chi(r) = V \Omega_d \beta \int dr r^{d-1} C_{\text{conn}}(r) , \quad (2.155)$$

where V is the volume, Ω_d is the angular volume of the d dimensional space, and we used the fluctuation-dissipation relation (2.154) to introduce the connected correlation function in the last identity. If we now use the critical scaling form of the connected correlation function, eq. (2.148),

$$\begin{aligned} (V \Omega_d)^{-1} \int d^d x \int d^d y \chi(\vec{x}, \vec{y}) &= \beta \int_a^L dr r^{d-1} r^{2-d-\eta} e^{-r/\xi} \\ &= \beta \xi^d \xi^{d-1} \xi^{2-d-\eta} \int_{a/\xi}^{L/\xi} du u^{d-1} u^{2-d-\eta} e^{-u} \\ &= \beta c(L/\xi, a/\xi) \xi^{2-\eta} . \end{aligned} \quad (2.156)$$

where $c(L/\xi, a/\xi)$ is the value of the last integral. In the infinite size limit, $L/\xi \rightarrow \infty$, taking also the limit $a/\xi \rightarrow 0$, $c(L/\xi, a/\xi)$ reaches a constant and the integrated susceptibility diverges with the correlation length at the critical point since, in general, $\eta < 2$.

2.7.2 Critical exponents & universality

When studying the observables close to the critical point one realises that they depend on the distance from the critical point in the form of power laws

$$X \sim \theta^n \quad (2.157)$$

where X is the observable, θ the distance to criticality and $n > 0$ the exponent. It is clear that these exponents measure the *strength of the singularity* at the critical point in the sense that all derivatives $d^m X / d\theta^m$ with $m > n$ diverge for $\theta \rightarrow 0$, and the smaller the n the sooner this happens.

Let us focus on a magnetic case and use its natural notation. In zero field the order parameter increases as

$$m \sim (T_c - T)^\beta \quad (2.158)$$

with β one critical exponent (not related to inverse temperature!). At T_c and as a function of the conjugate field,

$$m \sim h^{1/\delta} . \quad (2.159)$$

The divergence of the linear susceptibility at T_c is characterised by two exponents

$$\chi \sim \begin{cases} (T - T_c)^{-\gamma} & T > T_c , \\ (T_c - T)^{-\gamma'} & T < T_c . \end{cases} \quad (2.160)$$

The specific heat also diverges at T_c :

$$C_V \sim \begin{cases} (T - T_c)^{-\alpha} & T > T_c, \\ (T_c - T)^{-\alpha'} & T < T_c. \end{cases} \quad (2.161)$$

While the values of T_c are material dependent, all ferromagnetic transitions of systems in $d = 3$ with an order parameter of the same dimensionality, and the same *symmetries*, could be described by the same – within error bars – critical exponents! This feature indicated the existence of *universality classes*, *i.e.* groups of systems for which the details of the microscopic interactions do not matter, and whose macroscopic critical behaviour is identical.

We recall that we have already calculated the exponents in the naive mean-field approximation for any d or, equivalently, for the fully connected ferromagnetic model with $p = 2$ (Curie Weiss), and in the Landau scalar field theory. They read

$$\alpha = \alpha' = 0, \quad \beta = \frac{1}{2}, \quad \gamma = \gamma' = 1, \quad \delta = 3, \quad \eta = 0, \quad \nu = \frac{1}{2}, \quad (2.162)$$

and are independent of d . η and ν are exponents characterizing the correlation function and the correlation length that we defined in (2.148) and (2.149). These values are to be confronted to the experimental ones. In ferromagnetic phase transitions with Ising symmetry they are given in Table 2 in dimensions $d = 2$ and $d = 3$ and they are compared to the mean-field values.

Name	n	d	β	$\alpha = \alpha'$	$\gamma = \gamma'$	δ	ν	η	
Ising	1	2	1/8	0	7/4	15	1	1/4	exact
Ising	1	3	0.325	0.11	1.24	4.82	0.63	0.032	approx
Ising	1	$d \geq 4$ (MF)	1/2	0	1	3	1/2	0	exact
XY	2	3	0.33	0	1.33	5	0.66	0	approx
Heisenberg	3	3	0.35	-0.14	1.4	5	0.7	0.04	approx
$O(n)$	10	3	0.44	-0.61	1.72		0.87	0.025	approx
$O(n)$	$n \rightarrow \infty$	3	1/2	-1	2		1	0	exact

Table 2: Critical exponents in various universality classes. n is the dimension of the order parameter, *i.e.* the number of components of the spin. d is the dimension of real space. $d=1$ for Ising and $d_l = 2$ for Heisenberg. $d_u = 4$ in both cases.

The fact that very different systems share the same critical properties, the mere existence of universality classes, suggested that it should be possible to describe critical behaviour within a unique framework. The fact that the mean-field critical exponents were slightly different from the ones observed was not very important as a quantitative disagreement but it was from a fundamental point of view. Something important was going on and called for an explanation.

In the rest of this Subsection we introduce and discuss the concepts that allowed one to acquire a qualitative and quantitative understanding of critical phenomena. The ideas and methods introduced actually go beyond this problem and have been exported to other situations like dynamical processes in and out of equilibrium.

2.7.3 The correlation length

Let us go back to the analysis of spatial correlation functions and the the very important concept of correlation length.

Discussion

The correlation length is the distance over which the *fluctuations* of the microscopic degrees of freedom are significantly correlated.

A simple way to understand its meaning is the following. Take a macroscopic sample and measure some macroscopic observable under some external conditions, *i.e.* temperature T and pressure P . Now, repeat the measurement after cutting the sample in two pieces and keeping the external conditions unchanged. The result for the macroscopic observable is the same. Repeating this procedure, one finds the same result until the system size reaches the correlation length of the material.

When the correlation length is finite, a fluctuation within a region of length ξ has no effect outside of it. There is a separation of length-scales. When describing the system at a short length scale, $a \ll r \ll \xi$, the other boxes act as constant parameters with respect to the chosen one. At a longer length scale, $\xi \ll r$, the microscopic details enter only through average values like the mean density or the averaged magnetisation.

Systems with finite correlation lengths look uniform, that is to say, they are statistically translational invariant over distances $r \gg \xi$. The measurement of any observable on different boxes of linear size r is Gaussian distributed about its mean and the variance decreases with r/ξ (due to the central limit theorem). Global measurements do not reflect the microscopic details.

At finite temperature, no system is fully ordered. There are *droplets* of the wrong phase within the correct one, due to *thermal agitation*. The size of these droplets will be a function of temperature and at a given instant, a snapshot of the system reveals the existence of a number of them with different sizes. One expects though that they have a well-defined average (taken, for instance, over different snapshots taken at different times).

The average size of the thermally agitated droplets can be taken as a qualitative indication of the value of the correlation length.

(We will give a more precise definition below.) Consequently

Systems with diverging correlation length have fluctuations, or droplets, of all sizes.

These systems are no longer translational invariant over any finite length scale. Instead, they are *scale invariant* under simultaneous rescaling of the quantities of interest and the length. There is a *self-similar* structure and if one looks at it with different microscopes one essentially sees the same. A localised fluctuation has an effect over the whole system and no subsystem is statistically independent of the others. Still, knowledge of the behaviour at a given scale allows one to derive what happens at all scales through the *scaling transformation*.

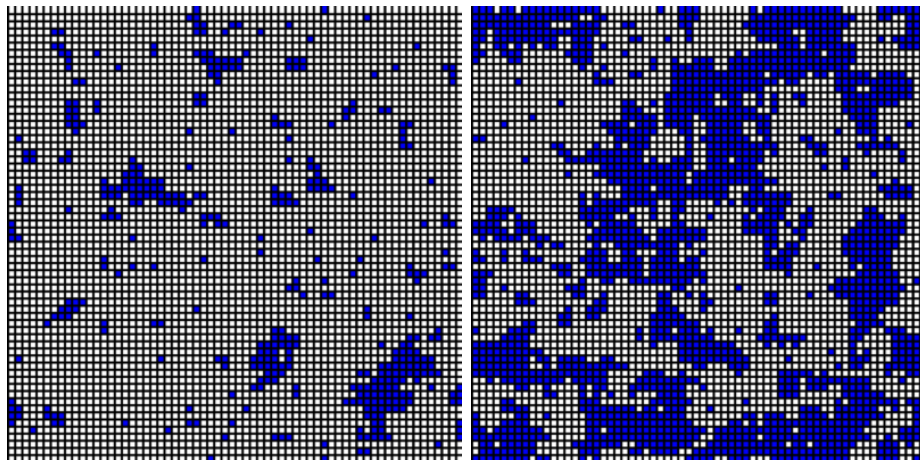


Figure 2.16: Two snapshots of an equilibrium spin configuration in a $2d$ Ising model, one below T_c (left) and on at T_c (right).

The fact that one finds coherent structures at all lengths at the critical point means that there is no spatial scale left in the problem and then all scales participate in the critical behaviour.

In second order phase transitions, the correlation length is usually very short, of the order of a few lattice spacing, at low temperature. It increases when approaching T_c from below, it diverges at T_c , and then decreases again in the high temperature phase when getting away from the critical point, see Fig. 2.16 for two snapshots of the $2d$ Ising model, one well in the ordered phase and the other one at the critical point which illustrate these properties.

Whether fluctuations influence the critical behaviour depends on the space dimensionality d . In general, fluctuations become less important with increasing dimensionality. In sufficiently low dimensions, *i.e.* at and below the *lower critical dimension* d_l , $d \leq d_l$, fluctuations are so strong that they completely destroy the ordered phase at all (nonzero)

temperatures and there is no finite temperature phase transition. Between d_l and the *upper critical dimension* d_u , order at low temperatures is possible, there is a finite temperature phase transition, and the critical exponents are influenced by fluctuations (and depend on d). Finally, for $d > d_u$, fluctuations are unimportant for the critical behaviour, and this is well described by mean-field theory. The exponents become independent of d and take their mean-field values. For example, for Ising ferromagnets, $d_l = 1$ and $d_u = 4$ and for Heisenberg ferromagnets $d_l = 2$ and $d_u = 4$.

In first order phase transition the correlation length is finite for all values of the parameters.

An example: the Ising chain

Let us discuss the correlation length in a simple solvable case, the Ising model in $d = 1$ with, say, open boundary conditions. In this case, the finite temperature connected correlation function equals the normal correlation since

$$C_{kl}^{\text{conn}} = \langle s_k s_l \rangle - \langle s_k \rangle \langle s_l \rangle = \langle s_k s_l \rangle = C_{kl} \quad (2.163)$$

since $\langle s_k \rangle = 0$ at any $T > 0$. Introducing, for convenience, different coupling constants $K_i = \beta J_i$ on the links, C_{kl} reads

$$C_{kl} = \mathcal{Z}^{-1} \sum_{\{s_i = \pm 1\}} e^{\sum_i K_i s_i s_{i+1}} s_k s_l = \mathcal{Z}^{-1} \frac{\partial}{\partial K_k} \frac{\partial}{\partial K_{k+1}} \cdots \frac{\partial}{\partial K_{l-1}} \mathcal{Z} . \quad (2.164)$$

At the end of the calculation one takes $K_i = K = \beta J$ for all i . Thus, at finite temperature the connected correlation between any two spins can be computed as a number of derivatives (depending on the distance between the spins) of the partition function conveniently normalised. Using the change of variables $\eta_i = s_i s_{i+1}$, one finds

$$\mathcal{Z} = \sum_{\{\eta_i = 1\}} e^{\sum_i K_i \eta_i} = 2 \prod_{i=1}^{N-1} 2 \cosh(K_i) \rightarrow 2(2 \cosh \beta J)^{N-1} . \quad (2.165)$$

Taking the distance between the chosen spins s_k and s_l to be $r_k - r_l = r$ the correlation function is then given by

$$C(r) = [\tanh(\beta J)]^r = e^{r \ln[\tanh(\beta J)]} = e^{-r/\xi} \quad (2.166)$$

with

$$\xi = \frac{1}{\ln \coth(\beta J)} \quad \text{and} \quad \xi \sim e^{4J/(T-T_c)} \quad \text{at} \quad T \sim 0 . \quad (2.167)$$

In this one dimensional example we found an *essential singularity*, an exponential divergence, of the correlation length when approaching $T_c = 0$ from above. In general, in higher d , one has a power law divergence.

2.7.4 Droplet theory

The droplet theory, developed by M. E. Fisher building upon previous attempts, is based on an approximation of the full partition sum, in which it is written as a sum over droplet excitations on top of the ground state.

Domain-wall stiffness

Ordered phases resist spatial variations of their order parameter. This property is called *stiffness* or *rigidity* and it is absent in high-temperature disordered phases.

More precisely, in an ordered phase the *free-energy cost* for changing one part of the system with respect to another part far away is proportional to $k_B T$ and usually diverges as a power law of the system size. In a disordered phase the information about the reversed part propagates only a finite distance (of the order of the correlation length, see below) and the stiffness vanishes.

Concretely, the free-energy cost of installing a *domain-wall* in a system, gives a measure of the stiffness of a phase. The domain wall can be imposed by special boundary conditions. Compare then the free-energy of an Ising model with linear length L , in its ordered phase, with periodic and anti-periodic boundary conditions on one Cartesian direction and periodic boundary conditions on the $d - 1$ other directions of a d -dimensional hypercube. The \pm boundary conditions forces an interface between the regions with positive and negative magnetisations. At $T = 0$, the minimum energy interface is a $d - 1$ flat hyper-plane and the energy cost is

$$\Delta U(L) \simeq \sigma L^\theta \quad \text{with} \quad \theta = d - 1 \quad (2.168)$$

and $\sigma = 2J$ the *interfacial energy per unit area* or the *surface tension* of the domain wall.

Droplets - generalisation of the Peierls argument

In an ordered system at finite temperature domain walls, surrounding *droplet fluctuations*, or domains with reversed spins with respect to the bulk order, are naturally generated by thermal fluctuations. The study of droplet fluctuations is useful to establish whether an ordered phase can exist at low (but finite) temperatures. One then studies the free-energy cost for creating large droplets with thermal fluctuations that may destabilise the ordered phase, in the way usually done in the simple Ising chain (the Peierls argument).

Indeed, temperature generates fluctuations of different size and the question is whether these are favourable or not. These are the *droplet excitations* made by simply connected regions (domains) with spins reversed with respect to the ordered state. Because of the surface tension, the minimal energy droplets with linear size or radius L will be compact spherical-like objects with volume L^d and surface L^{d-1} . The surface determines their energy and, at finite temperature, an entropic contribution has to be taken into account as well. Simplifying, one argues that the free-energy cost is of the order of L^θ , that is L^{d-1} in the ferromagnetic case but can be different in disordered systems.

Summarising, the free-energy cost of an excitation of linear size L is expected to scale as

$$\Delta F(L) \simeq \sigma(T)L^\theta . \quad (2.169)$$

The sign of θ determines whether thermal fluctuations destroy the ordered phase or not. For $\theta > 0$ large excitations are costly and very unlikely to occur; the order phase is expected to be stable. For $\theta < 0$ instead large scale excitations cost little energy and one can expect that the gain in entropy due to the large choice in the position of these excitations will render the free-energy variation negative. A proliferation of droplets and droplets within droplets is expected and the ordered phase will be destroyed by thermal fluctuations. The case $\theta = 0$ is marginal and its analysis needs the use of other methods.

As the phase transition is approached from below the surface tension $\sigma(T)$ should vanish. Moreover, one expects that the stiffness should be independent of length close to T_c and therefore, $\theta_c = 0$.

Above the transition the stiffness should decay exponentially

$$\Delta F(L) \simeq e^{-L/\xi} \quad (2.170)$$

with ξ the equilibrium correlation length.

2.8 Scaling and the renormalisation group

Scaling concepts are fundamental in describing the behaviour of systems made of a large number of constituents, interacting non-linearly, and according to laws that are sometimes poorly understood. The idea is to isolate a few relevant variables that characterise the behaviour at a certain length (and time scale) and to postulate simple *scaling relations* between them. When there is only one independent variable, the scaling relations take the form of power laws with exponents that are not necessarily rational numbers.

Scaling arguments apply to many different physical situations (in and out of equilibrium) and they can be explained using *renormalisation* ideas. In most cases, the renormalisation approach does not have a formal basis. It is in the context of critical phenomena in equilibrium that scaling and renormalisation can be derived systematically.

In the discussion of critical phenomena we have defined 6 critical exponents (α for the specific heat, β for the order parameter, γ for the susceptibility, δ for the order parameter at the critical point as a function of the conjugate field, η for the correlation function and ν for the correlation length). But, actually, not all these exponents are independent. It was soon observed that the *experimental data* pointed towards simple relations between the exponents.

2.8.1 Homogeneity & scaling

The solution of the Curie-Weiss ferromagnet yields an expression of the free-energy density as a function of the auxiliary variable x which, at the saddle point level, is to be

identified with the order parameter m . In terms of the latter,

$$f(t, h) = \min_m \left(\frac{t}{2} m^2 + u m^4 - h m \right) = \begin{cases} -\frac{1}{16} \frac{t^2}{u} & \text{for } h = 0, t < 0, \\ -\frac{3}{4^{4/3}} \frac{h^{4/3}}{u^{1/3}} & \text{for } h \neq 0, t = 0, \end{cases} \quad (2.171)$$

with t the reduced temperature $(T - T_c)/T_c$. We do not write explicitly the dependence on u in the function f since this parameter does not control the phase transitions. These parameter dependencies and, in particular, the singularities can be collected in the form

$$f_{\text{sing}}(t, h) = |t|^2 g_f(h/|t|^\Delta) \quad \text{with} \quad -g_f(y) \sim \begin{cases} \frac{1}{u} & \text{for } y \sim 0, t < 0, \\ \frac{y^{4/3}}{u^{1/3}} & \text{for } y \rightarrow \infty, \end{cases}$$

and $\Delta = \frac{3}{2}$ (2.172)

with Δ the *gap exponent*.

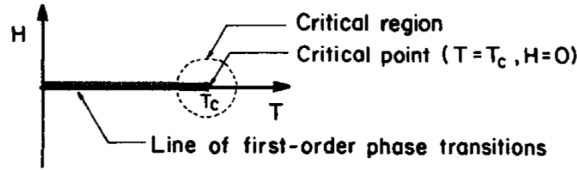


Figure 2.17: The phase diagram of the Ising model in $d \geq 2$.

The form above is an example of an homogeneous function of the parameters. A real function of n variables is said to be *homogeneous* if

$$f(b^{p_1} x_1, \dots, b^{p_n} x_n) = b^{p_f} f(x_1, \dots, x_n) \quad (2.173)$$

for any scaling real factor b and powers p_1, \dots, p_n . Then

$$f(x_1, \dots, x_n) = b^{-p_f} f(b^{p_1} x_1, \dots, b^{p_n} x_n) \quad (2.174)$$

and choosing b so that $b^{p_n} x_n = 1$ one writes

$$\begin{aligned} f(x_1, \dots, x_n) &= x_n^{p_f/p_n} f(x_n^{-p_1/p_n} x_1, x_n^{-p_2/p_n} x_2, \dots, 1) \\ &= x_n^{p_f/p_n} \tilde{f}(x_n^{-p_1/p_n} x_1, x_n^{-p_2/p_n} x_2, \dots, x_n^{-p_{n-1}/p_n} x_{n-1}). \end{aligned} \quad (2.175)$$

In this way, the resulting function \tilde{f} has one less independent variable and the remaining ones are ratios of the original ones and powers of the one that has been eliminated:

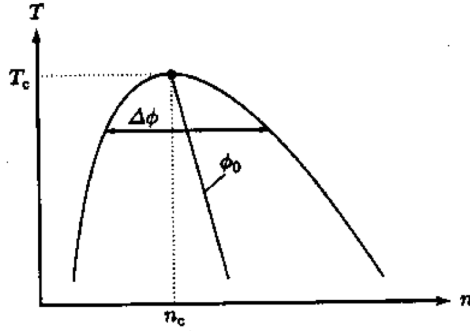


Fig. 4.4.3. Schematic phase boundary for the liquid-gas transition showing the asymmetry of the order parameter about the critical density.

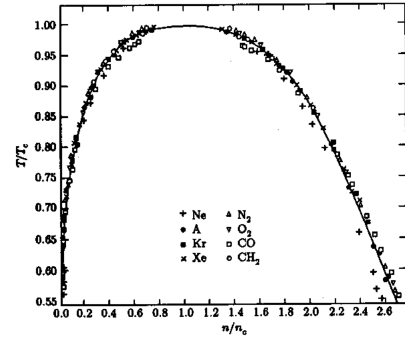


Fig. 4.4.4. Phase boundary in units of reduced temperature and density for eight different molecular fluids near their liquid-gas transitions. Note the universal behavior and the fact that the solid line is $\Delta\phi \propto (T_c - T)^{1/3}$ with $\beta = 1/3$ rather than the mean-field result $\beta = 1/2$. [E.A. Guggenheim, *J. Chem. Phys.* 13, 253 (1945)]

Chaikin - Lubensky #19

Figure 2.18: The gas-liquid transitions at constant pressure. At very low density and low temperature, at the left of the curve the system is a gas, at very large density and still low temperature, at the right of the curve the system is a liquid. In the region below the curve there is coexistence of gas and liquid. Above the curve the system goes continuously from a gas to a liquid when increasing the density. The critical line behaves as $|\rho_l - \rho_g| \sim |T - T_c|^\beta$ with $\beta \sim 0.327$ close to the maximum. Note that scaling holds as far as $T/T_c \sim 0.55$!

$x_j/x_n^{p_j/p_n}$ with $j = 1, \dots, N-1$ in the example. We note that f_{sing} for the Curie Weiss mean-field theory is of this form, with $x_1 = h$, $x_{n=2} = |t|$, $p_1/p_2 = \Delta$ and $p_f/p_2 = 2$

The *homogeneity assumption* is that the singular part of the free-energy density, in finite dimensional systems, keeps a similar form to the one in Eq. (2.172)

$$f_{\text{sing}}(t, h) \simeq |t|^{2-\alpha} g_f(h/|t|^\Delta) \quad (2.176)$$

The exponent of the $|t|$ factor is chosen to be $2 - \alpha$ so as to recover the exponent α in the singularity of the heat capacity, $C_{\text{sing}} = \partial^2 f_{\text{sing}} / \partial t^2 \sim |t|^{-\alpha}$ for $h \rightarrow 0$.

Since the free-energy density is analytic everywhere in the two-dimensional phase diagram (t, h) reported in Fig. 2.17 apart from at the $h = 0$ critical point $t = 0$, the critical exponent α , the gap exponent Δ and the scaling functions should be the same on both sides of the critical point, that is, for $t > 0$ and $t < 0$, close to $t = 0$, see [10] for a proof. This justifies $\gamma = \gamma'$ and $\alpha = \alpha'$ in this problem.

Surprisingly enough, *all* systems undergoing a ferromagnetic transition can be *scaled* in this way using the *same* functions g_m^\pm above and below the critical temperature, respectively! The way of checking this hypothesis is by plotting $m/|t|^\beta$ against $|h|/|t|^{\beta\delta}$ for different systems and looking for *data collapse*. Of course, we do not know the values of the universal exponents β and δ and the material dependent critical temperature T_c *a priori*, so we need to manipulate a bit the data before obtaining collapse. Note that the scaling law (2.177) is independent of the dimension d . An example of data collapse using the scaling relation (2.177) is given in Fig. 2.18.

It is interesting to note that scaling holds on a much wider window than the power law expressions defining the critical exponents.

2.8.2 Relation between exponents

From the scaling form (2.176) one derives the magnetisation density, the linear susceptibility and relations between the corresponding exponents:

$$m(t, h) = \frac{\partial f}{\partial h} = |t|^{2-\alpha-\Delta} g'_f(h/|t|^\Delta) = |t|^{2-\alpha-\Delta} g_m(h/|t|^\Delta) \quad (2.177)$$

and then

$$m \sim \begin{cases} |t|^\beta & \text{for } h|t|^{-\Delta} \rightarrow 0 \\ h^{1/\delta} & \text{for } h|t|^{-\Delta} \gg 1 \end{cases} \implies \begin{cases} g_m(y) \xrightarrow{y \rightarrow 0} 1 & \& \beta = 2 - \alpha - \Delta, \\ g_m(y) \xrightarrow{y \gg 1} y^{1/\delta} & \& \delta = \Delta/\beta. \end{cases} \quad (2.178)$$

Putting these two relations together

$$\beta = 2 - \alpha - \delta\beta \quad \Rightarrow \quad \boxed{\beta = \frac{2 - \alpha}{1 + \delta}} \quad (2.179)$$

From the susceptibility $\chi \sim |t|^{-\gamma}$, using $\chi \propto \partial^2 f / \partial h^2|_{h=0}$, one derives

$$\gamma = 2\Delta - 2 + \alpha \quad \Rightarrow \quad \boxed{\gamma = 2\beta\delta - 2 + \alpha} \quad (2.180)$$

Combining the exponent relations one deduces

$$\begin{aligned} \text{\textit{Rushbrooke's identity}} & \quad \alpha + 2\beta + \gamma = 2, \\ \text{\textit{Widom's identity}} & \quad \delta - 1 = \gamma/\beta. \end{aligned} \quad (2.181)$$

Note that these thermodynamic relations are independent of the dimension of space and that they do not involve the correlation length nor its divergence close to $t = 0$.

One now assumes that the correlation length also satisfies a scaling relation

$$\xi(t, h) \sim |t|^{-\nu} g_\xi(h/|t|^\Delta), \quad (2.182)$$

with $g_\xi(y \rightarrow 0) = \text{ct}$ and $g_\xi(y \gg 1) = y^{-\nu/\Delta}$, and that it is the only quantity that controls the divergence of all thermodynamic quantities. Then, the singular part of the free-energy density must behave as

$$-\beta f_{\text{sing}} = L^{-d} \underbrace{\ln Z}_{\text{adim}} \propto L^{-d} \left(\frac{L}{\xi} \right)^d = \xi^{-d} \sim |t|^{-\nu d} [g_\xi(h/|t|^\Delta)]^{-d}. \quad (2.183)$$

The third identity can be interpreted as the result of considering the system as the union of $(L/\xi)^d$ independent pieces, each contributing the same amount to the total free-energy. Since this expression has to equal (2.176) one must have

$$\text{\textcolor{red}{Josephson's identity}} \quad 2 - \alpha = \nu d . \quad (2.184)$$

This is a so-called *hyperscaling relation* since it involves the space dimension d . The mean-field values $\alpha = 0$ and $\nu = 1/2$ do not satisfy the hyperscaling relation.

Exploiting the fluctuation-dissipation relation, the linear susceptibility is expressed as an integral over space of the two point connected correlation (we do not write conn explicitly)

$$\chi \propto \int d^d x C(\vec{x}, \vec{y}) = \int d^d x |\vec{x} - \vec{y}|^{2-d-\eta} \sim \xi^{2-\eta} \sim |t|^{-\nu(2-\eta)} \quad (2.185)$$

and this should also be $\sim |t|^{-\gamma}$, hence

$$\boxed{\gamma = \nu(2 - \eta)} \quad (2.186)$$

Similarly, for the heat capacity C_V

$$C_V \propto \int d^d x C_E^c(\vec{x}, \vec{y}) = \int d^d x |\vec{x} - \vec{y}|^{2-d-\eta'} \sim \xi^{2-\eta'} \sim |t|^{-\nu(2-\eta')} \quad (2.187)$$

where $C_E^c(\vec{x}, \vec{y})$ is the energy-energy connected correlation function. This should also be $\sim |t|^{-\alpha}$, then

$$\boxed{\alpha = \nu(2 - \eta')} \quad (2.188)$$

Only two exponents are independent and allow us to characterise the singular behaviour of all thermodynamic observables.

Experimental and numerical measurements of the exponents confirm that the relations derived above are indeed satisfied.

2.8.3 Scale invariance

Scale invariance is the property of an object which does not change if all its scales are multiplied by a common factor. An illustrative movie showing this property in a random walk can be found in Wikipedia https://en.wikipedia.org/wiki/Scale_invariance. In Fig. 2.19 we show a snapshot of the bidimensional Ising model demonstrating this property. Many other examples can be found in [28]. The process of multiplying all relevant scales by the same constant, say λ is called a *dilatation* or *dilation*.

Near a critical point, fluctuations occur at all length scales, and thus the relevant theory to describe this particular point(s) in the phase diagram should be *scale-invariant*. As

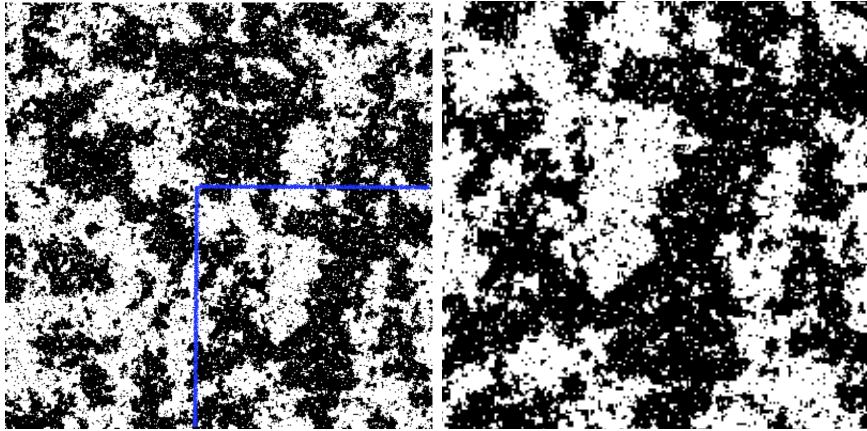


Figure 2.19: Left: a $2d$ Ising model configuration at the critical point. Right: the selection of the right-down box has been scaled up to the same size as the original figure. The two images look statistically the same, illustrating the self-similarity.

a consequence, the correlation functions are homogeneous at criticality, with the *dilation symmetry*

$$C(\lambda\vec{x}, \lambda\vec{y}) = \lambda^p C(\vec{x}, \vec{y}) , \quad (2.189)$$

which implies *scale invariance* or *self similarity*. When a snapshot of the system at the critical point is scaled by a factor λ the resulting image is self-similar to the original one, that means that statistically it looks the same. This property is a hallmark of *fractal geometry* [30, 31]. In $d = 2$ *dilation symmetry* implies *conformal symmetry* and the latter has been used to construct effective theories at criticality.

Therefore, critical fluctuations are described by a scale-invariant statistical field theory. For a system d spatial dimensions, the corresponding statistical field theory is formally similar to a d -dimensional *conformal field theory* (CFT). The *scaling dimensions* in such problems are critical exponents, and one can in principle compute these exponents in the appropriate CFT.

2.8.4 Finite Size Scaling

A real system is large but finite, $1 \ll N \sim 10^{23} < \infty$. Finite size effects will then play a role in the phase transition, which is rounded by the fact that $N < \infty$. Finite size effects become important when $\xi \sim L$, the linear size of the system, say $L \sim 1\text{cm}$ for an actual sample. A rough estimation of how close to T_c one needs to get to see deviations from critical scaling shows that finite size effects are quite negligible in experiments but are certainly not in numerical simulations or transfer matrix studies and have to be taken into account very carefully when trying to compare numerical data to analytical predictions. Note that periodic boundary conditions suppress boundary effects and then reduces finite size effects.

The theory of finite-size scaling formulated by Fisher [34] explains how the singular behaviour of thermodynamic quantities at the critical point of a phase transition emerges when the size of the system becomes infinite. Concretely, it is a way of extracting values for critical exponents and the critical parameter, e.g. the critical temperature, by observing how measured quantities vary as the size L of the system changes. Usually, this theory is presented in a phenomenological way although it can also be justified with a renormalisation group treatment, see *e.g.* [35], and the scaling forms have been derived in some solvable cases, see *e.g.* [36].

The first remark is that an observable A that would diverge in the infinite size limit is rounded in finite size systems. The evolution with size is sketched in Fig. 2.20. One

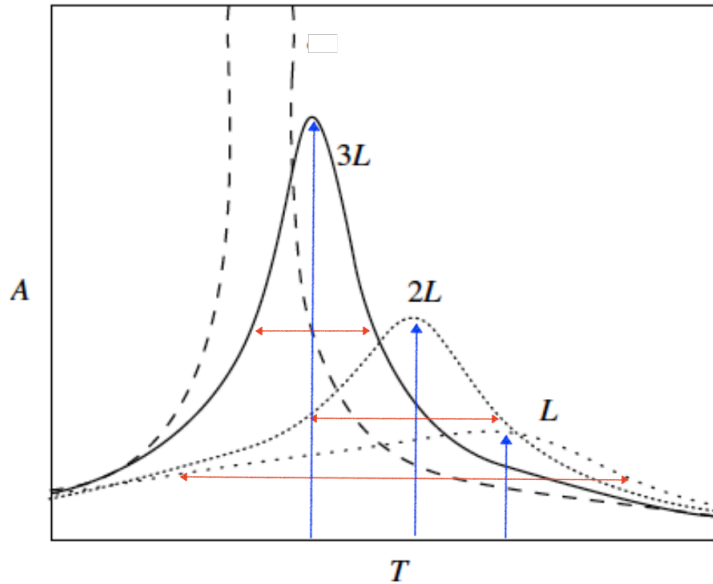


FIG. 1. Typical behaviour of a physical quantity A vs temperature close to the critical point for various system sizes. Figure taken from Thijssen^[8].

Figure 2.20: Sketch of the evolution of a susceptibility with system size, image from [37].

observes:

- A shift in the position of the maximum with respect to the infinite size critical temperature, which can be described by,

$$T_c(L) - T_c(L \rightarrow \infty) \text{ decreases as a power law of } L. \quad (2.190)$$

- The width of the peak, measured at half height, for example,

$$\Delta T(L) \text{ decreases as a power law of } L. \quad (2.191)$$

- The peak height

$$A_{\max}(L) \text{ increases as a power law of } L. \quad (2.192)$$

In a finite size system there are three length scales: a microscopic one, a , related to the range of the interactions (e.g., the lattice spacing for short-range interactions), the correlation length, ξ , and the system size, L . Thermodynamic quantities depend, then, on the adimensional ratios, ξ/a , and ξ/L . The *finite size scaling hypothesis* postulates that close to the critical point the microscopic length dependence disappears, $\xi/a \rightarrow \infty$, and only the ξ/L dependence remains.

Take the example of the magnetic susceptibility per spin, χ , in a problem with a second order phase transition and write it in terms of the correlation length, ξ , over which critical fluctuations are correlated. One has

$$\left. \begin{aligned} \chi &\simeq |T - T_c|^{-\gamma} \\ \xi &\simeq |T - T_c|^{-\nu} \end{aligned} \right\} \implies \chi \simeq \xi^{\gamma/\nu}, \quad (2.193)$$

where we have explicitly used the algebraic divergence of ξ with exponent ν . In a system of finite size, the correlation length is cut-off by the system size. As long as $\xi < L$ the susceptibility should behave as in the infinite size system with, at most, exponentially decaying correction with L/ξ , whereas for $\xi > L$ the susceptibility must be rounded. One therefore writes

$$\chi = \xi^{\gamma/\nu} \chi_0\left(\frac{L}{\xi}\right) \quad \text{with} \quad \chi_0(y) \sim \begin{cases} \text{cst} & y \gg 1 \\ x^{\gamma/\nu} & y \rightarrow 0 \end{cases} \quad (2.194)$$

The effect of the finite size is to round the critical point singularity over a region of parameter space in which $\xi \sim L$.

In anisotropic systems in which d' directions are finite and $d - d'$ are infinite the critical behaviour undergoes a *dimensional reduction* and the critical behaviour is the one of the $d - d'$ dimensional system.

These expressions, though perfectly correct, are not very useful for the analysis of numerical data since ξ is still unknown. It is convenient at this stage to go back to an expression in terms of the reduced distance from the critical point $t = (T - T_c)/T_c$. After some rearrangements

$$\chi = L^{\gamma/\nu} \tilde{\chi}(L^{1/\nu}t) \quad \text{with} \quad \tilde{\chi}(y) \sim y^{-\gamma} \chi_0(y^\nu) \quad \text{and} \quad \tilde{\chi}(y) \sim \begin{cases} y^{-\gamma} & y \gg 1 \\ \text{cst} & y \rightarrow 0 \end{cases} \quad (2.195)$$

Note that we have first written the observable in terms of the correlation length to be able to compare the latter to the system size, and we then came back to an expression in which the distance to criticality appears. The function $\tilde{\chi}$ is the *scaling function* of the intensive susceptibility and $L^{1/\nu}t$ the *scaling variable*. $\tilde{\chi}$ is finite at the origin, that is, at the critical point and falls off algebraically. $\tilde{\chi}$ does not depend on the lattice geometry but it may depend on the boundary conditions.

Compared to the scalings mentioned above:

- The peak height scales as $L^{\gamma/\nu}$.
- The peak position scales as $L^{-1/\nu}$.
- The peak width also scales as $L^{-1/\nu}$.

(For the moment we have not discussed infinite order phase transitions. We postpone the extension of finite size arguments in these case.)

Data collapse

Notably, the function χ has no further dependence on L and this is the property that is exploited to determine the exponents ν and γ by measuring χ in systems with different sizes. One proceeds as follows. By measuring χ at different temperatures close to the expected critical one and for different systems sizes one obtains a set of $\chi_L(t)$. Inverting Eq. (2.195)

$$\chi_L(t)L^{-\gamma/\nu} = \tilde{\chi}(L^{1/\nu}t) , \quad (2.196)$$

and plotting the right-hand-side as a function of the scaling variable $L^{1/\nu}t$ the points should fall on a master curve *if and only if* one uses the correct values of the exponents γ and ν , and the critical temperature T_c , which enters the calculation of the reduced temperature t .

Figure 2.21 shows on the left a sketch of the evolution of the extensive susceptibility of the order parameter with size in a second order phase transition, and on the right as scaling plot of the same quantity in Monte Carlo data [37] for the $2d$ Ising model. In the simulations shown, the best data collapse is obtained for $\gamma = 1.76 \pm 0.01$, $\nu = 1.00 \pm 0.05$ and $T_c/J = 2.27 \pm 0.01$. These values are in good agreement with the exact known values of $\gamma = 7/4$, $\nu = 1$ and $T_c/J = 2.269$.

The same method can be applied to other intensive quantities diverging at criticality

$$o_L(t)L^{-\gamma_o/\nu} = \tilde{o}(L^{1/\nu}t) \quad (2.197)$$

with γ_o their corresponding critical exponent. If one prefers to work with the extensive quantity $O_L = L^d o_L$ an additional power L^{-d} should be included in the left-hand-side.

Finite size scaling can also be applied to the study of quantum critical phenomena in a way that we will discuss when entering the field of quantum statistical physics. We anticipate that the mapping between quantum problems in d dimensions and classical problems in $d+1$ with the additional periodic dimension being of length $\beta\hbar$, makes finite size scaling very important in this context.

The order parameter

Near the critical point, the finite size corrections to the scaling form of the order parameter, eq. (2.177), are

$$m \sim |t|^\beta g_m\left(\frac{t}{|h|^\Delta}, \frac{\xi}{L}\right) = |t|^\beta g_m\left(\frac{t}{|h|^\Delta}, \frac{1}{|t|^\nu L}\right) = L^{-\beta/\nu} \tilde{g}_m\left(\frac{t}{|h|^\Delta}, |t|^\nu L\right) \quad (2.198)$$

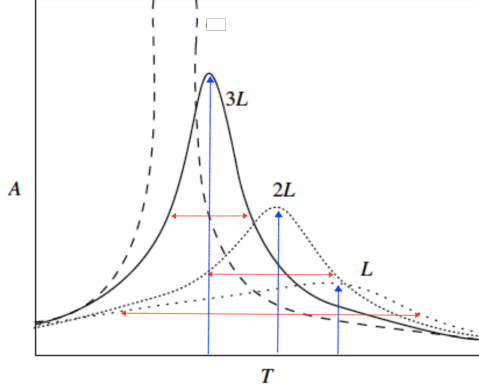


FIG. 1. Typical behaviour of a physical quantity A vs temperature close to the critical point for various system sizes. Figure taken from Thijssen⁸.

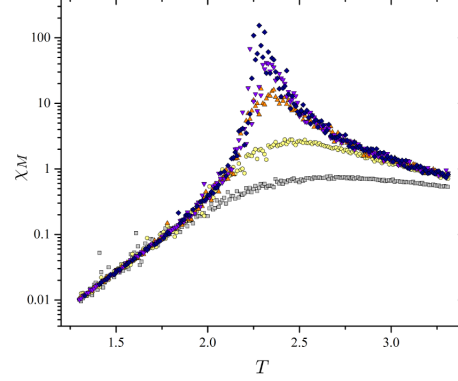


FIG. 3. (Color online) Magnetic susceptibility per site χ_M vs temperature T for different lattice sizes $L = 5$ (squares), 10 (circles), 25 (up triangles), 50 (down triangles) and 100 (diamonds) for the 2D Ising model.

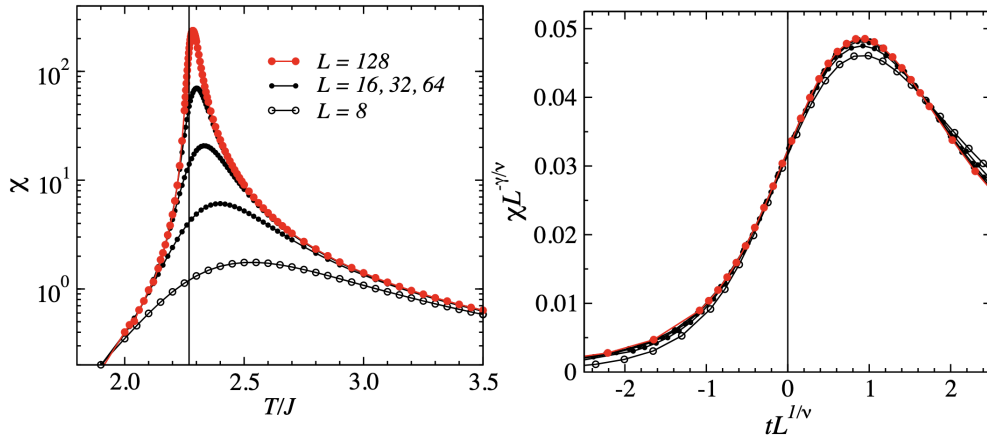


Figure 2.21: Left: A sketch of the typical behaviour of an intensive susceptibility close to the critical point. Right: the scaling plot. Figures above from [37]. In the bottom the bare and scaled susceptibility [38].

This finite-size-scaling *Ansatz* can be verified by plotting $mL^{\beta/\nu}$ versus $|t|h^{-\Delta}$ and $|t|^\nu L$. Of course, there are different ways of writing the arguments (and hence the function) in the right-hand-side. If a data collapse emerges, this gives the shape of the scaling function. The finite-size behaviour is determined from the critical exponents of the infinite system.

The Binder cumulant - location of T_c

A variation of the *kurtosis*⁸ of the order parameter, say O , in a system with linear size

⁸The kurtosis is a statistical measure that defines how heavily the tails of a distribution differ from the tails of a normal distribution. In other words, kurtosis identifies whether the tails of a given distribution contain extreme values. It is a scaled version of the fourth moment of the distribution: $K(X) = \langle (X -$

L is the so-called Binder parameter [40, 41],

$$U_L = 1 - \frac{\langle O^4 \rangle_L}{3\langle O^2 \rangle_L^2}, \quad (2.199)$$

and it is used to locate the critical point in systems with second order phase transitions.

In the disordered phase, the order parameter is Gaussian distributed with zero mean and variance σ_L^2 . Thus, $\langle O^4 \rangle_L = 3\sigma_L^4$, $\langle O^2 \rangle_L = \sigma_L^2$, and $U_L = 0$. In an ordered spontaneously symmetry broken phase, the order parameter is distributed as two narrow peaks centred at non-vanishing values. In the large L limit one can approximate the peaks by delta functions, and then $U_L = 2/3$. For finite L , there must be a crossover between these two extreme values when tuning the control parameter across the phase transition.

The critical parameter is the unique point where the different curves cross in the thermodynamic limit, since

$$U_L = g_U(tL^{1/\nu}). \quad (2.200)$$

In the infinite size limit U is a discontinuous function of the control parameter.

Exercise 2.18 Reflect upon this statement.

An example of the generic discussion above is again given by the $2d$ Ising case, in which the order parameter is the magnetisation density. Above T_c its distribution is a Gaussian centred at zero, whereas below T_c the distribution tends towards two Gaussians centred at $m = \pm|m_{\text{eq}}|$ where m_{eq} is the spontaneous magnetisation of the infinite size systems.

Above the critical point, with symmetry unbroken, the Binder parameter decreases with increasing system size while below it, in a symmetry-breaking magnetic phase, the behaviour is the opposite and U_L increases with L . These trends are shown in Fig. 2.22, where data for the $2d$ Ising model with system sizes in the range $L \in [32, 162]$ are displayed. The curves cross at a single point and, because the behaviour at the critical point is close to universal, only a set of relatively small system sizes need be considered to identify the critical parameter, with no need for complicated extrapolations of very large systems to the thermodynamic limit.

The value of the Binder cumulant at criticality in the thermodynamic limit, $U_{L \rightarrow \infty}$, is a measure of the deviation of the distribution function of the order parameter from a Gaussian function. $U_{L \rightarrow \infty}$ is not a universal quantity in the sense that it depends on the boundary conditions, the shape of the system, and even lattice structure.

The Binder parameter also satisfies scaling, in the form of Eq. (2.200) and data collapse allows for the determination of ν .

Fluctuations of macroscopic observables

A direct consequence of having a diverging correlations length is that the critical measure-to-measure fluctuations of global observables like, for instance, the magnetisation

$\mu)^4)/\langle(X - \mu)^2\rangle^2$ and for any univariate normal distribution it equals 3. One also notes that the kurtosis is a dimensionless ratio.

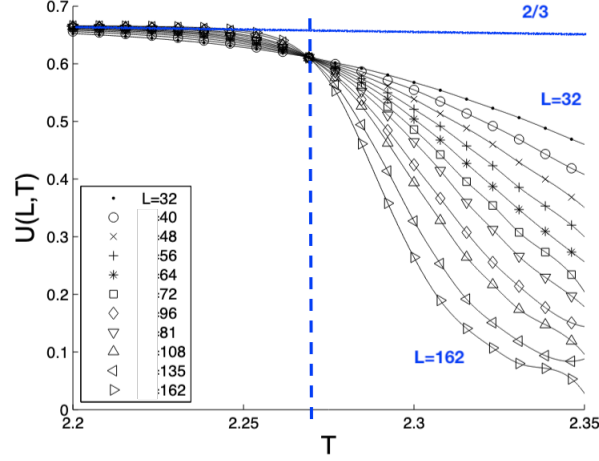


Figure 2.22: The Binder cumulant of the 2d Ising model. Data from [43] with the estimate $T_c/J = 2.26903 \pm 0.0005$ cfr. Onsager's exact value $T_c/J = 2/\ln(1 + \sqrt{2}) \sim 2.26919$.

density, are not Gaussian. The reason is simple, if $L < \xi$, a global measurement is not the result of an average over many uncorrelated regions and, thus, one cannot use the central limit theorem to argue for a normal distribution of fluctuations. In the regime in which L is finite with respect to ξ , finite size scaling implies

$$p_L(m) = L^{\beta/\nu} \Pi\left(mL^{\beta/\nu}, \frac{\xi}{L}\right). \quad (2.201)$$

Recently, the study of critical fluctuations of macroscopic observables received much attention. The best adapted model for this analysis is the 2d XY model, that is critical on a finite interval of temperatures (and not only at a single precise value of T_c) [29].

2.8.5 The renormalisation group

We identified two important properties of the critical behaviour:

- At the critical point fluctuations at all length scales have to be taken into account since ξ diverges. Concomitantly, large structures of ordered spins exist.
- Microscopic details should not matter much, since there is universality.

The renormalisation group is engineered in such a way to explain how short-range couplings generate a *collective phenomenon* observable at *all* length scales. It relates different scales making the expected *scale invariance* appear. The method is general and

it does not rely on a special model, being thus apt to treat very different models with similar global behaviour, the *universality* property.

We will start the discussion with a treatment of the Ising chain that illustrates how a reduction of the number of degrees of freedom induces a *flow in the coupling constants*. This motivated Kadanoff to introduce *block spins*, with large numbers of the original ones, and thus eliminate large numbers of degrees of freedom which should be irrelevant at the transition. The new Hamiltonian ruling the behaviour of the block spins needs to be deduced. The concrete way to do it, and from it derive the scaling relations and critical exponents, was developed by Wilson in the early 70s. We explain it afterwards.

This *renormalisation group* ideas gave a totally new way of understanding condensed-matter and particle physics phenomena. They transformed the picture of phase transitions that developed in the 60s – with the understanding of concepts like scaling, universality and correlations – into a calculation tool. Wilson got the Nobel Prize in Physics in 1982.

2.8.6 Decimation in the one dimensional Ising chain

The idea is to reduce the number of degrees of freedom by a factor $b > 1$ at each step of a transformation, $N \mapsto N/b = N'$, in such a way that

$$\mathcal{Z} = \sum_{\{s_i = \pm 1\}} e^{-\beta \mathcal{H}(\{s_i\})} = \sum_{\{s'_I = \pm 1\}} e^{-\beta \mathcal{H}'(\{s'_I\})} \quad (2.202)$$

where s_i are the original $i = 1, \dots, N$ Ising spins, and s'_I are $I = 1, \dots, N/b$ remaining Ising spins. We need to find the relation between the Hamiltonians \mathcal{H} and \mathcal{H}' , which will actually have exactly the same form in this special model, though with different parameters (this is not always the case, in exact form, in other more complicated models and some approximation procedure has to be implemented). The transformation searched for applies then on the parameters.

For concreteness, take an open chain with N odd, $N \pm 1$ even, and write the partition function in the way

$$\mathcal{Z} = \sum_{\{s_i = \pm 1\}} \exp[K(s_1 s_2 + s_2 s_3) + K(s_3 s_4 + s_4 s_5) + \dots + K(s_{N-2} s_{N-1} + s_{N-1} s_N)] \quad (2.203)$$

with $K = \beta J$. The spins with even labels s_2, s_4, \dots, s_{N-1} appear only once in the parenthesis singled out in this way of writing \mathcal{Z} . One can now perform the partition sums over the even $(N-1)/2$ spins, an operation which is called *decimation*, and find

$$\begin{aligned} \mathcal{Z} = \sum_{\{s_I = \pm 1\}} & \{ \exp[K(s_1 + s_3)] + \exp[-K(s_1 + s_3)] \} \times \dots \\ & \times \{ \exp[K(s_{N-2} + s_N)] + \exp[-K(s_{N-2} + s_N)] \} \end{aligned} \quad (2.204)$$

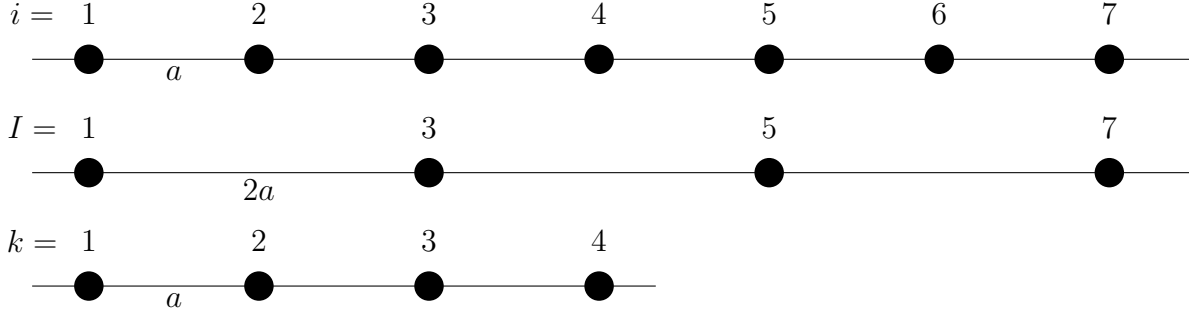


Figure 2.23: The 1d Ising chain. The original chain, the decimated one, and the rescaled final one. In the example, $N = 7$, the decimated spins are $(N - 1)/2 = 3$ and the remaining ones $(N + 1)/2 = 4$. Every second spin has been integrated away in the partition sum. Any distance r in the original lattice becomes $r' = r/2$ in the new one, measured in the units of the lattice spacing.

where the partition sum runs over $\{s_I = \pm 1\}$ with $I = 1, 3, \dots, N$. The aim is to find a transformation of the parameter K such that,

$$\exp[K(s_I + s_{I+2})] + \exp[-K(s_I + s_{I+2})] = f(K) \exp(K' s_I s_{I+2}) \quad (2.205)$$

for all $s_I = \pm 1$ and $s_{I+2} = \pm 1$. In other words, the condition to keep the same Ising model form in the new Hamiltonian. Two conditions should be imposed for $s_I = \pm 1, s_{I+2} = \pm 1$:

$$\begin{aligned} \exp(2K) + \exp(-2K) &= f(K) \exp(K') & s_I s_{I+2} &= 1, \\ 2 &= f(K) \exp(-K') & s_I s_{I+2} &= -1, \end{aligned} \quad (2.206)$$

and we find

$$f(K) = 2 \exp(K') \quad \text{and} \quad \cosh(2K) = \exp(2K') \quad (2.207)$$

which imply

$$\boxed{K' = \frac{1}{2} \ln \cosh(2K)} \quad \text{and} \quad \boxed{f(K) = 2(\cosh(2K))^{1/2}} \quad (2.208)$$

One can see that $K' < K$ for all $K \geq 0$.

The relation between K' and K can be seen as a recurrence

$$K_{n+1} = \frac{1}{2} \ln \cosh(2K_n) \quad (2.209)$$

with n labelling the step of the decimation, starting from $K_0 = K$. For $K_n = 0$, $K_{n+1} = 0$ as well. The derivative of the right-hand-side with respect to K_n at $K_n = 0$ vanishes. In

the large K_n limit the right-hand-side goes as $K_n - (\ln 2)/2$. If one looks for the *fixed points* of this relation, imagined as a recurrence, one imposes

$$K^* = \frac{1}{2} \ln \cosh(2K^*) \quad \Longrightarrow \quad \boxed{K^* = 0 \quad \text{and} \quad K^* \rightarrow \infty} \quad (2.210)$$

Clearly, for any $K_n \neq 0, \infty$, $K_{n+1} < K_n$, and the $K^* = 0$ is an *attractive fixed point* while $K^* \rightarrow \infty$ is a *repulsive* one. The phase transition at $T = 0$ corresponds to the repulsive fixed point $K^* \rightarrow \infty$. Close to this repulsive fixed point the recursion can be approximated by

$$e^{2K_{n+1}} \sim \frac{1}{2} e^{2K_n} \quad K_n \gg 1 \quad (2.211)$$

$$K_{n+1} \sim K_n^2 + \mathcal{O}(K_n^4) \quad K_n \sim 0 \quad (2.212)$$

See Fig. 2.24 for a graphical representation of this recurrence.

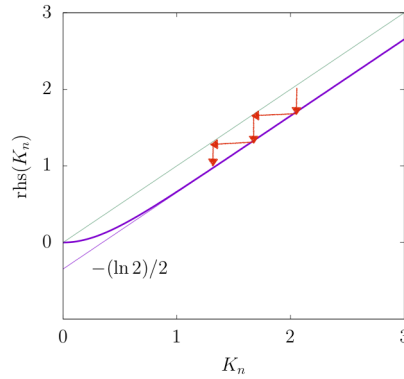


Figure 2.24: A graphical representation of the recurrence (2.209).

The partition function becomes

$$\mathcal{Z}(N, K) = (f(K))^{(N-1)/2} \sum_{\{s_k = \pm 1\}} \exp[K' \sum_k s_k s_{k+1}] \quad (2.213)$$

with the new index k running over $k = 1, 2, \dots, (N+1)/2$, with the normal splitting 1 between consecutive values. Comparing we have

$$\mathcal{Z}(N, K) = (f(K))^{(N-1)/2} \mathcal{Z}((N+1)/2, K'). \quad (2.214)$$

Since we expect $\ln \mathcal{Z}(N, K)$ to be extensive, $\ln \mathcal{Z}(N, K) = N\zeta(K)$ then

$$\begin{aligned} \ln \mathcal{Z}(N, K) &= (N-1)/2 \ln f(K) + \ln \mathcal{Z}((N+1)/2, K') \quad \Longrightarrow \\ N\zeta(K) &= (N-1)/2 \ln f(K) + (N+1)/2 \zeta(K') \end{aligned} \quad (2.215)$$

and in the large N limit

$$\boxed{\zeta(K') = 2\zeta(K) - \ln[2(\cosh(2K))^{1/2}]} \quad (2.216)$$

(note that, apart from a factor $-\beta$, ζ is the free-energy density.)

The process described in the previous paragraph is a *flow* in the space of parameters. Starting from any non-zero value of the coupling constant the iteration converges to $K^* = 0$. There are then two *fixed points*, a *stable* fixed point at $K^* = 0$ or infinite temperature (to which trajectories are attracted) and an *unstable* fixed point $K^* \rightarrow \infty$ or zero temperature from which trajectories depart. The stable fixed point represents the high temperature paramagnetic phase while the unstable fixed point is the critical $T = 0$ point. The critical behaviour can be obtained from the dependence of $\zeta(K)$ on the parameter $K - K_c = K - K^*$ with $K^* \rightarrow \infty$ or, better suited for an expansion, the translation of eq. (2.216) in terms of T and the expansion around $T^* = 0$.

If one solved $K(K')$ instead of $K'(K)$ as we have just done, the *recursion relations* are

$$\boxed{K = \frac{1}{2}(\cosh(\exp(2K')))^{-1}, \quad \zeta(K) = \frac{1}{2} \ln 2 + \frac{1}{2}K' + \frac{1}{2}\zeta(K'),} \quad (2.217)$$

which yield $K > K'$. The flow then goes in the opposite direction and it is represented in Fig. 2.25.

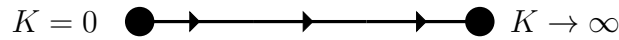


Figure 2.25: The flow of the coupling constant according to Eqs. (2.217) in the one dimensional Ising chain.

The recursive relations can be used to evaluate the free-energy as a function of K . The trick is to start from a very small value of the coupling strength K' ($T \rightarrow \infty$) for which the spins are effectively uncoupled and $\ln \mathcal{Z} = N \ln 2$, and then progressively increase K following the rules in eq. (2.217). The results of this procedure are given in the Table in Fig. 2.26 which is reproduced from [33]. The agreement between the values generated this way and the results of the exact calculation are quite amazing.

Exercise 2.19 Repeat the calculation above for the ferromagnetically coupled one dimensional Ising chain under an external magnetic field. Find the recursion relations and study the flow. Details can be found in [44].

Let us now investigate the evolution of the *correlation length*. It is extracted from the decay of the spatial correlation

$$C(\vec{x}, \vec{y}) = \langle s(\vec{x})s(\vec{y}) \rangle \simeq e^{-|\vec{x}-\vec{y}|/\xi(K)} \quad \text{for} \quad a \ll |\vec{x} - \vec{y}| \ll L, \quad (2.218)$$

Table I. Values of ζ for the 1D Ising model calculated from the recursion formulas Eqs. (31) and (32) of the renormalization group and from the exact formula derived from Eq. (9). ζ is related to the partition function Z through Eq. (28).

K	$\zeta(K)$	
	Renormalization group	Exact
0.01	$\ln 2$	0.693 197
0.100 334	0.698 147	0.698 172
0.327 447	0.745 814	0.745 827
0.636 247	0.883 204	0.883 210
0.972 710	1.106 299	1.106 302
1.316 710	1.386 078	1.386 080
1.662 637	1.697 968	1.697 968
2.009 049	2.026 876	2.026 877
2.355 582	2.364 536	2.364 537
2.702 146	2.706 633	2.706 634

Figure 2.26: This Table is reproduced from [33] and shows how the iterative procedure (2.217) starting from the uncoupled problem converges after a relative small number of steps to the exact partition function.

where we did not need to consider the connected correlation since $\langle s_m \rangle = 0$ at all non-zero temperatures. $\xi(K)$ is a dimensionfull quantity, i.e. $\xi(K) = \bar{\xi}(K)a$, with a carrying length units. Proceeding by definition

$$C(\vec{x}, \vec{y}) = \frac{1}{Z(K)} \sum_{\{s_i = \pm 1\}} s_m s_n e^{K \sum_{i=1}^N s_i s_{i+1}} \quad \text{with} \quad \vec{x} = ma\hat{e}_x, \quad \vec{y} = na\hat{e}_x \quad (2.219)$$

and close to the critical ($T = 0$) point

$$C(\vec{x}, \vec{y}) \sim e^{-|m-n|a/\xi(K)}. \quad (2.220)$$

We notice that the correlation length has **units of length** but, when measured in units of the lattice spacing, $\xi(K)/a$, it is just a number. Say, for example, $a = 1\text{cm}$, and $\xi(K) = 10a = 10\text{cm}$, with $\xi(K)/a = \bar{\xi}(K) = 10$.

For concreteness, take m and n to be odd (in the sketch in Fig. 2.23 this could be $m = 3$ and $n = 5$ for example). Integrate away the spins with even label. The spins to be correlated are not concerned and the result of the partition sums over the even-labeled spins is the same as the one above. We have

$$C(\vec{x}, \vec{y}) = \frac{1}{(f(K))^{\frac{N-1}{2}} Z\left(\frac{N+1}{2}, K'\right)} \sum_{\{s_I = \pm 1\}} s_m s_n (f(K))^{\frac{N-1}{2}} e^{K' \sum_{I=1}^N s_I s_{I+1}} \quad (2.221)$$

The factors $(f(K))^{(N-1)/2}$ in numerator and denominator cancel:

$$C(\vec{x}, \vec{y}) = \frac{1}{Z\left(\frac{N+1}{2}, K'\right)} \sum_{\{s_I = \pm 1\}} s_m s_n e^{K' \sum_{I=1}^N s_I s_{I+1}}. \quad (2.222)$$

We now rename the spins, with $k = (I + 1)/2$ in the new partition sum, so as to let them run from 1 to $(N + 1)/2$, with unitary label splitting. However, the lattice spacing in the decimated model has been expanded to $2a$ (from a in the original one), see the second row in Fig. 2.23. The right-hand-side is then rewritten as

$$C(\vec{x}, \vec{y}) = \frac{1}{\mathcal{Z}\left(\frac{N+1}{2}, K'\right)} \sum_{\{s_k = \pm 1\}} s_{\frac{(m+1)}{2}} s_{\frac{(n+1)}{2}} e^{K' \sum_{k=1}^{(N+1)/2} s_k s_{k+1}}, \quad (2.223)$$

where the right-hand-side concerns a problem with coupling strength K' , $(N + 1)/2$ spins and lattice spacing $2a$. In order to recover a model with the same lattice spacing we need to rescale space to recover the original lattice spacing

$$2a \mapsto a \quad (2.224)$$

and let the new model look exactly like the old one, see the third row in Fig. 2.23. All distances are now halved with respect to the original ones.

Let us go back to the correlation length analysis. After decimation, the correlation length measured in units of the lattice spacing (the adimensional one) has been divided by two. That is

$$\xi = \bar{\xi}(K)a = \bar{\xi}'(K')2a \quad \Rightarrow \quad \bar{\xi}'(K') = \bar{\xi}(K)/2 \quad (2.225)$$

In the example, $\xi = 10\text{cm}$ is obtained from $\bar{\xi}(K) = 10$ and $\bar{\xi}'(K') = 5$. Thus, we have

$$\bar{\xi}'(K') = \bar{\xi}(K)/2. \quad (2.226)$$

Think now in terms of the flow from low temperatures to high temperatures, that is, going from high K to $K' < K$ via the recursion. At very high K the recursion is approximated by $K' \sim K - (\ln 2)/2$, and this gives the reduction of K in each step of the decimation. Thus, the number of steps \bar{n} needed to reduce K from its original value to something $\mathcal{O}(1)$ is

$$K - \bar{n} \frac{\ln 2}{2} = \mathcal{O}(1) \quad \Rightarrow \quad \bar{n} \sim \frac{2K}{\ln 2}. \quad (2.227)$$

Looking at the evolution of the adimensional correlation length in reversed direction

$$\bar{\xi}(K) = 2\bar{\xi}'(K') \quad \text{and after } \bar{n} \text{ steps} \quad \bar{\xi}(K) = 2^{\bar{n}} \bar{\xi}'(K_{\bar{n}}). \quad (2.228)$$

If we require $\bar{\xi}'(K_{\bar{n}})$ to be $\mathcal{O}(1)$,

$$\bar{\xi}(K) = 2^{\bar{n}} \mathcal{O}(1) \quad (2.229)$$

and using now (2.227) to get K of order one,

$$\bar{\xi}(K) = 2^{\frac{2K}{\ln 2}} \mathcal{O}(1) \quad \Rightarrow \quad \boxed{\bar{\xi}(K) \sim e^{2K}} \quad (2.230)$$

Note that one can now go back to the dimensionfull correlation length $\xi(K) \sim ae^{2K}$ and the numerical factor in front of the exponential is not really important. What is important here is the exponential divergence with $T \rightarrow 0$.

Exercise 2.20 It is instructive to look at the Ising chain from a different angle. First, show, for example using the transfer matrix method, that the spatial correlation function between two points at distance na is exactly given by $C(na) = \tanh^n(K)$. Study this form in the large n limit and prove that the adimensional correlation length (measured in units of a) grows as $\xi(K) \sim e^{2K}$ as a function of K . Second, notice that the recursion relation between K and K' , eq. (2.208), can also be written as $\tanh K' = \tanh^2 K$. Use this form to deduce the relation between the adimensional correlation lengths.

Exercise 2.21 The recursion $\tanh K' = \tanh^2 K$ can be thought of as a recursion on the “magnetisation” observable $m'(K') = (m(K))^2$. The correlation length, expressed in terms of m behaves as $\bar{\xi}(m'(K')) = \bar{\xi}(m(K))/2$. Therefore, $\bar{\xi}(m^2) = \bar{\xi}(m)/2$. Find the solution to this equation and use it to show the exponential divergence of ξ .

A similar procedure can be applied to the $d > 1$ problem. In this case, however, the decimation of spins cannot be done exactly: one does not obtain the same Hamiltonian as the original one after having decimated the spins. Terms with next-nearest neighbours, as well as terms with products of four spins, with new coupling constants K_{nn} and K_4 , are generated. Some intuition is then needed to decide what to do with these new terms. There are a number of successful recipes to approximate the iteration in the literature. An exercise sheet will give an example of one of these.

This example showed that

effective coupling constants should be viewed as scale-dependent quantities.

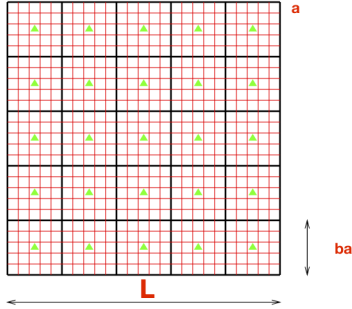
The decimation related a lattice model with spacing a , and coupling constants K (and H), to another lattice model with spacing $2a$, and coupling constants K' (and H'). We will see below how to generalise this procedure to a transformation with scale b of a generic model and find the flow in terms of b .

2.8.7 Kadanoff’s block spins, renormalisation & re-scaling

Kadanoff showed that a diverging correlation length and the associated scale invariance imply (under some more or less mild assumptions) the scaling hypothesis, the ensuing scaling laws postulated by Widom and the relations between critical exponents, which we discussed in the previous Subsection.

The idea is the following [32, 33]. Take, for concreteness, an Ising model in equilibrium at temperature T , with adimensional parameters

$$K \equiv \beta J \qquad H = \beta h \qquad (2.231)$$



Number of degrees of freedom

$$b^d \mapsto 1$$

New lattice spacing

$$a' = ba$$

Length rescaling

$$x'_\alpha \mapsto x_\alpha/b$$

$$\xi'_\alpha \mapsto \xi_\alpha/b$$

Figure 2.27: Block spins in a square lattice model. In this representation we placed the original spins, s_i , at the centres of the white boxes delimited by the red squares. The linear size of the system is $L = 25a$. The black boxes, B , with linear size ba ($5a$ in the sketch) are then the regions over which the spins are summed over to define the block spins, s_I . The latter are placed at the centres of the black boxes, on the green dots. The lattice spacing for the block spins S_I is $a' = ba$. $N = 25^2$, $b = 5$ and $N' = 25^2/5^2 = 25$.

in the Boltzmann factor. Since the system has a correlation length ξ (which depends on temperature), the spins placed within a region of linear size $ba \ll \xi$ (with a the microscopic length scale and b a numerical factor) are strongly correlated and, basically, act as a single unit. One can then define $N' = Nb^{-d}$ averaged spins,

$$s_I \equiv \sum_{i \in B_I} s_i, \quad (2.232)$$

which are placed on a lattice with spacing $a' = ab$. Here b is just an adimensional number and $I = 1, \dots, N'$. Such new spins, s_I , vary between $-b^d$ and b^d , the completely aligned configurations, and are not Ising variables any longer. For larger and larger blocks they are not bounded. In order to keep them bounded, one needs to apply a *renormalisation*:

$$s'_I = Z_b s_I \quad \text{such that} \quad s'_I = \pm 1 \quad (2.233)$$

When we justified the Landau approach with the coarse-graining procedure, we used a normalisation equal to the box size, $Z_b = b^{-d}$ in the current notation, which coincides with the un-normalised block spin value for perfectly aligned spins within the box. Now, we want to take into account the spin fluctuations that will certainly exist within the box at the critical point. Thus, we normalise with a smaller denominator which corresponds to a larger factor Z_b . All in all, the *block spins* are defined as

$$s'_I = Z_b \sum_{i \in B_I} s_i = b^{-x} \sum_{i \in B_I} s_i \quad (2.234)$$

with x an exponent, $0 < x < d$ to be determined requiring (2.233). Note that there are many configurations of the original spins that yield the same value of s_I .

The correlation length in absolute units clearly remains unchanged under the change of variables (we are simply looking at the same physical problem in terms of new variables). However, if one measures it in units of the lattice spacing, it turns out that the one for the block spin system is significantly reduced with respect to the original one, just because the lattice spacing has increased by a factor b ,

$$\xi = \bar{\xi}a = \bar{\xi}'a' = (\bar{\xi}'b)a \implies \bar{\xi}' = \bar{\xi}/b < \bar{\xi}. \quad (2.235)$$

Note that $\bar{\xi}$ and $\bar{\xi}'$ are numbers. Thus, one can interpret the block spin system as being *farther away* from criticality since

$$\bar{\xi} = \frac{\xi}{a} > \frac{\xi}{a'} = \bar{\xi}' \quad \text{or} \quad \bar{\xi} > \frac{\bar{\xi}}{b} \quad (2.236)$$

and at a new reduced temperature t_b with $|t_b| > |t|$.

As already said, the new lattice has an enlarged lattice spacing, $a' = ba$, and for larger and larger blocks the lattice spacing would continue to grow. One can then shrink the lattice, in other words, apply a *scale transformation* to redefine the spin positions

$$\vec{x}' = \vec{x}/b \implies x'_\alpha = x_\alpha/b \quad \alpha = 1, \dots, d \quad (2.237)$$

The block spins are now Ising variables placed on the vertices of a smaller lattice with $N' = N/b^d$ sites but the same lattice spacing a as the original one.

After these transformations the Hamiltonian should be written in terms of the block renormalised spins, $\mathcal{H}'(\{s_I\})$. The form of this new Hamiltonian needs not be the same as the one of the original one. In general one writes

$$\mathcal{H}'(\{s'_I\}) = R_b \mathcal{H}(\{s_i\}) \quad (2.238)$$

with R_b representing the transformations performed with length scale b . The final idea is that at the critical point, and at distances larger than the scale b , the two Hamiltonians should give equivalent descriptions of the system, since the scale at which one observes the system's behaviour should be irrelevant:

$$\mathcal{H}'(\{s'_I\}) = \mathcal{H}(\{s_i\}) \quad \xi \gg r \gg ba \gg a \quad (2.239)$$

At criticality a *fixed point* Hamiltonian should then describe the system's behaviour, as a consequence of *scale invariance* and *self-similarity*.

The transformation R_b should then have a fixed point,

$$\mathcal{H}^* = R_b \mathcal{H}^* \quad \text{for arbitrary } b \quad (2.240)$$

Since one expects that the renormalisation transformations compose in such a way that coarsening at distance $\ell_1 \times \ell_2$ can be achieved by coarsening first at distance $\ell_1 = b_1 a$ and then at distance $\ell = b_2 a$, R_b should also satisfy the properties

$$R_{b_1} R_{b_2} = R_{b_1 b_2} \quad \implies \quad R_{b^n} = \underbrace{R_b R_b \dots R_b}_{n \text{ times}} = (R_b)^n . \quad (2.241)$$

The coupling constant flow

Let us write a completely generic Hamiltonian, as a series including all possible terms,

$$\mathcal{H}(\{s_i\}) = - \sum_A J_A s_A \quad (2.242)$$

with J_A the coupling constants and s_A representing zero, one, two, *etc.* groups of spins. For example, for the two body Ising model under a magnetic field, $J_0 = 0$, $J_1 = h$ and $s_A = s_i$, $J_2 = J$ and $s_2 = s_i s_j$, and J_A with $A > 2$ equal to zero. It is convenient to work with adimensional coupling constants that, in this formulation, arise from

$$-\beta \mathcal{H}(\{s_i\}) = \sum_A \beta J_A s_A = \sum_A K_A s_A . \quad (2.243)$$

Collect all the adimensional coupling constants in $[K] = (K_1, \dots, K_n, \dots)$ and follow their renormalisation, $[K'] = R_b[K]$, calling R_b the renormalisation transformation using a coarse-graining scale $\ell = ba$, with a the lattice spacing.

The transformations listed above should then lead to transformations of the adimensional parameters

$$[K'] = R_b[K] \quad (2.244)$$

which *flow*. In general, this is a complicated non-linear function. By eliminating degrees of freedom one obtains a system with less of them but with, possibly, more complicated interactions (*e.g.* generation of more than two-body interactions from a pairwise interaction problem). However, the power of the method resides in the fact that near the critical point the new Hamiltonian can be argued to keep a similar form to the one of the original one. If new terms are generated through the coarse-graining procedure, one argues that they are either irrelevant, that is to say, they become less and less important after successive iteration of the coarse-graining, or that only a few such new terms are generated.

Now, since the transformation only involves changes at *short length scales* it cannot generate singularities. Then, R_b should be analytic and hence expandable in Taylor series

$$K'_\alpha = \sum_\beta R_{\alpha\beta}(b) K_\beta + \dots , \quad (2.245)$$

where the sum runs over the elements of $[K]$ and we changed the notation to write the dependence on the scale between parenthesis (b).

Back to the Ising model with two control parameters

This model has two coupling constants, $K_1 = \beta h$ and $K_2 = \beta J \equiv K$, and all other ones are identical to zero at the start. Without loss of generality, but for presentation convenience, we assume now that these parameters are measured with respect to their values at the critical point. This means that $K_1 = \beta_c h \equiv H$ and $K_2 = (T_c(J) - T)/T_c(J) \equiv K$.

The transformation then is

$$K' = A(b)K + B(b)H + \dots, \quad H' = C(b)K + D(b)H + \dots, \quad (2.246)$$

where the dots are higher order terms. The zero-th order terms of the series expansion in (2.245) vanish since we now measure the parameters with respect to the critical point and $K_c = H_c = 0$. For $b = 1$ there is no transformation and one must recover identities; therefore, $R_{\alpha\alpha}(1) = 1$ for all α , which implies $B(1) = C(1) = 0$ and $A(1) = D(1) = 1$. The simultaneous spin and magnetic field reversal symmetry implies that the transformation must remain unchanged under $\{s_i\} \mapsto -\{s_i\}$, $H \mapsto -H$ and $K \mapsto K$. Therefore, $B(b) = C(b) = 0$. We are left with

$$K' = A(b)K + \dots, \quad H' = D(b)H + \dots, \quad (2.247)$$

$A(1) = D(1) = 1$. Finally, one can readily exploit the properties (2.241) and argue that $A(b_1)A(b_2) = A(b_1b_2)$ and $D(b_1)D(b_2) = D(b_1b_2)$ since one should recover the same effect after applying two transformations in a row with different b 's or just one with the product of the two b 's. Then, $A(b) = b^{y_t}$ and $D(b) = b^{y_h}$:

$$\boxed{K' = b^{y_t}K + \dots, \quad H' = b^{y_h}H + \dots} \quad (2.248)$$

Say one starts from a Hamiltonian \mathcal{H} which is slightly away from criticality with a large but finite correlation length, $\xi(K, H)$. After the transformation, we have already argued in Eq. (2.235) that the new correlation length measured in units of the new lattice spacing is shorter and the system moved away from criticality. Therefore, the exponents must be positive

$$\boxed{y_t > 0, \quad y_h > 0} \quad (2.249)$$

Finally, dropping the higher order terms in (2.248)

$$\boxed{K' = b^{y_t}K, \quad H' = b^{y_h}H} \quad (2.250)$$

Equation (2.239) sets an identity between the original and block spin Hamiltonians at criticality. The total free-energies of the original and block spin systems should also be the same

$$F(K', H') = F(K, H) \quad \text{with} \quad \begin{cases} F(K, H) = Nf(K, H) \\ F(K', H') = N'f(K', H') \end{cases} \quad (2.251)$$

and then

$$f(K, H) = b^{-d} f(K', H') . \quad (2.252)$$

Therefore,

$$\boxed{f(K, H) = b^{-d} f(K b^{y_t}, H b^{y_h})} \quad (2.253)$$

and this is just the *homogeneity property* we have already discussed phenomenologically, now proved *via* the block spin argument and the fixed point requirement.

Up to now nothing fixes the block scale b and we can then choose it at will; taking

$$b = |K|^{-1/y_t} \quad (2.254)$$

and defining $\Delta = y_h/y_t$ and $2 - \alpha \equiv d/y_t$, one is simply left with

$$f(K, H) = |K|^{2-\alpha} g_f(H/|K|^\Delta) , \quad (2.255)$$

which can also be written as

$$\boxed{f(t, h) = |t|^{2-\alpha} g_{\text{sing}}(h/|t|^\Delta)} \quad (2.256)$$

with h the proper magnetic field, $t = (T - T_c)/T_c$, and g_{sing} a slightly different scaling function from g_f , appearing just in the same way as when we argued phenomenologically.

This is the scaling form postulated in (2.176) which we have now derived. We know already that from it one can derive the scaling relations and the relations between the exponents characterising the thermodynamic observables.

Now, to make contact with the critical exponent ν , let us study the evolution of the correlation length, and focus on a single control parameter K . The critical point K_c must be a *fixed point* of the transformation,

$$K_c = R_b(K_c) \quad \text{and} \quad \xi(K_c) \rightarrow \infty . \quad (2.257)$$

Linearising $R_b(K)$ around K_c

$$R_b(K) = R_b(K_c) + \left. \frac{dR_b(K)}{dK} \right|_{K=K_c} (K - K_c) , \quad (2.258)$$

with $R_b(K_c) = K_c$. If we *assume* that ξ diverges as a power of the distance to criticality, $\xi \sim |K - K_c|^{-\nu}$, then

$$\frac{\xi(R_b(K))}{\xi(K)} \sim \left[\frac{R_b(K) - R_b(K_c)}{K - K_c} \right]^{-\nu} = \left[\left. \frac{dR_b(K)}{dK} \right|_{K_c} \right]^{-\nu} \quad (2.259)$$

and using

$$\frac{\xi(R_b(K))}{\xi(K)} = \frac{1}{b} \quad (2.260)$$

we deduce

$$\boxed{\nu = \frac{\ln b}{\ln \left. \frac{dR_b(K)}{dK} \right|_{K_c}}} \quad (2.261)$$

Notably, an analytic $R_b(K)$ can produce a non-analytic $\xi(K)$.

We recall that the composition of two coarse-graining indicated that

$$R_b(K) = b^{y_t} K \quad \implies \quad \frac{dR_b(K)}{dK} = b^{y_t} . \quad (2.262)$$

The transformed parameter is $b^{y_t} K$, in the first iteration, and after n such iterations, $K^{(n)} = (b^{y_t})^n K = b^{ny_t} K$. Replacing above

$$\boxed{\nu = \frac{1}{y_t}} \quad (2.263)$$

We now *prove* that the transformations proposed lead to an algebraic divergence of ξ . The evolution of the correlation length is

$$\bar{\xi}(K_n) = \bar{\xi}(b^{ny_t} K) = b^{-n} \bar{\xi}(K) \quad (2.264)$$

b is still arbitrary. Choosing $b^{-n} = (b/K)^{-1/y_t} = (bK^{-1})^{-1/y_t}$ and multiplying the last equation by b^n ,

$$\bar{\xi}(K) = (bK^{-1})^{1/y_t} \bar{\xi}(b) = (b^{1/y_t} \bar{\xi}(b)) K^{-1/y_t} \sim K^{-1/y_t} \quad (2.265)$$

In the last term we have simply eliminated the prefactor $(b^{1/y_t} \bar{\xi}(b))$ which is a finite number ($\bar{\xi}(b)$ is just the correlation length far from criticality and it takes some finite small value). We have therefore found that $\xi(K)$ goes indeed as a power of K . Finally, since $\xi(t) \sim K^{-\nu}$,

$$\nu = 1/y_t \quad (2.266)$$

This argument justifies the scaling relations but it has one flaw, the fact that one can easily verify that the assumption in (2.239) does not hold in general. Some other assumptions are needed.

The general procedure

The renormalisation group procedure is based on the construction of coarse-grained variables. Above we focused on the example of a spin model, as a particularly clear problem, and we constructed Kadanoff's block spins. Here we repeat the same procedure in slightly more general terms.

Compute the Hamiltonian by expressing the original energy in terms of the coarse-grained variables. If new terms are generated through the coarse-graining procedure argue that they are either irrelevant, that is to say, they become less and less important

after successive iteration of the coarse-graining, or that only a few such new terms are generated. Collect all the adimensional coupling constants in $[K] = (K_1, \dots, K_n)$ and follow their renormalisation, $[K'] = R_b[K]$, calling R_b the renormalisation transformation using a coarse-graining scale ba , with a the lattice spacing.

The new coupling constants, $[K']$, and the new correlation length, $\xi[K']$, become functions of the previous ones

$$[K'] = R_b[K] , \quad \xi([K']) = \xi([K])/b . \quad (2.267)$$

With each iteration we are observing the system at a new scale – the scale of the blocks instead of the original one – and we are deriving the effective energy that describes the system at this scale. The *flow* generated in this way – in the space of models that translates into the space of parameters once new terms in the energy are no longer generated – approaches a fixed point that represents the critical point. At the critical point the renormalisation procedure must reach a stable fixed point. This means that the parameters should no longer change

$$[K'^*] = R_b[K^*] = [K^*] , \quad (2.268)$$

and the correlation length

$$\xi([K']) = \xi([K])/b , \quad (2.269)$$

should also reach a fixed value

$$\xi([K^*]) = \xi([K^*])/b , \quad (2.270)$$

and this can be satisfied by

$$\xi^* = 0 \quad \text{or} \quad \xi^* \rightarrow \infty \quad (2.271)$$

only. The former is called a *trivial* and the latter the *critical* fixed point.

Critical behaviour is given by the behaviour of the trajectories in parameter space close to the fixed points. Linearising the transformations close to one of them

$$\begin{aligned} K'_\alpha(b) - K_\alpha^* &= R_{\alpha\beta}(b)(K_\beta - K_\beta^*) \implies \\ \delta K'_\alpha(b) &= R_{\alpha\beta}(b)\delta K_\beta \quad \text{with} \quad R_{\alpha\beta}(b) = \left. \frac{\partial K'_\alpha(b)}{\partial K_\beta} \right|_{[K^*]} \end{aligned} \quad (2.272)$$

(sum over repeated indices is assumed). This is a vectorial linear equation and, to solve it, we diagonalise the matrix $R_{\alpha\beta}(b)$ using its eigenvalues $\lambda_i(b)$ and (left) orthonormal eigenvectors $u_\alpha^i(b)$, with i a label that identifies each of them,

$$u_\alpha^i(b) R_{\alpha\beta}(b) = \lambda_i(b) u_\beta^i(b) \quad \text{for each } i \quad (2.273)$$

$$u_\beta^i(b) u_\gamma^i(b) = \delta_{\beta\gamma} \quad \text{summed over } i \quad (2.274)$$

Multiplying now Eq. (2.272) on the left by u_α^i :

$$\begin{aligned} u_\alpha^i(b) \delta K'_\alpha(b) &= u_\alpha^i(b) R_{\alpha\beta}(b) u_\beta^j(b) u_\gamma^j(b) \delta K_\gamma \\ &= \lambda_i(b) \delta^{ij} u_\gamma^j(b) \delta K_\gamma \\ &= \lambda_i(b) u_\alpha^i(b) \delta K_\alpha \end{aligned} \quad (2.275)$$

which, for the “rotated” couplings $\kappa_i \equiv u_\alpha^i \delta K_\alpha$, reads

$$\delta \kappa'_i(b) = \lambda_i(b) \delta \kappa_i \quad (2.276)$$

or in matricial notation

$$\mathbb{U}(b) \delta \mathbb{K}'(b) = \mathbb{U}(b) \mathbb{R}(b) \mathbb{U}^T(b) \mathbb{U}(b) \delta \mathbb{K} = \mathbb{D}(b) \mathbb{U}(b) \delta \mathbb{K} \quad (2.277)$$

exploiting the fact that $\mathbb{U}^T \mathbb{U} = \mathbb{I}$. If $[K^*]$ lie on a critical surface, then a subset of the eigenvectors span the space tangential to the critical surface at $[K^*]$.

From the composition of the RG transformation we know that $\lambda_i(b) = b^{y_i}$, thus

$$y_i = \frac{d \ln \lambda_i(b)}{d \ln b} \quad (2.278)$$

Indeed, although for the treatment of models on a lattice we used integer b , it is convenient to think of b as being $1^+ = e^{\delta\tau}$, where $\delta\tau \rightarrow 0^+$, in which case the iteration procedure becomes continuous, as well as the evolution of the effective couplings $[K_b]$, driven by b or the “time” variable τ . This justifies having written a differential equation.

One characterises the RG (exponent) eigenvalues y_i by their sign:

- $y_i > 0$ – *relevant*, with the corresponding $\kappa_i(b)$ coupling growing under coarse-graining, i.e., getting away from the fixed point
- $y_i < 0$ – *irrelevant*, with the $\kappa_i(b)$ coupling vanishing under coarse-graining, i.e., approaching the fixed point
- $y_i = 0$ – *marginal*, with the flow of the $\kappa_i(b)$ coupling determined by the higher order terms in the couplings of the RG transformation.

Some comments are in order:

- An RG transformation cannot change the phase of the system, since dilution cannot generate order from disorder and vice versa.
- The critical points are repulsive fixed points of the RG.
- If we start above the critical temperature then the system should evolve to the free fixed point, characterised by $T \rightarrow \infty$.

- In contrast, if we start below the critical temperature then we should end up at the “ground state” fixed point $T = 0$.
- If the flow begins on the critical surface it then stays on this surface.

Differential equations for the evolution of these constants can then be written, and one can define the *β -function*

$$\beta(K) = \frac{d \ln K_b}{d \ln b} \quad (2.279)$$

giving the variation of the coupling constant close to the fixed point under an infinitesimal transformation of the scale of observation. At the critical point, which is a fixed point of the transformation, $\beta(K_c) = 0$, since then K does not change under iteration.

One still needs to prove that Kadanoff’s assumptions are valid. In the TD, cases in which these transformations can be carried out will be discussed, and explicit values for the critical exponents evaluated.

A renormalisation transformation is a scale transformation that leaves the partition function invariant. Since the thermodynamic properties of a system are governed by the partition function, the physics is preserved.

2.9 Geometric description of second order phase transitions

Thermal features of physical systems and in particular their second order phase transitions can in many cases be described by the structural properties of connected geometric objects, or clusters. The increase of the correlation length near the critical point is paralleled by the increase of the average cluster radius, and its divergence to the formation of an infinite cluster. Percolation theory is the natural framework to study the properties of cluster-like structures.

2.9.1 Geometric and FK clusters

Take an Ising model in its ordered low temperature phase. As temperature is taken to approach T_c larger and larger fluctuations arise and regions of the samples reverse with respect to the background. Very early researchers tried to relate the thermodynamic phase transition to the percolation of, initially, the *geometric domains* in which parallel nearest neighbour spins on the lattice are attached together. Computer simulations proved that although in $d = 2$ these clusters do indeed undergo *critical percolation* at T_c in $d = 3$ they percolate at a T_p which is lower than T_c . Moreover, the critical exponents predicted by critical percolation of these clusters in $d = 2$ were not in agreement with the ones derived from the non-analyticities of the free-energy density.

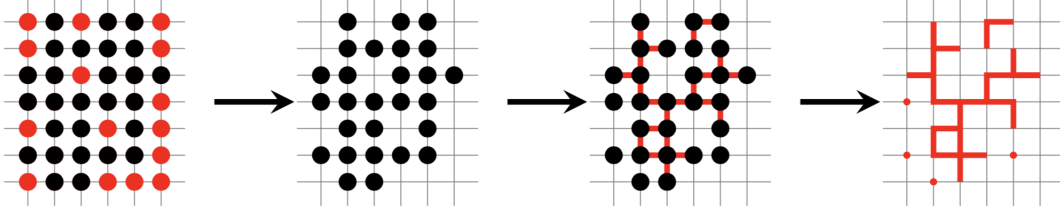


Figure 2.28: Sketch of the construction of a FK cluster. A domain is identified. The bonds between nearest-neighbour aligned spins (represented with black dots on the lattice sites) are erased using the FK procedure. Two FK disconnected clusters remain. The surviving bonds are highlighted on the edges of the lattice. The figure is taken from [46].

It was later noticed that the relevant clusters that characterise the fluctuations close to the critical point are not the obvious geometric domains (which are too large) but, instead, probabilist structures constructed using temperature dependent bond weights, which go under the name of *Fortuin-Kasteleyn clusters* [45]. The thermodynamic and geometric formalisms lead to the same criticality: the critical temperatures T_c as well as the corresponding critical exponents coincide.

The Fortuin-Kasteleyn (FK) clusters are constructed as follows. Starting with a spin domain, one first draws all bonds linking nearest-neighbour spin on the cluster and then erases bonds with a temperature dependent probability $e^{-\beta J}$. In such a way, the original bond-cluster typically diminishes in size and may even get disconnected. As example of the construction of FK clusters from the geometric ones in the $2d$ Ising model is displayed in Fig. 2.28 (figure extracted from [46]). Under the Fortuin-Kasteleyn (FK) transformation, the partition sum of the Ising model can be written as summation over such random cluster configurations:

$$\mathcal{Z} = \sum_G (e^{2K} - 1)^{N_{\text{bond}}} \left(\frac{1}{2} \right)^{N_c} \quad (2.280)$$

with N_{bond} the number of bonds in the cluster and N_c the number of clusters in the configuration and the summation runs over all possible subgraphs of the lattice.

At the critical point the FK clusters are *fractal* with *fractal dimension* $D_{\text{FK}} = (d + 2 - \eta)/2$, where η is the usual static critical exponent. A possible definition of the fractal dimension is given by the *box counting construction* in which one counts the number of boxes of linear size ϵ that are needed to cover the set and computes $D = \lim_{\epsilon \rightarrow 0} [\ln N(\epsilon) / \ln(1/\epsilon)]$. Another way to evaluate D is by relating the *mass of the cluster*, or just the number of elements in it, to its radius of gyration *via* $M \sim R_g^D$. As an example, for the bidimensional critical Ising class $\eta = 1/4$ and $D_{\text{FK}} = (2 + 2 - 1/4)/2 = 15/8$.

Accordingly, the equilibrium two-point correlation can also be written as

$$C(r) = r^{-2(d-D_{\text{FK}})} f(r/\xi) \quad (2.281)$$

The FK clusters are used in improved Monte Carlo methods tailored to beat *critical slowing down* of the fact that a single flip stochastic evolution becomes exceedingly slow close to the critical point. In *cluster Monte Carlo* Swendsen-Wang methods [?] full clusters of spins are updated at each time step with a probability that respects detailed balance, thus ensures the approach to thermal equilibrium, but is much faster in terms of computer time, than naive ones.

2.9.2 Percolation

The understanding of *fluid flow in porous media* needs, as a first step, the understanding of the static geometry of the connected pores. The typical example, that gave the name to the problem, is coffee percolation, where a solvent (water) filter or trickle through the permeable substance that is the coffee grounds and in passing picks up soluble constituents (the chemical compounds that give coffee its color, taste, and aroma).

Another problem that needs the comprehension of a static random structure is the one of *conduction across a disordered sample*. Imagine that one mixes randomly a set of conducting and insulating islands. Whether the mix can conduct an electric current from one end to the other of the container is the question posed, and the answer depends on the structure formed by the conducting islands.

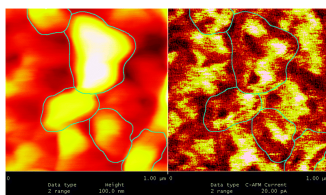


Figure 2.29: A measurement of the topography (left) and local current (right) in an inhomogeneous mixture of good and bad conducting polymers [53]. The brighter the zone the more current passing through it. Several grains are contoured in the left image.

Percolation [49, 50, 51, 52] is a simple *geometric* problem with a *critical threshold*. It is very helpful since it allows one to become familiar with important concepts of *critical phenomena* such as fractals, scaling, and renormalisation group theory in a very intuitive way. Moreover, it is not just a mathematical model, since it is at the basis of the understanding of the two physical problems mentioned above among many others.

In this Section we describe its simplest setting as well as some of its variants.

Dilution

Site dilute lattices with missing vertices are intimately related to the site percolation problem. Imagine that one builds a lattice by occupying a site with probability p (and not occupying it with probability $1 - p$). For $p = 0$ the lattice will be completely empty

while for $p = 1$ it will be totally full. For intermediate values of p , on average, order pL^d sites will be occupied, with L the linear size of the lattice. *Site percolation theory* is about the geometric and statistical properties of the structures thus formed. In particular, it deals with the behaviour of the clusters of nearest neighbour occupied sites.

Similarly, one can construct bond dilute lattices and compare them to the *bond percolation* problem.

The site percolation problem describes, for example, a binary alloy or dilute ferromagnetic crystal, also called a doped ferromagnet. The question in this context is how much dilution is needed to destroy the ferromagnetic order in the sample at a given temperature. The bond percolation problem corresponds to a randomly blocked maze through which the percolation of a fluid can occur. Many other physical problems can be set in terms of percolation: the distribution of grain size in sand and photographic emulsions, the vulcanisation of rubber and the formation of cross-linked gels, the propagation of an infection, etc.

The main interest lies on characterising the statistical and geometric properties of the *clusters* on a lattice of linear size L as a function of the probability p . The clusters are connected ensembles of nearest neighbour sites. Their easiest geometric property is their *size*, defined as the number of sites that compose them. Other geometric properties are also interesting and we will define them below.

The percolation problem is specially interesting since it has a threshold phenomenon, with a critical value p_c at which a first spanning cluster that goes from one end of the lattice to the opposite in at least one of the Cartesian directions appears. For $p < p_c$ there are only finite clusters, for $p > p_c$ there is a *spanning cluster* as well as finite clusters.

The first natural question is whether the value p_c depends on the particular sample studied or not, that is to say, whether it suffers from *sample-to-sample fluctuations*. All samples are different as the sites erased or the links cut are not the same. The threshold value is therefore a random variable and it does not take the same value for different samples. The ‘surprise’ is that the mean-square deviations of p_c from its mean value vanish as a power law with the system size,

$$\delta_{p_c}^2(N) \equiv \frac{1}{\mathcal{N}} \sum_{k=1}^{\mathcal{N}} (p_c^{(k)} - \bar{p}_c)^2 \simeq C^2 N^{-\nu}, \quad \bar{p}_c \equiv \frac{1}{\mathcal{N}} \sum_{k=1}^{\mathcal{N}} p_c^{(k)}, \quad (2.282)$$

with k labelling different measurements and \mathcal{N} counting its total number. N the number of sites in the sample. (C turns out to be 0.54 and $\nu = 1.3$ in $d = 2$.) In the infinite system size limit, p_c does not fluctuate from sample to sample.

One can then count the number of sites belonging to the largest cluster and compare this number to the total number of sites in the sample:

$$r_L(p) \equiv \frac{N_{\max}(p)}{N}. \quad (2.283)$$

This is, again, a fluctuating quantity that, in the infinite system size limit does no longer

fluctuate and defines

$$r_\infty \equiv \lim_{L \rightarrow \infty} r_L(p) . \quad (2.284)$$

The precise definition of the *critical threshold* p_c involves the infinite size limit and it can be given by

$$r_\infty(p) = \lim_{L \rightarrow \infty} r_L(p) = \begin{cases} 0 & \text{for } p < p_c \\ > 0 & \text{for } p > p_c \end{cases} \quad (2.285)$$

where $r_\infty(p)$ denotes the fraction of sites belonging to the largest cluster in the finite lattice with linear size L . In the magnetic application of percolation, this means that the magnetisation vanishes for $p < p_c$ and it takes the value that the magnetisation takes on the largest cluster for $p > p_c$ (as in both cases the magnetisation on the finite clusters is independent and averages to zero).

An equivalent definition of the *critical threshold* p_c is given by

$$P_\infty(p) = \lim_{L \rightarrow \infty} P_L(p) = \begin{cases} 0 & \text{for } p < p_c \\ 1 & \text{for } p > p_c \end{cases} \quad (2.286)$$

where $P_L(p)$ denotes the probability of there being a percolating cluster in the finite lattice with linear size L .

The percolation threshold p_c depends on the lattice geometry and its dimensionality. Moreover, it is not the same for bond percolation and site percolation. Exact results are known for special lattices as the Cayley tree. Examples of how these results are found are given in [49]. Numerical data for finite dimensional lattices are complemented by rigorous upper and lower bounds and the outcome of series expansions for the mean cluster value. Harris showed that $p_c \geq 1/2$ for the bond percolation problem on a planar square lattice and the numerics suggests $p_c = 1/2$. Fisher put several bounds on p_c on various $2d$ lattices for the site and bond problem. In particular, $p_c \geq 1/2$ for site percolation on planar regular lattices with no crossings. The values of p_c for some bidimensional lattices are given in Table 3.

The value of the percolation threshold, decreases for increasing spatial dimensionality. For cubic lattices, $p_c = 1$ in $d = 1$, $p_c \simeq 0.59$ in $d = 2$ and $p_c \simeq 0.32$ in $d = 3$. This implies that the case $p = 1/2$ is below threshold in $d = 2$ for all the lattices in Table 3 but above threshold in the cubic lattice in $d = 3$.

If one conducts a laboratory or a numerical experiment in a finite size array, the majority of the threshold values measured fall in a window centred at p_c of width $\delta(N)$. The infinite size limit is estimated by first taking the average at finite N and then performing an infinite size *extrapolation*

$$\bar{p}_c(N) = p_c + CN^{-\gamma} . \quad (2.287)$$

As, in general, the value $p_c = p_c(N \rightarrow \infty)$ cannot be computed analytically, numerical simulations are used to obtain it. The best algorithm to find the largest cluster is given in [54].

Lattice	n	p_c^{site}	p_c^{bond}
Honeycomb	3	0.70	0.65
Square	4	0.59	0.50
Kagomé	4	0.65	
Bowtie-a	5	0.55	
Triangular	6	1/2	0.35

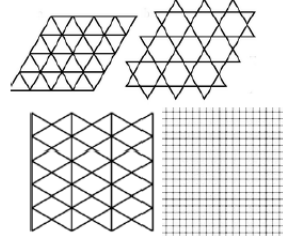


Table 3: Connectivities, n , and critical thresholds for percolation, p_c , for several two dimensional lattices shown in the figure on the right (the honeycomb lattice is missing). (In the case of the bow-tie lattice, $n = 5$ is the average between the connectivities of the sites with connectivities 4 and 6.)

The problem is quantitative characterised by a number of observables that depend on the *control parameter* p . The critical threshold p_c plays a role similar to the one of a thermodynamic transition in a physical problem. Several observables vanish and behave as *order parameters* and others diverge and behave as *susceptibilities* when the control parameter p approaches its critical value. Moreover, they do *algebraically* as in usual critical phenomena. Indeed, there is a large degree of universality in random percolation models: p_c is model dependent but the critical exponents depend only on the spatial dimension of the lattice. Microscopic details do not influence the behaviour close to p_c .

The cluster interfaces are also an interesting characterisation of the geometry of the clusters. The *domain wall* of a spin cluster is its external and internal contour, constructed as follows. One first generates a *dual lattice* by placing a site at the centre of each plaquette of the original lattice. Next, the links on the dual lattice that cross broken bonds on the original lattice are joined together. In this way, one finds a closed loop on the dual lattice that runs along the external, and possibly also internal, boundary of a spin cluster. The *hull* of a cluster is restricted to the external part of the contour, that is to say, one excludes the contribution of the holes of the cluster. The *hull-enclosed area* is the area, i.e. the total number of sites, inside the hull (the holes within the domains are thus filled). The lengths of the different contours existing on the dual lattice are computed by counting the number of broken bonds crossed by the boundary. The *external perimeter* is built by closing the narrow gates of the hull, making in this way a smoother version of the contour by eliminating the deep fjords.

Take a geometric object with a given property (area, length, etc.) generically called x that takes values X . For large but not necessarily infinite L , close to criticality, its probability distribution per lattice site or *number density*, $n_x(X)$, takes the form

$$n_x(X) \simeq X^{-\alpha_x} f_x(X^{\sigma_x}(p - p_c)) + n_{\text{fs}}(X/L^{D_x}). \quad (2.288)$$

The second term in the rhs are the finite size corrections while the first term is the only one remaining in the infinite size limit $L \rightarrow \infty$. The scaling function f_x is required to decay fast (it could be an exponential) for large arguments and to approach a constant

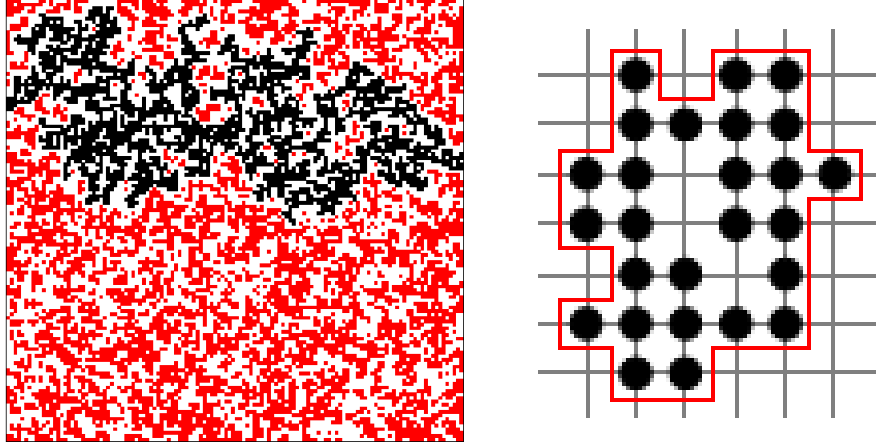


Figure 2.30: A percolating cluster highlighted in black and the hull of a cluster [48]. The domain wall will add to the red line the internal interface and the external perimeter will close the two fjords.

for small arguments. At p_c the decay is purely algebraic. $(p - p_c)^{1/\sigma_x}$ acts as cut-off and controls the crossover from a behaviour of “critical clusters” (power-law distributed) to that of non-critical clusters. A way to check this scaling form is to search *data collapse* by plotting

$$X^{\alpha_x} n_x(X) \quad \text{vs} \quad X^{\sigma_x} (p - p_c) \quad (2.289)$$

for the best choices of α_x and σ_x . The master curve yields the scaling function f_x that depends on the observable x as also do the exponents α_x and σ_x . For example, $n_x(X)$ can be the number of clusters with area $s = S$, $N_s(S)$, normalised by the number of lattice sites, $n_s(S) = N_s(S)/N$.

Exercise 2.22 Set the percolation problem on a one dimensional lattice. Show that $p_c = 1$. Demonstrate Eq. (2.288) for x being the cluster size s in the infinite system size limit, $L \rightarrow \infty$. Show that $\sigma_s = 1$ and find the scaling function $f_s(y)$. Identify an exponential cut-off and compute the characteristic length s_ξ from its decay.

The probability that a site belong to any cluster is, on the one side, equal to p and, on the other side, it can be written in terms of $n_s(S)$. For $p < p_c$ there are only finite size clusters and the *sum rule*

$$\sum_{S=1}^{\infty} S n_s(S) = p \quad (2.290)$$

holds.

Exercise 2.23 Verify the sum rule (2.290) in $d = 1$.

One can prove that the average size of the cluster diverges when approaching p_c from below, see [51] for an explicit calculation, and the way in which it does is also characterised

by a critical exponent

$$\langle S \rangle(p) \simeq |p_c - p|^{-\gamma_s} . \quad (2.291)$$

On the other side, one can use the definition and scaling Ansatz for $n_s(S)$ to show that $\langle S \rangle(p) \simeq |p - p_c|^{(\alpha_s - 3)/\sigma_s}$. Therefore, the equivalence of these two expressions requires

$$\gamma_s = \frac{3 - \alpha_s}{\sigma_s} . \quad (2.292)$$

Note that $\gamma_s > 0$ implies $\alpha_s < 3$.

The *pair connectedness correlation function* $g(\vec{r})$ is defined as the probability that a site at distance \vec{r} from an occupied site belong to the same cluster. The *correlation length* can be computed from

$$\xi^2 = \frac{\sum_{\vec{r}} r^2 g(\vec{r})}{\sum_{\vec{r}} g(\vec{r})} . \quad (2.293)$$

Close to the threshold the correlation length diverges as

$$\xi \simeq |p - p_c|^{-\nu} . \quad (2.294)$$

Exercise 2.24 Show that in $d = 1$, $g(r) = p^r$ and $\xi = -1/\ln p \simeq (1 - p)^{-1}$ close to p_c .

Another sum rule that one can easily show is $\sum_{\vec{r}} g(\vec{r}) = \langle S \rangle$.

The *strength of the percolating cluster*, $r(p)$, measures the proportion of sites on the lattice that belong to the infinite cluster and plays the role of an *order parameter* for the percolation transition. It vanishes as

$$r(p) \simeq (p - p_c)^\beta \quad \text{for} \quad p \gtrsim p_c \quad (2.295)$$

and the *transition is continuous*. For $p > p_c$ an occupied site can belong to the infinite cluster or it can be in one of the many finite clusters. Therefore, the sum rule (2.290) is modified to

$$r(p) + \sum_{S=1}^{\infty} S n_s(S) = p \quad (2.296)$$

where the sum runs only on finite clusters. From (2.295) and (2.296) with the scaling form of $n_s(S)$ one shows

$$r(p) \simeq |p - p_c|^{(\alpha_s - 2)/\sigma_s} \quad \Rightarrow \quad \beta = \frac{\alpha_s - 2}{\sigma_s} . \quad (2.297)$$

Several geometric properties of the clusters can also be studied. Take a site at \vec{r}_i in a cluster. The *centre of mass* of a cluster with mass S and the *radius of gyration* of the same cluster are

$$\vec{r}_{\text{cm}} = S^{-1} \sum_{j=1}^S \vec{r}_j \quad R_g^2 = S^{-1} \sum_{j=1}^S |\vec{r}_j - \vec{r}_{\text{cm}}|^2 \quad (2.298)$$

Exercise 2.25 Prove that $R_g^2 = (2S^2)^{-1} \sum_{ij} |\vec{r}_i - \vec{r}_j|^2$ with \vec{r}_i and \vec{r}_j the positions of two sites i and j on the cluster.

The *mass* of the percolating cluster, that is to say the number of sites S in it, depends on L the linear size of the system. One can write it as $M_L(p) = L^d P_L(p)$ where $P_L(p)$ was defined above in the infinite size limit and its definition is now extended to finite system size. At p_c the correlation length diverges and the percolating cluster is a *fractal* object. Accordingly, $M_L(p_c)$ does not scale as L^d but, instead, as

$$M_L \simeq L^{D_s} \quad \text{for} \quad L \ll \xi \quad (2.299)$$

with D_s a *fractal dimension*. If, instead, the linear size of the system is larger than the correlation length, one can divide the full system in cubic boxes of linear size $\ell \approx \xi$. Inside each box, the cluster is fractal and its mass scales as $M_\ell \approx \ell^{D_s} = \xi^{D_s}$. Adding together the independent contributions from all boxes,

$$M_L \simeq (L/\xi)^d \ell^{D_s} \quad \text{for} \quad L \gg \xi \quad (2.300)$$

These two limits can be joined into a single equation

$$M_L(\xi) \simeq L^{D_s} m\left(\frac{L}{\xi}\right) \quad \text{with} \quad m(y) \simeq \begin{cases} \text{const} & y \ll 1 \\ y^{d-D_s} & y \gg 1 \end{cases} \quad (2.301)$$

These relations imply that large clusters at $p \neq p_c$ appear fractal at length scales smaller than ξ and regular at longer length scales.

For generic clusters of size S and radius of gyration R_g the relation (2.299) generalises to

$$S \simeq R_g^{D_s} \quad (2.302)$$

Equation (2.301) is an example of finite size scaling, that for a generic observable X takes the form

$$X(p, L) = \xi^{-\beta_x/\nu} F_x[(p - p_c)L^{1/\nu}] = \xi^{-\beta_x/\nu} F_x[(L/\xi)^{1/\nu}] \quad (2.303)$$

where β_x is a quantity-dependent critical exponent and ν is the exponent of the power law divergence of the incipient cluster size. The scaling function F_x should have the limits $F_x(y \ll 1) = 1$ and $F_x(y \gg 1) = y^{-\beta_x/\nu}$.

Many quantities diverge at p_c and they can be expressed as a sum over clusters of all sizes. The main contribution to these sums comes from the size scale $s_\xi \simeq |p - p_c|^{-1/\sigma}$, as can be read from the scaling form of $n_s(S)$. Since one also expects this size to be given by $s_\xi \simeq \xi^D$ in terms of the fractal dimension D , one has

$$\xi^{D_s} \simeq \xi^{1/(\nu\sigma_s)} \quad \Rightarrow \quad D_s = 1/(\nu\sigma_s) \quad (2.304)$$

As in standard phase transitions, the exponents α_x , σ_x , β , ν depend on the dimension of space but do not depend on the lattice geometry. In dimension one and two they take

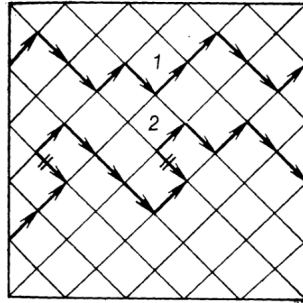


Fig. 26. Directed white bonds are shown by the solid lines with arrows; black bonds are shown by the thin lines. Flame propagates from left to right along path 1, and cannot propagate along path 2. Two segments of path 2 on which the fire would have to move against the wind are marked by two dashes.

Figure 2.31: Two paths of occupied bonds in the directed percolation problem, one along which a fire propagates from left to right and another one that does not allow propagation.

specially simple values. They are integer in $d = 1$ and fractions in $d = 2$. In particular, the fractal dimension of the clusters areas is $D_s = 1$ in $d = 1$ and $D_s = 91/48$ in $d = 2$. The interfaces (hulls, external perimeters, etc.) also have fractal properties that can be characterised with fractal exponents.

Physical phase transitions also admit a geometric description. In the 70s the surprise was that the clusters that characterise the phase transition are not the geometric ones. The idea was to study the clusters of the reversed fluctuations in the Ising model. While these percolate at T_c in $2d$, they do at a T_p that is strictly below T_c in $3d$. This indicates that the geometric clusters are not the correct one to describe criticality. Fortuin and Kasteleyn proposed to erase or keep the links between points belonging to the clusters with a probability distribution that depends on temperature. Having done this, the clusters reduce their size and while they still percolate at T_c in $2d$ they do at a higher temperature in $3d$ that coincides with T_c . The analysis of their critical exponents (α , σ , ν , ...) proved that they yield the correct thermodynamic exponents (β , γ , δ , ...).

Directed percolation

A figure extracted from [49] shows the definition of the directed percolation problem.

Away from the lattice

It is also possible to define percolation problems on the continuous space. This can be done, for example, by setting circles of equal radius R randomly on a plane. Two disks are considered to be nearest-neighbours if the centre of one falls into the other one. The path linking such centres then identified. Remote disks can be then connected via these paths and the question is whether the longest path runs from one border of the sample to an opposite one. In this problem there are, *a priori*, two independent parameters: the

concentration of the disks, i.e. their number over the size of the plane, N/L^2 , and their radius, R . The control parameter turns out to be the dimensional quantity NR^2/L^2 . This model is used to describe conduction in impurity semiconductors [49].

2.9.3 Mapping to the Potts model

The bond percolation problem can be easily mapped to the Potts model [95, 96], a simple generalisation of the Ising model,

$$H_J[s_i] = \sum_{\langle ij \rangle} \delta_{s_i s_j} \quad (2.305)$$

with spins s_i that take q values, $s_i = 1, \dots, q$ and δ_{ab} the Kronecker delta function, $\delta_{ab} = 1$ if $a = b$ and $\delta_{ab} = 0$ otherwise. The case $q = 2$ corresponds to the Ising model. In the limit $q \rightarrow 1$ the bond percolation properties are recovered in the way that we will describe below. This results is due to Kasteleyn and Fortuin [55, 56]. This connection between these two apparently different problems illustrates the use of an *analytical continuation* from integer q to real q as a tool to solve one problem (percolation) using a non-physical extension of another one (the Potts model). A similar mapping, though slightly more complicated, exists for the site percolation problem.

Each configuration of the bond percolation problem is associated to a sub-graph G' of the embedding graph G on which the problem is defined, that appears with probability

$$\pi(G') = p^{E(G')} (1 - p)^{M - E(G')} \quad (2.306)$$

where $E(G')$ is the number of edges in G' and M is the total number of edges in the original graph. Each sub-graph G' is not necessarily formed by a single component, so we will later call $c(G')$ the number of clusters in the sub-graph G' . (A cluster is defined as the ensemble of edges that are occupied and joined by a vertex on the lattice.) Any averaged property of the bond percolation problem can then be computed as

$$\langle A \rangle = \sum_{G'} A(G') \pi(G') = \sum_{G'} A(G') p^{E(G')} (1 - p)^{M - E(G')} \quad (2.307)$$

A could be, for example, the number of clusters.

The partition function of the Potts model reads

$$\begin{aligned} Z_J &= \sum_{\{s_i\}} e^{-\beta H_J[\{s_i\}]} = \sum_{\{s_i\}} e^{\beta J \sum_{\langle ij \rangle} \delta_{s_i s_j}} = \sum_{\{s_i\}} \prod_{\langle ij \rangle} e^{\beta J \delta_{s_i s_j}} \\ &= \sum_{\{s_i\}} \prod_{\langle ij \rangle} (1 + v \delta_{s_i s_j}) \end{aligned} \quad (2.308)$$

with

$$v = e^{\beta J} - 1. \quad (2.309)$$

The last identity can be readily checked, by considering the two possible outcomes for each factor in the product:

$$s_i = s_j \quad \Rightarrow \quad e^{\beta J} , \quad (2.310)$$

$$s_i \neq s_j \quad \Rightarrow \quad 1 . \quad (2.311)$$

Note that if one took $q = 1$, that is to say if $s_i = 1$ for all i , the partition function is identical to one, $Z_J = 1$.

The product $\prod_{\langle ij \rangle} (1 + v\delta_{s_i s_j})$ under the sum $\sum_{\{s_i\}}$ can now be expanded. Each term in the resulting sum is represented by a subgraph on the lattice in which all its edges coincide with the $v\delta_{s_i s_j}$ factors in the term. Let us explain how this works listing the first terms in the sum for a square lattice:

- the first term is just the product of number-of-edges= M 1s and equals 1. The sum over the spin configurations is fully unconstrained and yields a factor q^N .
- the second kind of term is the product of $M-1$ 1s and a factor $v\delta_{s_i s_j}$ and equals $v\delta_{s_i s_j}$. There are M ways of choosing this non-trivial factor. Moreover, it will give a non-vanishing result only if $s_i = s_j$ and there are q possibilities for this to happen. All these terms can be associated to isolated clusters with only two sites on the lattice. All the other spins on the graph are unconstrained and the sum over their configurations yields a factor q^{N-2} . Therefore, these terms are accompanied by an overall q^{N-1} factor.
- the third kind of term is the product of $M-2$ 1s and two factors $v\delta_{s_i s_j}$ and $v\delta_{s_k s_l}$. There are now three options for the two edges $\langle ij \rangle$ and $\langle kl \rangle$. They can be separated, when all indices are different, yielding two isolated clusters with two sites each. They can be joined together by one site, when e.g. $i \neq j = k \neq l$, and form a single cluster with three sites. They cannot be such that $i = k$ and $j = l$ since there is no double counting of links. The Kronecker delta imposes that all the spins on each individual cluster in the graph take the same value (out of the q possible ones) while the spins that are not on vertices belonging to the clusters are free to take any of the q possibilities.

The construction goes on along these lines.

The product is then represented as a sum over all possible subgraphs on the original graph. Each edge on each sub-graph is accompanied by a factor v . The sum over the spin configurations yields a factor q for each cluster in the sub-graph and a factor q^n with n the number of sites that do not belong to any cluster. In short,

$$Z_J = \sum_{G'} v^{E(G')} q^{c(G')} \quad (2.312)$$

where we called $E(G')$ the number of edges and $c(G')$ the number of clusters in the sub-graph G' , including as independent single-site clusters the sites that are alone. This model, for generic q is called the *random cluster model*.

The free-energy density of the Potts model is

$$-\beta f_J = N^{-1} \ln Z_J = N^{-1} \ln \sum_{G'} v^{E(G')} q^{c(G')} \equiv N^{-1} \ln \langle q^{c(G')} \rangle , \quad (2.313)$$

where we introduced the symbol $\langle\langle \dots \rangle\rangle$ to indicate the average over the subgraphs with weight $v^{E(G')}$. Now, we approximate this average in the $q \simeq 1$ limit:

$$\ln \langle\langle q^{c(G')} \rangle\rangle = \ln \langle\langle e^{\ln q^{c(G')}} \rangle\rangle = \ln \langle\langle e^{c(G') \ln q} \rangle\rangle . \quad (2.314)$$

Using

$$\ln q = \ln[1 + (q - 1)] \simeq (q - 1) + O((q - 1)^2) \quad (2.315)$$

then

$$\ln \langle\langle q^{c(G')} \rangle\rangle \simeq \ln \langle\langle e^{c(G')(q-1)} \rangle\rangle \simeq \ln [1 + \langle\langle c(G')(q - 1) \rangle\rangle] \simeq (q - 1) \langle\langle c(G') \rangle\rangle \quad (2.316)$$

Therefore,

$$-\beta f_J = N^{-1} \ln Z_J \simeq (q - 1) \langle\langle c(G') \rangle\rangle = (q - 1) \sum_{G'} v^{E(G')} c(G') . \quad (2.317)$$

The remaining average will be then average number of clusters in the percolation problem provided the statistical weight $v^{E(G')}$ in the Potts model be proportional to the one in the percolation problem (apart from an irrelevant constant $(1 - p)^M$ that does not depend on the sub-graph configuration)

$$\left(\frac{p}{1 - p} \right)^{E(G')} = v^{E(G')} \quad (2.318)$$

that implies

$$v = \frac{p}{1 - p} \quad \text{or} \quad p = 1 - e^{-\beta J} . \quad (2.319)$$

2.10 Models with continuous symmetry

The energy of spin models with continuous variables, such as the XY, Heisenberg or generic $O(n)$ models introduced in (2.3) and (2.4) in the absence of an applied field ($\vec{h} = \vec{0}$), is invariant under the simultaneous rotation of all the spin variables:

$$s_i^a \mapsto R^{ab} s_i^b . \quad (2.320)$$

(R^{ab} are the n^2 elements of a rotation matrix in an n -dimensional space. As all rotation matrices in real space it has real elements and it is orthogonal, that is to say, $R^T = R^{-1}$ with $\det R = \pm 1$.) This is a *continuous global symmetry* to be confronted to the *discrete global* spin reversal invariance, $s_i \mapsto -s_i$, of the Ising case. In group theoretical terms, the continuous symmetry is $O(n)$ and the discrete one is Z_2 .

The spontaneous magnetisation at zero temperature can point in any of the infinite equivalent directions constrained to satisfy (2.4). This gives rise to an *infinite degeneracy of ground states* that are translational invariant (in real space). These equilibrium states are controlled by a continuous variable, determining the direction on the n -dimensional

hypersphere of radius 1. The effect of thermal fluctuations depends on the dimensions of the real space d and the vector n . We analyse them below, especially in the case of $d = n = 2$.

In the Peierls argument, the energy of the low-lying excitations with respect to the ground state are one of the ingredients to estimate the free-energy variation under temperature fluctuations. For an Ising model the reversal of a domain has an energetic cost which is proportional to its surface. Instead, for continuous spins the energetic cost can be made arbitrarily small by turning the spins infinitesimally from site to site over a very long distance. It is therefore much easier to have such long-wave variations in the continuous models. This is related to the fact that the $2d$ XY model cannot sustain long-range order at any non-zero temperature.

In general, an excitation with vanishing cost in the long wave-length limit is called a *soft mode* and it is said to be *gapless*. (In quantum field theory gapless is also referred to as massless, while gapped are also called massive.)

First of all one may want to compute the average magnetisation $\vec{m} = \langle \vec{s}(\vec{r}) \rangle = \lim_{\vec{h} \rightarrow \vec{0}} \langle \vec{s}(\vec{r}) \rangle_{\vec{h}}$ where \vec{h} is a pinning field. Mermin's exact calculation [57, 58] (that we will not present here, see [8] for a description of the proof) leads to $\vec{m} = \vec{0}$ at all non-vanishing temperatures in the thermodynamic limit, excluding usual magnetic order at any finite temperature in this system. Hence,

there is no spontaneous symmetry breaking, and thus no long-range order, in the $2d$ XY model. The potential order parameter $\vec{m}(\vec{r}) = \langle \vec{s}(\vec{r}) \rangle$ vanishes at all temperatures in the thermodynamic limit.

Exercise 2.26 Study Mermin's proof [57, 58]. Look also at the proof of the bound on the spatial correlation function $\langle \vec{s}_i \cdot \vec{s}_j \rangle \leq (A/2) |\vec{r}_i - \vec{r}_j|^{(1-\epsilon)/(2\pi A)}$ of McBryan & Spencer [59, 60]. (Both apply beyond the spin-wave approximation, for the exact model). The fact that the correlation is bounded from above by a function that tends to zero asymptotically is another confirmation of the absence of long-range order in this model.

2.10.1 Spin waves

Let us consider one perfectly ordered ground state state. It is clear that if one slightly modifies the angle of the \vec{s} vector on neighbouring space points, the energy cost of such a perturbation vanishes in the limit of vanishing angle. These configurations are called *spin-waves* and they differ from the uniformly ordered state by an arbitrarily small amount.

In the particular case of the XY model, see Fig. 2.32, the local spins are constrained to rotate on the *plane*; therefore, each spin has only two components ($n = 2$) and it can be parametrised as

$$\vec{s}_i = (s_i^1, s_i^2) = |\vec{s}_i|(\cos \phi_i, \sin \phi_i) = (\cos \phi_i, \sin \phi_i) \quad (2.321)$$

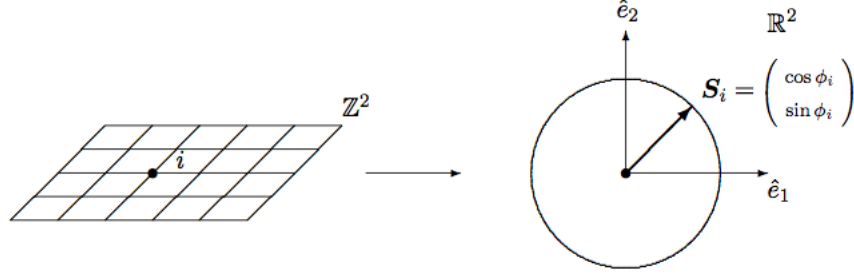


Figure 2.32: A sketch of the 2d XY model definition. On the left the square lattice in 2d, on the right the $n = 2$ spin vector.

where $0 \leq \phi_i \leq 2\pi$ is the angle with respect to the x axis of the plane on which the spin vector lives, on each d -dimensional lattice site i . The modulus of each vector spin is fixed to one. The Hamiltonian (2.3) then becomes

$$H(\{\vec{s}_i\}) \mapsto H(\{\phi_{ij}\}) = -\frac{J}{2} \sum_{\langle ij \rangle} \cos \phi_{ij} \quad (2.322)$$

where $\phi_{ij} = \phi_i - \phi_j$ is the angle between the spins at neighbouring sites i and j . Equation (2.322) remains invariant under the global translation of all angles, $\phi_i \rightarrow \phi_i + \phi_0$ by the same amount, that corresponds to the *global rotational invariance*. The zero-temperature equilibrium state, or ground state, is any of the fully aligned states $\phi_i = \phi$ for all i , with ϕ in $[0, 2\pi]$. There is, therefore, an *infinite degeneracy* of the ground state, as all possible orientations of the (saturated) magnetisation \vec{m} are equally probable. Any of these ground states has perfect *long-range order* since all spins point in the same direction. The ground state energy is $E_0 = -JNz/2$ with z the coordination number of the lattice and N the total number of spins in the system.

If one now assumes that at low enough T the angles between contiguous spins can only be small, $|\phi_i - \phi_j| \ll 2\pi$, the cosine in the Hamiltonian can be expanded to second order

$$\begin{aligned} H(\{\phi_i\}) &\simeq -\frac{Jz}{2}N + \frac{J}{4} \sum_{\langle ij \rangle} (\phi_i - \phi_j)^2 \\ &= E_0 + \frac{J}{4} \sum_{\vec{r}, \vec{a}} [\phi(\vec{r} + \vec{a}) - \phi(\vec{r})]^2 = H(\{\phi(\vec{r})\}) . \end{aligned} \quad (2.323)$$

In the last member we used a different parametrisation of the lattice sites in which they are identified by their positions \vec{r} with respect to the origin of a coordinate system, and the vectors \vec{a} point along all axes of the lattice. On a square lattice in $d = 2$, $\vec{a} = a\hat{e}_k$ with $k = x, y$, and has modulus a , the lattice spacing. If $\phi(\vec{r})$ is a slowly varying function of \vec{r} one can approximate the finite difference by a derivative, *e.g.*, along the x axis

$\phi(\vec{r} + \vec{a}) = \phi(\vec{r} + a\hat{e}_x) - \phi(\vec{r}) \simeq a\partial_x\phi(\vec{r})$ since typically, $a \ll |\vec{r}|$. Next, the sum over lattice sites is approximated by an integral $\sum_{\vec{r}} \dots \simeq a^{-d} \int d^d r \dots$, and we write

$$H(\{\phi(\vec{r})\}) \simeq E_0 + \frac{J}{4a^{d-2}} \int d^d r [\vec{\nabla}\phi(\vec{r})]^2 \quad (2.324)$$

where $d = 2$. We ended up with a quadratic form that, if we *relax the angular constraint* $\phi \in [0, 2\pi]$, acts on a *real unbounded field*

$$-\infty < \phi < \infty. \quad (2.325)$$

This is also called the *elastic representation* and the adimensional parameter βJ the *spin stiffness*. For βJ sufficiently large, lifting the angular constraint should be an acceptable approximation.

We note that if we use a Fourier transform $\phi_{\vec{k}} = V^{-1} \int d^d r e^{i\vec{k}\cdot\vec{r}} \phi(\vec{r})$, where $\phi_{\vec{k}}$ is now a complex function of \vec{k} , with $\vec{k} = 2\pi n/L \hat{e}_k$ and n an integer (see App. 2.A.2, the number of variables is not doubled since the Fourier components are constrained to satisfy $\phi_{\vec{k}}^* = \phi_{-\vec{k}}$), the Hamiltonian becomes one of independent harmonic oscillators or *modes*

$$H(\{\phi_{\vec{k}}\}) \simeq E_0 + \frac{(2\pi)^d J}{4a^{d-2}} \sum_{\vec{k}} k^2 |\phi_{\vec{k}}|^2. \quad (2.326)$$

The contribution of the *long wave-length* modes, that is to say, small $k = 2\pi/\lambda$, is expected to be very small due to the k^2 factor.

Exercise 2.27 Show that the spin wave approximation on a square lattice $H \sim (J/2) \sum_{\langle ij \rangle} (\phi_i - \phi_j)^2$ reads, in Fourier representation, $H \sim (J/2) \sum_{\vec{k}} \gamma(\vec{k}) |\phi_{\vec{k}}|^2$ with $\gamma(\vec{k}) = (2/N)[2 - \cos(k_x a) - \cos(k_y a)]$. Back in real space, express the spin wave Hamiltonian as $H = (J/2) \sum_{i \neq j} \phi_i G(\vec{r}_i, \vec{r}_j) \phi_j$ with the spin wave *propagator* $G(\vec{r}_i, \vec{r}_j) = \sum_{\vec{k}} \gamma(\vec{k}) e^{-i\vec{k}\cdot(\vec{r}_i - \vec{r}_j)}$. Note that the sum $\sum_{i \neq j}$ runs now over the whole lattice and not just the nearest neighbour sites. Construct the Boltzmann weight of the angles ϕ_i as a Gaussian probability, with a vectorial representation $\vec{\phi} = (\phi_1, \phi_2, \dots, \phi_N)$.

Exercise 2.28 Use the results in the previous exercise, and the properties of Gaussian probabilities, to prove that the average magnetisation density, $m = N^{-1} \sum_i \langle \cos \phi_i \rangle$ vanishes as $N^{-1/(8\pi\beta J)}$ with N the number of spins. Discuss the different thermodynamic limits at $T = 0$ and $T > 0$. Notice that this magnetisation can be quite important even for rather large systems.

From the harmonic Hamiltonian (2.324), assuming a smooth character of the field $\phi(\vec{r})$, one finds that the equation for the field configurations that minimise the energy is

$$\nabla^2 \phi(\vec{r}) = 0. \quad (2.327)$$

This equation is identical to the *Laplace equation* for the electrostatic potential in the absence of any charge density. It admits the trivial solution $\phi(\vec{r}) = \text{cst}$, that is just the ground state configuration.

The interest is in computing the *spin-spin correlation function*

$$G(\vec{r}) \equiv \langle \vec{s}(\vec{r}) \cdot \vec{s}(\vec{0}) \rangle = \text{Re} \langle e^{i[\phi(\vec{r}) - \phi(\vec{0})]} \rangle = e^{-\frac{1}{2} \langle [\phi(\vec{r}) - \phi(\vec{0})]^2 \rangle} \equiv e^{-\frac{1}{2} g(r)} , \quad (2.328)$$

where the second identity holds for Gaussian fields with zero average.⁹ $G(\vec{r})$ here is a space-dependent correlation function and its Fourier transform is called the *structure factor*. Since there is no perturbation breaking the systems *isotropy*, one can expect this quantity to be a function of the modulus of the position vector and not of its direction; therefore, one should find that the result is given by a $G(r)$. Next, one should analyse whether the correlation function, at long distances, converges to a finite value (*long-range order*) or zero (no long-range order). Some details of this calculation (which can be found in many textbooks) are given in Sec. 2.6.2 and App. 2.A.3. They lead to

$$\frac{J a^{2-d}}{k_B T} g(r) \simeq \begin{cases} \Omega_d / (d-2) (\pi/L)^{d-2} & d > 2 , \\ (2\pi)^{-1} \ln(r/L) & d = 2 , \\ r/2 & d = 1 , \end{cases}$$

that imply

$$G(r) \simeq \begin{cases} e^{-\text{const } k_B T} & d > 2 & \text{long-range order} , \\ (r/L)^{-\eta(k_B T/J)} & d = 2 & \text{quasi-long-range order} , \\ \exp[-k_B T / (2Ja)] r & d = 1 & \text{short-range order} \end{cases}$$

The behaviour is special in $d = 2$. Interestingly enough, we find that the $2d$ XY model does not support long-range order but its correlation function decays algebraically at all non-zero temperatures in the Gaussian approximation. One can prove that higher order terms in the gradient expansion do not change this behaviour for $d = 2$ and two component spins. The long range order is eliminated by the accumulation of small phase fluctuations.

This is the kind of decay found *at a critical point*, $G(r) \simeq r^{-(d-2+\eta)}$, so the system behaves as at criticality at all temperatures. This does not seem feasible physically (at least at very high temperature the decay should be exponential) and, indeed, we shall see that other excitations, not taken into account by the continuous expansion above, are responsible for a phase transition of a different kind, a so-called *topological phase transition*. After these have been taken care of, the low- T phase remains well described by the spin-wave approximation but the high- T one is dominated by the proliferation of topological defects.

The exponent $\eta(k_B T/J)$ continuously depends on temperature,

$$\eta(k_B T/J) = \frac{k_B T}{2\pi J} . \quad (2.329)$$

This is a signature of the *criticality of the low- T phase*. The criticality is also accompanied by other special features, such as, for example, the non-trivial fluctuations of the “failed”

⁹Gaussian identity: $\int_{-\infty}^{\infty} \frac{dz}{\sqrt{2\pi\sigma^2}} e^{-\frac{z^2}{2\sigma^2}} e^{iz} = \int_{-\infty}^{\infty} \frac{dz}{\sqrt{2\pi\sigma^2}} e^{-\frac{1}{2}(\frac{z}{\sigma} - i\sigma)^2} e^{-\frac{\sigma^2}{2}} = e^{-\frac{\sigma^2}{2}} .$

order parameter $m = N^{-1} \langle |\sum_{i=1}^N \vec{s}_i| \rangle$ for finite system size [63]. Indeed, the thermally averaged value of the order parameter m has abnormally large finite size corrections. Within a spin wave calculation one finds $m = (1/(2N))^{k_B T/(8\pi J)}$ with the expected vanishing value in the thermodynamic limit but rather large values at low temperature and finite sizes, see Ex. 2.28. Monte Carlo simulations demonstrate that the distribution function, $P(y)$ with $y = N^{-1} |\sum_{i=1}^N \vec{s}_i|$ is a universal asymmetric form with interesting characteristics.

2.10.2 High temperature expansions

A first quantitative hint on the fact that there must be a phase transition in the $2d$ XY model came from the study of the high temperature expansion [64, 65]. The method is very similar to the one used to study Ising spin systems. With the aim of developing a small β Taylor expansion, the partition function is written as

$$Z = \int \prod_i d\phi_i e^{\frac{\beta J}{2} \sum_{\langle ij \rangle} \cos(\phi_i - \phi_j)} = \int \prod_i d\phi_i \prod_{\langle ij \rangle} e^{\frac{\beta J}{2} \cos(\phi_i - \phi_j)}. \quad (2.330)$$

Exploiting the periodicity of the exponential of the cos, one can use several tricks to derive

$$G(r) = e^{-r/\xi} \quad \text{with} \quad \xi = a / \ln(4k_B T / J) \quad (2.331)$$

an exponential decay of the correlation function (see [10] for details).

One way to derive this result is to write the correlation function

$$G(r) = \langle \cos(\theta(\vec{r}_i) - \theta(\vec{r}_j)) \rangle, \quad (2.332)$$

expand the exponential to first order in $K = \beta J$, and notice that the resulting product leads to a term with just one $\cos(\vec{r}_i) - \theta(\vec{r}_j)$ and other terms with a multiplicity of similar factors with the angles involved placed on neighbouring sites on the lattice. The identities

$$\int_0^{2\pi} d\theta_j \cos \theta(\theta_i - \theta_j) = 0, \quad (2.333)$$

$$\int_0^{2\pi} d\theta_j \cos \theta(\theta_i - \theta_j) \cos \theta(\theta_j - \theta_k) = \frac{1}{2} \cos \theta(\theta_i - \theta_k), \quad (2.334)$$

force the products to yield non zero results only if they correspond to path on the lattice that join the positions at which the correlation $G(r)$ is calculated. Since K is assumed to be small, the leading contribution is the one given by the shortest path and one recovers (2.331). (We assumed there is a single shortest path, which is not strictly true. The multiplicity of shortest paths changes the correlation length expression but not the exponential decay of the correlation function.)

This calculation strongly suggests that there must be a phase transition between the high temperature disordered phase and a low temperature phase, the latter with, possibly,

the quasi long-range order predicted by the spin-wave approximation. (It was argued that higher order terms in the gradient expansion around the zero temperature ground state do not destroy the quasi long-range order at low temperatures since they are irrelevant in the RG sense [10].)

2.10.3 Vortices and the Kosterlitz-Thouless transition

The failure of the spin-wave approximation at high temperatures is rooted in that it only allows for small and smooth deviations (*gradient expansion*) about the ferromagnetically ordered state. In particular, it excludes configurations in which the angular field is singular at some isolated point(s). In other words, only *single-valued* functions ϕ satisfying,

$$\sum_{nn} [\phi(\vec{r}) - \phi(\vec{y})] \mapsto \oint_C d\vec{y} \cdot \vec{\nabla} \phi(\vec{y}) = 0 \quad (2.335)$$

for any closed path C are admitted in the spin-wave expansion. However, in the 2d XY model, only the spin \vec{s}_i should be single-valued and the original Hamiltonian (2.322) defined on the lattice has a *discrete symmetry*

$$\phi_i - \phi_j \rightarrow \phi_i - \phi_j + 2\pi q \quad \text{with} \quad q \in \mathbb{Z} \quad (2.336)$$

that is lost in the continuous approximation (2.324). This symmetry, which is actually a *local* one since one can use different q on different bonds, permits the existence of *vortices*, a particular kind of *topological defects*. These excitations are the ones that kill the simple spin-wave prediction of there being quasi long-range order at all temperatures, as explained by Kosterlitz & Thouless in the series of papers [67, 68, 69]. Kosterlitz & Thouless (together with Haldane) were retributed the Nobel Prize in 2016 for having exhibited a new class of phase and phase transitions, qualified as *topological*.

Topological defects are configurations, in this case spin configurations, that are local minima of the potential energy and that *cannot* be smoothly transformed into the ground state, in this case the configuration in which all the spins are aligned, by a continuous transformation of variables, in this case a continuous rotation of all spins.

In a continuous description of the lattice problem, this means that there is no transformation of the kind

$$\vec{s}(\vec{r}) \mapsto R(\vec{r})\vec{s}(\vec{r}) \quad (2.337)$$

with a continuous rotation matrix $R(\vec{r})$ that transforms the configuration with a topological defect into one of the ground state (continuously transformable into a spin-wave state).

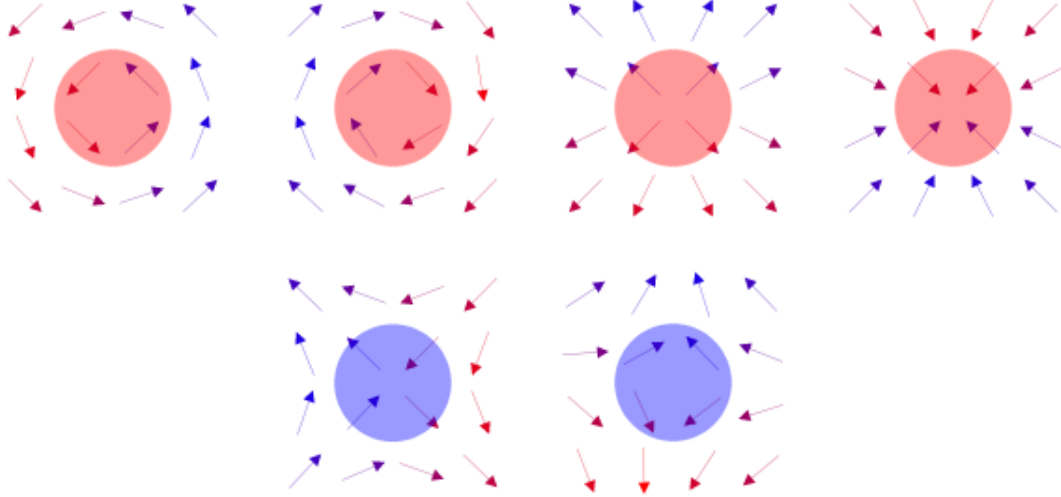


Figure 2.33: Four examples of vortices with charge $q = 1$ (first line) and two examples of anti-vortices with $q = -1$ (second line), see Eq. (2.338) for the definition of q . Figures borrowed from [70].

On the lattice a vortex configuration is such that

$$\sum_{nni, j \in C} (\phi_i - \phi_j) = 2\pi q \quad (2.338)$$

with q an integer ensuring that the spin be single-valued on each site of the lattice, the *charge* of the vortex. These are spin configurations for which in going around a closed path the angle rotates by $2\pi q$. The discrete nature of the charge, makes impossible to continuously deform the configuration to the uniformly ordered state in which the charge is zero. The center of the vortex is located on a site of the *dual lattice*.

In the continuous limit, valid far from the center of the vortex where the discontinuity sits and lattice effects can be important, vortex configurations are *local minima* of the Hamiltonian

$$\frac{\delta H}{\delta \phi(\vec{r})} = 0 \quad \text{and} \quad \frac{\delta^2 H}{\delta \phi(\vec{r}) \delta \phi(\vec{y})} \quad \text{positive definite} \quad (2.339)$$

where the second condition ensures their stability. Indeed, $\phi(\vec{r}) = \text{cst}$ is not the only field configuration that minimises the energy. Vortex configurations, $\phi(\vec{r})$, in which the field has a *singularity* at the location of a point-like *charge*, also satisfy the conditions above.

A vortex configuration located at the origin $\vec{r} = \vec{0}$ can be written as

$$\phi(\vec{r}) = q\varphi(\vec{r}) + \phi_0 \quad (2.340)$$

with q the *integer charge* and $\varphi(\vec{r})$ the polar angle (angle with the horizontal x axis) of the space point \vec{r}

$$\varphi(\vec{r}) = \arctan\left(\frac{y}{x}\right) \quad (2.341)$$

and ϕ_0 an additive constant. As an example, let us take $q = 1$ and $\phi_0 = 0$. One can easily construct the spin configuration associated with this $\phi(\vec{r})$, that is $\vec{s}(\vec{r}) = (\cos \phi(\vec{r}), \sin \phi(\vec{r}))$. The arrows point as in the third panel in the first line in Fig. 2.33. Another choice is to use $q = 1$ and $\phi_0 = \pi/2$, leading to a configuration in which the spins turn anti-clockwise as in the left Fig. 2.36. Finally, one can use $q = 1$ and $\phi_0 = \pi$ to construct a configuration in which all spins point inwards, as in the last snapshot in the first line in Fig. 2.33.

All the configurations with the same q can be continuously transformed into one another. In the cases listed in the previous paragraph, $q = 1$, and

$$\vec{s}(\vec{r}, t) = (\cos(\varphi + t), \sin(\varphi + t)) \quad (2.342)$$

with t a real parameter, taking the values $t = 0, \pi/2$ and π in these particular cases. However, there is no parameter t that makes this configuration be one with another charge q' ; this excludes the transformation into a constant field with $q' = 0$.

The *divergence at the origin of the gradient* of the configuration $\phi(\vec{r}) = q\varphi(\vec{r}) + \phi_0$ with $\varphi(\vec{r})$ in (2.340) is

$$\begin{aligned} \vec{\nabla}\phi(\vec{r}) &= q\vec{\nabla}\varphi(\vec{r}) = q\vec{\nabla} \arctan\left(\frac{y}{x}\right) = -q\frac{y}{x^2} \frac{1}{1 + \frac{y^2}{x^2}} \hat{e}_x + q\frac{1}{x} \frac{1}{1 + \frac{y^2}{x^2}} \hat{e}_y \\ &= -q\frac{y}{x^2 + y^2} \hat{e}_x + q\frac{x}{x^2 + y^2} \hat{e}_y = -q\frac{r \sin \varphi}{r^2} \hat{e}_x + q\frac{r \cos \varphi}{r^2} \hat{e}_y \end{aligned}$$

and

$$\boxed{\vec{\nabla}\phi(\vec{r}) = \frac{q}{r} \hat{e}_\varphi} \quad (2.343)$$

where we used $\hat{e}_\varphi = \cos \varphi \hat{e}_y - \sin \varphi \hat{e}_x$. One clearly sees the divergence for $r \rightarrow 0$. The problem is *spherically symmetric* in the sense that the modulus of the gradient of the field only depends on the modulus of r , $|\vec{\nabla}\phi(\vec{r})| = f(r)$. Moreover, $\vec{\nabla}\phi(\vec{r})$ points along a circle around the center of the vortex, that is to say, perpendicularly to the radius ($\hat{e}_\varphi \cdot \hat{e}_r = 0$).

We now check that the *Laplacian of the angular field* ϕ vanishes for all $r \neq 0$:

$$\vec{\nabla} \cdot \vec{\nabla}\phi(\vec{r}) = q \frac{2xy}{(x^2 + y^2)^2} - q \frac{2xy}{(x^2 + y^2)^2} = 0.$$

At the origin one has to be more careful because of the divergence of the gradient. We proved in this way that the proposed configuration satisfies the extremisation equation. One can also check that it is a *local minimum* of the energy.

Taking a circle with radius R and centred at the centre of the vortex, the *circulation of the angular field* ϕ in (2.340)-(2.349) around C yields

$$\oint_C d\phi(\vec{r}) = \oint_C d\vec{l} \cdot \vec{\nabla}\phi(\vec{r}) = \int_0^{2\pi} R d\varphi \hat{e}_\varphi \cdot \frac{q}{R} \hat{e}_\varphi = 2\pi q. \quad (2.344)$$

Note that this result is independent of the radius of C . Actually, in a single vortex configuration the angle winds around the topological defect for any contour C around the centre of the vortex¹⁰

$$\oint_C d\phi(\vec{r}) = \oint_C d\vec{l} \cdot \vec{\nabla} \phi(\vec{r}) = 2\pi q . \quad (2.345)$$

(Note that the spin has to point in the same direction after coming back to the starting point of the circulation, this condition implies that q must be an integer.) The integral yields this non-vanishing result for all paths C that encircle the centre of the vortex and vanishes on paths that do not. The position of the vortex corresponds to a singularity in the field that is constructed with the *coarse-graining* procedure (the continuous space limit we used to build the field). The discrete nature of the charge makes it impossible to find a continuous deformation which returns the state to the uniformly ordered configuration in which the charge is zero. (One justifies the continuous treatment of the spin rotation by taking a curve around the vortex core with a sufficiently large “radius” so that the variations in angle will be small and the lattice structure can be ignored. The continuous approximation fails close to the core of the vortex.) A vortex creates a distortion in the phase field $\phi(\vec{r})$ that persists infinitely far from the centre of the vortex.

The electromagnetic analogy, that is explained in detail in the book by Chaikin & Lubensky [74], is such that

$$\begin{array}{lll} \text{magnetic induction} & \vec{B} & \leftrightarrow \vec{\nabla} \phi \\ \text{electric current density} & \vec{J} & \leftrightarrow \vec{\mathcal{M}} = \vec{\nabla} \times \vec{\nabla} \phi \\ \text{vector potential} & \vec{\nabla} \times \vec{A} & \leftrightarrow \vec{\nabla} \phi \end{array} \quad (2.346)$$

The current density is singular at the location of the centre of the vortices as

$$\vec{\mathcal{M}}(\vec{r}) = 2\pi \sum_i q_i \delta(\vec{r} - \vec{r}_i) \hat{e}_z = 2\pi \rho(\vec{r}) \hat{e}_z \quad (2.347)$$

where \vec{r} lives on the two dimensional plane and \hat{e}_z is perpendicular to it. $\rho(\vec{r})$ is the charge density constituted by point-like charges located at positions \vec{r}_i .

Several singular configurations are shown in Fig. 2.33, with vortices ($q = 1$) in the first row and antivortices ($q = -1$) in the second row (figures borrowed from [70]). A simple visualisation of the winding angle is sketched in Fig. 2.34. Vortices with higher charge are also possible (though as they have a higher energetic cost they are less common), see Fig. 2.35. A vortex and a nearby anti-vortex configuration are shown in Fig. 2.36 and some constant spin lines around vortex-antivortex pairs are shown in Fig. 2.37. The latter appear bounded in the low temperature phase, see Fig. 2.38.

An angular configuration with M vortices with charge q_i situated at the points \vec{r}_i is

$$\phi(\vec{r}) = \sum_i^M q_i \arctan \left(\frac{(\vec{r} - \vec{r}_i)_y}{(\vec{r} - \vec{r}_i)_x} \right) \quad (2.348)$$

¹⁰Recall Gauss' divergence theorem $\int dV \vec{\nabla} \cdot \vec{F} = \int dS \hat{n} \cdot \vec{F}$, where the volume integral on the left transforms into the surface integral on the right. Applied to a volume in two dimensions and $\vec{F} = \vec{\nabla} \phi$, one goes from eq. (2.343) to eq. (2.345) for a single vortex with charge q .

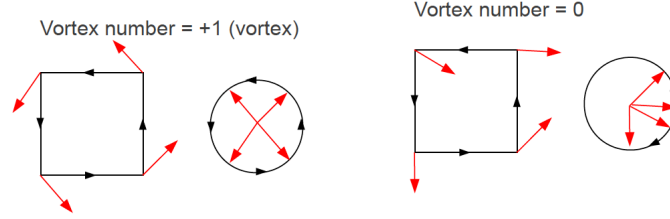


Figure 2.34: A graphical way to visualise the charge of a vortex. One places on the circle an arrow corresponding to the “first” (arbitrary choice) spin. One takes the next spin on the plaquette, conventionally turning in anti-clockwise order, and places a second arrow on the circle. One repeats the procedure until the last spin on the plaquette. The points on the circle are numbered according to the order of the spins on the plaquette, $1, \dots, 4$ in these examples. If the points make one turn on the circle the charge is $q = 1$. If it has made an anti-turn the charge is $q = -1$. If they make more than one turn the charge is higher than 0.

where the sub-scripts x and y indicate the horizontal and vertical components.

Let us evaluate the *energy of a single vortex* configuration. We have already argued that the vortex configuration satisfies

$$\vec{\nabla}\phi(\vec{r}) = \frac{q}{r} \hat{e}_\varphi \quad (2.349)$$

where, without loss of generality, we set the origin of coordinates at the center of the vortex, φ is the angle of the position \vec{r} with respect to the x axis, and q is the charge of the vortex. Using the expression (2.324) where $\vec{\nabla}\phi(\vec{r})$ is replaced by (2.349),

$$E_{1 \text{ vortex}} = \frac{J}{2} \int d^2r [\vec{\nabla}\phi(\vec{r})]^2 = \frac{J}{2} q^2 \int_0^{2\pi} d\varphi \int_a^L dr r \frac{1}{r^2} = \pi J q^2 \ln \frac{L}{a} \quad (2.350)$$

with L the linear dimension of the system. The energy of a single vortex

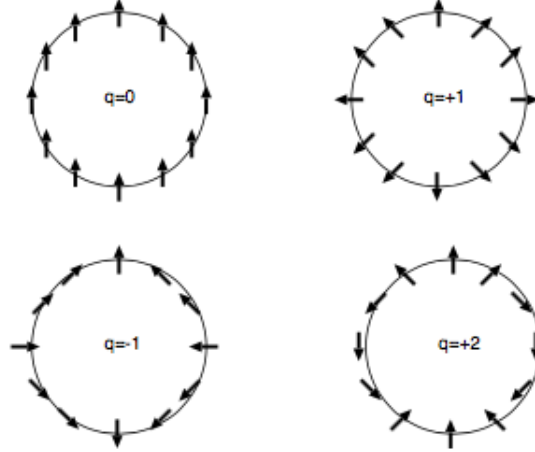
- increases quadratically with its charge
- diverges logarithmically in the infinite size limit

and one might conclude that these configurations cannot exist in equilibrium at any temperature. However, as already discussed when presenting Peierls argument applied to the Ising chain, at finite T one needs to estimate the *free-energy* difference between configurations with and without a vortex to decide for their existence or not. The *configurational entropy of a single vortex* is $S = k_B \ln \mathcal{N} = k_B \ln(L/a)^2$ since in a $2d$ lattice the centre of the vortex can be located on $(L/a)^2$ different sites. Then

$$\Delta F = F_{1 \text{ vortex}} - F = (\pi J q^2 - 2k_B T) \ln(L/a) \quad (2.351)$$

Both energy and entropy of a single vortex configuration grow as $\ln L$. The variation of the free-energy changes sign at $k_B T = \pi J q^2 / 2$ therefore *there cannot be isolated vortices in equilibrium below*

$$k_B T_{KT} = \pi J / 2 \quad (2.352)$$

Figure 2.35: Four vortices with charges $q = 0, 1, -1, 2$.

but they can at higher temperatures. Indeed, at $T > T_{KT}$, isolated vortices proliferate (favoured by the entropic contribution), destroy the quasi long-range order and make correlations decay exponentially on a length-scale given by the typical spacing between vortices

$$G(r) \simeq e^{-r/\xi(T)} \quad \xi(T) \simeq e^{b|T-T_{KT}|^{-1/2}} \quad (2.353)$$

close to T_{KT} . This very fast divergence of the correlation length, $\nu \rightarrow \infty$, can be rigorously proven with an RG analysis [69] that we shall not present here.

The estimate of T_{KT} just given represents only a bound for the stability of the system towards the condensation of topological defects. Pairs (dipoles) of defects may appear at larger couplings or lower temperatures.

Although the energy of a single vortex diverges as $\ln L$, the energy of a *bound pair* of vortex-antivortex does not diverge, since, the total vorticity of the pair vanishes, see the Fig. 2.37 taken from [7]. Below T_{KT} vortices exist only in bound pairs with opposite vorticity held together by a logarithmic confining potential

$$E_{pair}(\vec{r}_1, \vec{r}_2) = -\pi J q_1 q_2 \ln(|\vec{r}_1 - \vec{r}_2|/a) . \quad (2.354)$$

This expression follows uniquely from the fact that at distances much larger than the pair's size there is no net vorticity, so the energy of the pair must be finite, and as the pair's size diverges E_{pair} should yield the sum of the energies for an isolated vortex and an isolated antivortex. (A more detailed calculation uses an integral over a contour in the $2d$ plane that excludes the centers of the vortices. In particular, this approach allows one to show that a sum over the energies of the single vortices appears multiplied by $\sum_i q_i$ and this divergence is eliminated if the total vorticity is zero, i.e. $\sum_i q_i = 0$.) Such pairs can thus be thermally excited, and the low temperature phase will host a gas of such pairs.

The insight by Kosterlitz and Thouless was that at a certain temperature T_{KT} the pairs will break up into individual vortices. It is this vortex pair unbinding transition that will take the system to a high temperature phase with exponentially decaying correlations.

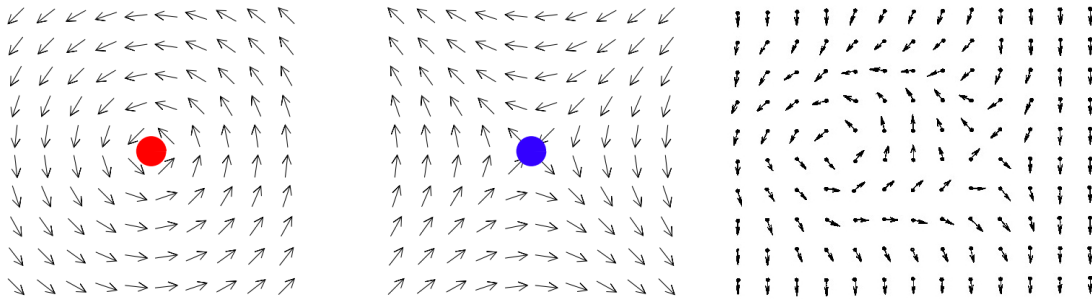


Figure 2.36: A vortex and a near-by anti-vortex configuration as they may appear bounded in the low temperature phase.

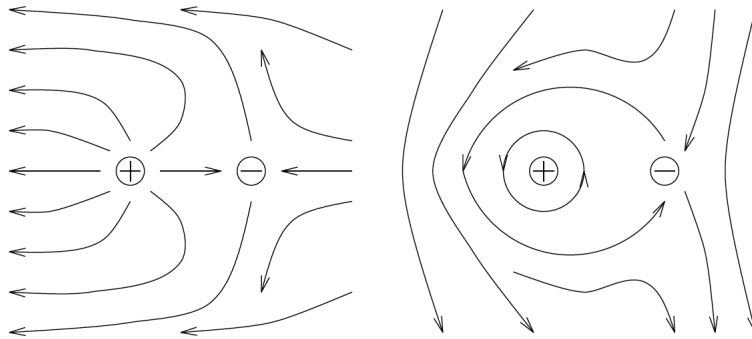


Figure 2.37: Lines of spin direction close to a vortex-antivortex pair. As one observes the spin configurations far from the vortex cores, the lines of constant spin are smooth.

The (single) vortices and anti-vortices act as if they were two point particles with charges $q = +1$ and $q = -1$ interacting with a $1/r$ force. Since this corresponds to the Coulomb interaction in two dimensions, the physics of the topological defects is just like the physics of a two-dimensional *neutral Coulomb gas*. Note that the energy increases if one tries to unbind – separate – the vortices in the pair. The vortices remain paired and do not change much the behaviour in the low temperature phase. The correlation still decays as a power-law and there is no spontaneous symmetry breaking in this phase since the order parameter vanishes – in agreement with the Mermin-Wagner theorem that we discuss below. In terms of the electrostatic analogy, the high temperature phase is a

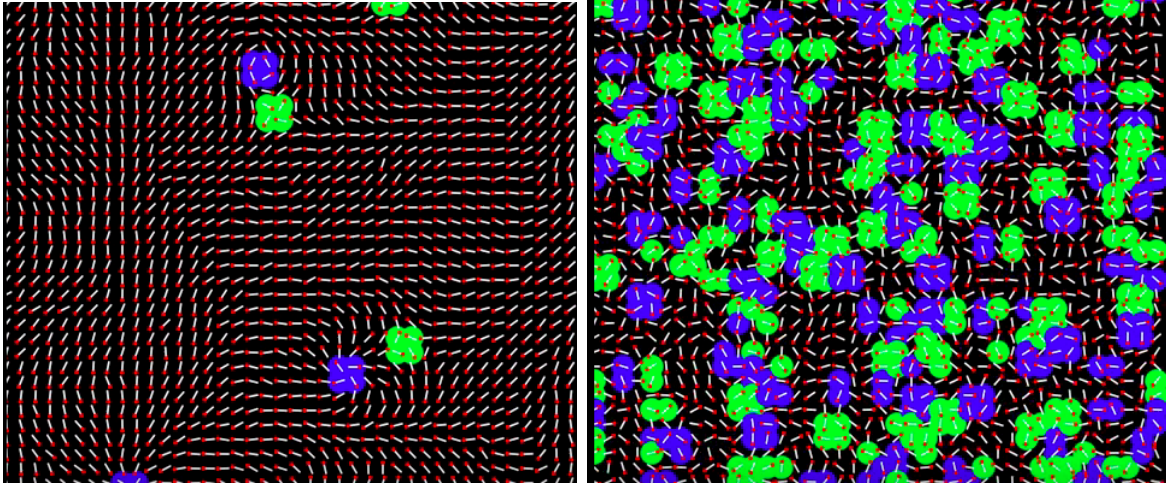


Figure 2.38: At low T there are few vortices and they are bound in pairs. At high T there are many more vortices, they are free and can separate apart. Image taken from [71].

plasma. A detailed description of the vortex influence on the equilibrium properties of the $2d$ XY goes beyond the scope of these Lectures. A detailed description can be found in several book, in particular in [8].

This argument shows that two qualitatively different equilibrium states exist at high and low T but it does not characterize the transition. The naive order parameter vanishes on both sides of the transition but there is still a topological order, with the spin-spin correlation decaying exponentially on one side (high T) and as a power law on the other (low T) of the transition.

In contrast to usual continuous phase transitions, the KT-transition does not break any symmetry. The free-energy density has an essential singularity at the critical temperature. The full low-temperature phase is critical in the sense that the correlation length diverges and the correlation function decays as a power law.

2.10.4 The Villain model

Villains's idea is to use a Gaussian approximation on the lattice which preserves the local symmetry $\phi_i - \phi_j \rightarrow \phi_i - \phi_j + 2\pi q$ with q an integer, and allows for large variations

of the angle from site to site. Concretely,

$$H_{\text{harm}} \sim \frac{J}{2} \sum_{ij} (\theta_i - \theta_j - 2\pi m(\theta_i - \theta_j))^2 \quad (2.355)$$

$$\text{with the function } m(\theta_i - \theta_j) = \begin{cases} 1 & \theta_i - \theta_j > \pi \\ -1 & \theta_i - \theta_j < -\pi \\ 0 & |\theta_i - \theta_j| < \pi \end{cases}$$

A further idea is to consider that, at least at low temperatures, $m(\theta_i - \theta_j)$ are *independent degrees of freedom* taking the values $m_{ij} = \pm 1, 0$ with the symmetric property $m_{ij} = -m_{ji}$.

$$H_{\text{Villain}} \sim \frac{J}{2} \sum_{ij} (\theta_i - \theta_j - 2\pi m_{ij})^2 \quad (2.356)$$

The next step in Villain's development is to introduce the *vortex-less* and *vortex carrying* variables φ_i and ψ_i , respectively, and propose $\phi_i = \varphi_i + \psi_i$. Then expanding the square and arguing that the ψ_i can be chosen so that the cross term vanishes one arrives at a Hamiltonian with decoupled fields.

Villain's model will be studied in TD5.

2.10.5 Numerical evaluation

Distinguishing a second order phase transition from a Kosterlitz-Thouless one is a daunting challenge. See, *e.g.*, [75] for a recent effort to verify the scalings expected. A useful method is based on the scaling properties of the kurtosis of the (pseudo) order parameter or Binder parameter [76, 77].

2.10.6 Applications

From the Nobel Lecture: *In 1972 J. Michael Kosterlitz and David J. Thouless identified a completely new type of phase transition in two-dimensional systems where topological defects play a crucial role. Their theory applied to certain kinds of magnets and to superconducting and superfluid films, and has also been very important for understanding the quantum theory of one-dimensional systems at very low temperatures.*

Other two dimensional systems, notably those of particles in interaction that would like to form solids at sufficiently low temperature and high densities, also fall into the scheme of the Kosterlitz-Thouless phase transitions. Indeed, in 1934, Peierls argued that thermal motion of *long-wave length phonons* will destroy the long-range order or a two dimensional solid in the sense that the mean square deviation of an atom from its equilibrium position increases logarithmically with the size of the system [?]. He also proposed a model, just atoms sitting on a lattice in $2d$ and linked together by Hookean springs, that has quasi long-range order at all temperatures [72]. Quasi long range order means in this context that the mean square deviation of an atom from its equilibrium position increases

logarithmically with the size of the system. It was later understood that the mechanism for destabilising this critical phase is through the unbinding of topological defects that are of a different kind from the ones we studied here. (For more details, see, for example [the slides](#) that I included in my web page and the Subsection below.)

For similar reasons, the expectation value of the *superfluid order parameter* in a two dimensional Bose fluid is zero. In 1978, Bishop and Reppy studied the superfluid transition of a thin two dimensional helium film absorbed on an oscillating substrate. The observation results on superfluid mass and dissipation supported the Kosterlitz-Thouless picture of the phase transition in a two dimensional superfluid. The jump in the superfluid density at the transition given by Kosterlitz and Thouless is in good agreement with estimates from experiment.

2.10.7 The Mermin-Wagner theorem

What happens in $d = 2$ and below? Indeed, the logarithmic behaviour of the angle correlation function in the XY model or the transverse correlation in the generic $O(n)$ model, see below, are signatures of the fact that this is a special dimension.

In 1968, using a mathematical inequality due to Bogoliubov, Mermin showed that the magnetisation density m is strictly zero at all $T > 0$ in the $2d$ XY model. This proof is part of what is nowadays called the Mermin-Wagner theorem.

The *Mermin-Wagner theorem* is often quoted as stating that for any system with short-range interactions there is a *lower critical dimension* below which no spontaneous broken symmetry can exist at finite temperature [58]. In other words, fluctuations are so large that any ordering that breaks a continuous symmetry is destroyed by thermal fluctuations. $d_c = 1$ for discrete symmetries and $d_c = 2$ for systems with continuous symmetries. The absence of long-range order in the $2d$ XY case, for example, is demonstrated by the fact that the finite temperature correlation decays to zero at long distances – albeit as a power law – and thus there is no net magnetisation in the system.

However, the statement above is not totally correct. What Mermin proved is that some order parameters (like the magnetisation for the $2d$ XY model or the one associated to translational order in $2d$ particle systems in interaction) cannot take a non-zero value at any non-vanishing temperature. This does not exclude that *other* order parameters could do it. This is indeed what happens in the problem of $2d$ melting, where the translational order parameter vanishes at all non-zero temperatures but a less obvious order parameter, associated to orientational order, does not. The system can therefore sustain long-range orientational order at finite temperatures while it cannot maintain translational order.

The Mermin-Wagner theorem [58] is known as Coleman-Weinberg theorem/result in field theory [61]. Independently of Mermin & Wagner, Hohenberg developed a similar argument in the context of Bose quantum liquids and superconductors [62].

2.10.8 About universality

The picture described above has been developed based on the analysis of the 2d XY model in which planar spins are placed on the vertices of a regular lattice, with nearest neighbour pairwise interactions $-J\cos\theta_{ij}$ with θ_{ij} the angle between the two spins. Interestingly enough, the nature of the transition can change dramatically if the interaction term takes other forms that still respect rotational invariance. The potential $2[1 - \cos^{2p^2}(\theta_{ij}/2)]$, that interpolates between the conventional one for $p = 1$ and a much steeper well for large p^2 was used by Domany, Schick and Swendsen [78] to show that the transition crosses over from BKT to first order for large p^2 . In particular, for $p^2 = 50$ the transition is very sharp with a huge peak in the specific heat and many other elements of a first order phase transition. The reason for this behaviour is that the typical temperature for the unbinding of vortex-antivortex pairs is pushed to very high values, beyond the ones at which other kinds of excitations drive the discontinuous transition. Similarly, other examples of models expected to have BKT transitions, such as the 2d Coulomb gas, were shown to comply with the expectations only at low density and depart towards a first order phase transition at higher density.

The phenomena just described seem to be in contradiction with the picture that emerges from the renormalisation group theory according to which systems in the same universal class (having the same symmetry of the order parameter and same dimensionality) should exhibit the same type of phase transition with identical values of critical exponents. However, a rigorous proof that planar spin models of the XY kind with a sufficiently narrow potential undergo first order phase transitions was provided by van Enter & Shlosman [79] and the fact that with a simple change of parameter one can change the order of the transition was thus confirmed.

2.10.9 On interface energies

In a continuous spin model the cost of an interface is proportional to its surface divided by its thickness (note that spins can smoothly rotate from site to site to create a thick interface). The thickness of the interface depends on the details of the model, temperature, *etc.* This means that interfaces are much easier to create in continuous spin models than in discrete ones. One can then expect to have lower critical dimensions for continuous spin models than for discrete ones.

2.10.10 $O(n)$ model: Goldstone modes

We lift here the constraint on the modulus of the vector spins and we let it fluctuate. It is simple to derive a continuum limit of the lattice model in analogy with the Landau approach. One first coarse-grains the two-component spin to construct a n -component field

$$\vec{\psi}(\vec{r}) = \ell^{-d} \sum_{i \in V_{\vec{r}}} \vec{s}_i. \quad (2.357)$$

Let us first focus on the *d dimensional $O(2)$ model*, where the field has just two com-



Figure 9.2. A 'Mexican hat' potential.

Figure 2.39: A Mexican hat potential, figure taken from [9].

ponents. One proposes a Landau ψ^4 action for the field $\vec{\psi}$,

$$F[\vec{\psi}] = \int d^d r \left[\frac{1}{2} [\vec{\nabla} \vec{\psi}(\vec{r})]^2 + \frac{T - T_c}{T_c} \psi^2(\vec{r}) + \frac{\lambda}{4!} \psi^4(\vec{r}) + \vec{h} \vec{\psi}(\vec{r}) \right] \quad (2.358)$$

and parametrises the field by its modulus and angle,

$$\vec{\psi}(\vec{r}) = |\phi_0(\vec{r})| (\cos \phi(\vec{r}), \sin \phi(\vec{r})) \quad (\text{or } \vec{\psi}(\vec{r}) = |\phi_0(\vec{r})| e^{i\phi(\vec{r})}). \quad (2.359)$$

to rewrite the Landau free-energy of a generic configuration in the absence of the external field \vec{h} as

$$F[\phi_0, \phi] = \int d^d r \left[\frac{1}{2} (\vec{\nabla} \phi_0(\vec{r}))^2 + \frac{T - T_c}{T_c} \phi_0^2(\vec{r}) + \frac{\lambda}{4!} \phi_0^4(\vec{r}) \right] \quad (2.360)$$

$$+ \frac{\phi_0^2}{2} \int d^d r [\vec{\nabla} \phi(\vec{r})]^2. \quad (2.361)$$

The first term is just similar to the Landau free-energy of a *massive scalar field* configuration in the Ising model. The second-term quantifies the free-energy of the spin-wave configurations (in higher dimensions topological defects also exist, for example, in $d = 3$ this model has vortex lines with linear singularities). The local angle is simply a *massless scalar field* in d dimensional space. The correlation functions of the ϕ field behave as

$$\langle \phi(\vec{r}) \phi(\vec{y}) \rangle \sim (2 - d)^{-1} |\vec{r} - \vec{y}|^{2-d} \quad (2.362)$$

in the large $|\vec{r} - \vec{y}|$ limit for $d = 1, 2$. The behaviour is logarithmic in $d = 2$ (the $2d$ XY model). The correlation reaches a constant in $d > 2$.

Let us now focus on the generic *d dimensional $O(n)$ model*. The free-energy à la Landau is the one in Eq. (2.358)

$$F[\vec{\psi}] = \int d^d r \left[\frac{1}{2} (\vec{\nabla} \vec{\psi}(\vec{r}))^2 + \frac{T - T_c}{T_c} \psi^2(\vec{r}) + \frac{\lambda}{4!} \psi^4(\vec{r}) + \vec{h} \vec{\psi}(\vec{r}) \right] \quad (2.363)$$

where $\psi^2 \equiv \sum_{a=1}^N \psi_a^2$ is the result of a sum over n components. The potential $V(\psi^2)$ has the Mexican hat form sketched in Fig. 2.39 (credit to A. M. Tsvelik), with extrema at

$$\vec{\psi} = \vec{0} \quad \text{or} \quad \psi^2 = -\frac{4!}{2\lambda} \frac{T - T_c}{T_c} \quad (2.364)$$

Clearly, the latter exists only if $T < T_c$ and we focus on this range of temperatures. It is clear that the condition on ψ^2 admits an infinite number of solutions, in other words, there is a *ground state manifold*, corresponding to the circular bottom of the valley in the Mexican hat potential. The pinning field \vec{h} can then be used to force the system to choose one among all these degenerate directions in the n dimensional space, in which the field “condenses”. Let us suppose that this is the n th direction that we therefore call *longitudinal*. The rotation symmetry in the remaining *transverse* $n - 1$ directions remains unbroken and the symmetry is therefore spontaneously broken to $O(n - 1)$. The expected values of such a configuration is then

$$\langle \psi_a(\vec{r}) \rangle = \psi \delta_{an} \quad (2.365)$$

while the fluctuations are

$$\begin{aligned} \psi_n(\vec{r}) &= \langle \psi_n(\vec{r}) \rangle + \delta\psi_n(\vec{r}) \\ \psi_{a \neq n}(\vec{r}) &= \delta\psi_{a \neq n} \end{aligned} \quad (2.366)$$

(think of the case $n = 3$, choosing the n direction to be the z vertical one and the rotations around this axis). Replacing these forms in the Landau free-energy one finds that the longitudinal mode is massive while the transverse ones are massless (just decoupled Gaussian fields).

The correlation functions, $C_{ab}(\vec{r}) = \langle \psi_a(\vec{r}) \psi_b(\vec{0}) \rangle$, can be written as

$$C_{ab}(\vec{r}) = \delta_{ab} [C_L(r) \delta_{an} + C_T(r)(1 - \delta_{an})] . \quad (2.367)$$

We recall that a and b label the components in the n -dimensional space. C_L is the *longitudinal* correlation (parallel to an infinitesimal applied field that selects the ordering direction, $\vec{h} = h \hat{e}_n$) and C_T is the *transverse* (orthogonal to the applied field) one. A simple calculation shows that the longitudinal component behaves just as the correlation in the Ising model. It is a massive scalar field. The transverse directions, instead, are massless: there is no restoring force to the tilt of the full system. These components behave just as the angle in the XY model, $C_T(\vec{r}) \sim r^{2-d}$ (the power law decay becomes a logarithm in $d = 2$). These are called *Goldstone modes* or *soft modes*.

2.10.11 The Higgs mechanism

A particular feature of models with continuous symmetry breaking in *gauge theories* is that gauge fields acquire a mass through the process of spontaneous symmetry breaking. Take the classical Abelian field theory

$$\mathcal{L}[A_\mu, \phi] = \int d^d r \left[-\frac{1}{4} F_{\mu\nu} F^{\mu\nu} + (D_\mu \phi)^* (D^\mu \phi) + V(\phi) \right] \quad (2.368)$$

with $F_{\mu\nu} = \partial_\mu A_\nu - \partial_\nu A_\mu$, $D_\mu = \partial_\mu + ieA_\mu$ and ϕ a complex field. The potential is

$$V(\phi) = \mu(\phi^*\phi) + \lambda(\phi^*\phi)^2 \quad (2.369)$$

with $\mu < 0$ and $\lambda > 0$. The ϕ configuration that renders V minimum is such that $\phi_0^*\phi_0 = -2\mu/\lambda$. Without loss of generality one can choose ϕ_0 to be real through a uniform rotation over all space. It is easy to verify that replacing ϕ by $(\phi_0 + \delta\phi) + i\phi_2$ where ϕ_2 is an imaginary part (playing the role of the transverse components in the analysis of the $O(n)$ model) one finds that the quadratic Lagrangian does not have a ϕ^2 term (massless field) but instead a quadratic term in A appears. The gauge field acquired a mass (there is also a $A_\mu \partial^\mu \phi_2$ term that can be eliminated with a change of variables).

This phenomenon has been discovered in the study of superconductors by P. W. Anderson. Indeed, one can find a short account of the historic development in Wikipedia: *The mechanism was proposed in 1962 by Philip W. Anderson, who discussed its consequences for particle physics but did not work out an explicit relativistic model. The relativistic model was developed in 1964 by three independent groups Robert Brout and François Englert, Peter Higgs and Gerald Guralnik, Carl Richard Hagen, and Tom Kibble. Slightly later, in 1965, but independently from the other publications the mechanism was also proposed by Alexander Migdal and Alexander Polyakov at that time Soviet undergraduate students. However, the paper was delayed by the Editorial Office of JETP, and was published only in 1966. The Nobel Prize was given to F. Englert and P. Higgs in 2013 "for the theoretical discovery of a mechanism that contributes to our understanding of the origin of mass of subatomic particles, and which recently was confirmed through the discovery of the predicted fundamental particle, by the ATLAS and CMS experiments at CERN's Large Hadron Collider".*

2.11 Melting in two dimensions

Consider a sufficiently dense system so that it should be a solid, possibly in a crystalline phase and evaluate the effect of thermal fluctuations. Does the solid melt? Which are the mechanisms leading to melting? Which is the order of the phase transition taking the solid into a liquid?

These questions received an answer that draw consensus around the fact that the transition is of first order in $d = 3$. However, the situation is trickier in $d = 2$. We discuss this case below.

2.11.1 Positional vs. orientational order

In the 30s Peierls [82] and Landau [80, 81] argued that it is not possible to find long-range *positional* order in low dimensional systems with short-range interactions.

Peierls used the simplest possible model for a solid, one of beads placed on a d -dimensional lattice, with Hookean couplings between nearest-neighbours, in canonical equilibrium, that is to say, a *harmonic solid*. The question he asked was whether such a

system could sustain periodic order over long distances under thermal fluctuations, and he concluded that this is not possible in $d \leq 2$, while it is in $d \geq 3$. Landau based his arguments instead on his theory of phase transitions and reached the same conclusion. In the 60s, the numerical simulations of [84] pointed towards a first order phase transition between solid and liquid. A more general proof of absence of crystalline order in $2d$, that does not rely on the harmonic approximation but uses a classical limit of Bogoliubov's inequality [85], was given later by [86].

An equilibrium amorphous state has a uniform averaged density $\langle \rho \rangle = \rho_0$, while a zero temperature crystalline state has a periodic one

$$\rho(\vec{r}) = \sum_i \delta(\vec{r} - \vec{R}_i) \quad (2.370)$$

with i a label that identifies the particles or lattice sites, and \vec{R}_i the position of the i th vertex of the lattice. At zero temperature a perfectly ordered state, with periodic density is allowed for all $d \geq 1$. However, thermal fluctuations make the atoms vibrate around their putative lattice sites, and the instantaneous position of the i th atom becomes

$$\vec{r}_i = \vec{R}_i + \vec{u}_i = \vec{R}_i + \vec{u}(\vec{R}_i) \quad (2.371)$$

with $\vec{u}_i = \vec{u}(\vec{R}_i)$ its displacement from \vec{R}_i . A simple way to see the lack of positional order in low dimensions (and the existence of it in higher dimensions) is to compute the mean-square displacement of the atoms assuming thermal equilibrium. Take a generic pair-wise potential

$$U_{\text{tot}} = \frac{1}{2} \sum_{ij} U(\vec{r}_i - \vec{r}_j) = \frac{1}{2} \sum_{ij} U(\vec{R}_i - \vec{R}_j + \vec{u}_i - \vec{u}_j) . \quad (2.372)$$

Indeed, the total harmonic potential energy is [83]

$$\begin{aligned} U_{\text{tot}} &= U_{\text{gs}} + \frac{1}{2} \sum_{ij} \sum_{\mu\nu} (u_i^\mu - u_j^\mu) \frac{\partial^2 U}{\partial r_i^\mu \partial r_j^\nu} (\vec{R}_i - \vec{R}_j) (u_i^\nu - u_j^\nu) \\ &= U_{\text{gs}} + \frac{1}{2} \sum_{ij} \sum_{\mu\nu} u_i^\mu D_{\mu\nu}(\vec{R}_i - \vec{R}_j) u_j^\nu \end{aligned} \quad (2.373)$$

where $U_{\text{gs}} = \frac{1}{2} \sum_{i \neq j} U(\vec{R}_i - \vec{R}_j)$, and in the second term μ, ν run from 1 to d , $D_{ij}^{\mu\nu} \equiv D_{\mu\nu}(\vec{R}_i - \vec{R}_j) = \delta_{ij} \sum_k \phi_{ik}^{\mu\nu} - \phi_{ij}^{\mu\nu}$ and $\phi_{ik}^{\mu\nu} = \partial^2 U(\vec{r}) / \partial r_i^\mu \partial r_k^\nu$. Three symmetries of the couplings follow immediately $D_{ij}^{\mu\nu} = D_{ji}^{\nu\mu}$, $D_{ij}^{\mu\nu} = D_{ji}^{\mu\nu}$ (from the inversion symmetry of a Bravais lattice), and $\sum_i D_{ij}^{\mu\nu} = 0$ (from the uniform translation invariance of the full lattice). After a Fourier transform U_{tot} becomes

$$U_{\text{tot}} = U_{\text{gs}} + \frac{1}{2} \sum_{\vec{k}} \sum_{\mu\nu} \tilde{u}_\mu^*(\vec{k}) \tilde{D}_{\mu\nu}(\vec{k}) \tilde{u}_\nu(\vec{k}) , \quad (2.374)$$

where $\tilde{u}_\mu(\vec{k}) = \sum_i e^{i\vec{k}\cdot\vec{r}_i} \vec{u}_i$ and $\tilde{u}_\mu^*(\vec{k}) = \tilde{u}_\mu(-\vec{k})$ since \vec{u}_i is real. Next one needs to estimate the \vec{k} dependence of $\tilde{D}_{\mu\nu}(\vec{k})$. Using the symmetries of $D_{ij}^{\mu\nu}$, its Fourier transform $\tilde{D}_{\mu\nu}(\vec{k})$ can be recast as

$$\tilde{D}_{\mu\nu}(\vec{k}) = -2 \sum_{\vec{R}} D_{\mu\nu}(\vec{R}) \sin^2(\vec{k} \cdot \vec{R}/2) \approx -2 \sum_{\vec{R}} D_{\mu\nu}(\vec{R}) (\vec{k} \cdot \vec{R}/2)^2, \quad (2.375)$$

after a small \vec{k} approximation. It is now possible to further assume

$$\tilde{D}_{\mu\nu}(\vec{k}) \mapsto k^2 A_{\mu\nu} \quad (2.376)$$

where the important k^2 dependence has been extracted. U_{tot} thus becomes the energy of an ensemble of harmonic oscillators. The equipartition of quadratic degrees of freedom in canonical equilibrium yields

$$\langle \tilde{u}_\mu^*(\vec{k}) \tilde{u}_\nu(\vec{k}) \rangle = \frac{k_B T}{k^2} A_{\mu\nu}^{-1} \quad (2.377)$$

and a logarithmic divergence of the displacement mean-square displacement

$$\Delta u^2 \equiv \langle |\vec{u}(\vec{r}) - \vec{u}(\vec{r}')|^2 \rangle \sim k_B T \ln |\vec{r} - \vec{r}'| \quad \text{in } d = 2 \quad (2.378)$$

follows as a consequence of the logarithmic divergence of the integral $\int d^2k k^{-2}$.

An even simpler derivation of the same result goes as follows. Take the harmonic Hamiltonian $H = \frac{\epsilon}{2} \int d^d \vec{r} (\nabla \vec{u})^2$ as a starting point. The excitation of a spin-wave with wavelength L (wave vector $2\pi/L$) then requires an energy $E \approx L^d (2\pi/L)^2 \propto L^{d-2}$ that diverges with L for $d = 3$, is independent of L for $d = 2$ (marginal case) and decreases as L^{-1} for $d = 1$.

The divergence of the mean-square displacement in Eqn. (2.378) implies that any atom displaces a long distance from each other and hence no long-range order is possible in $d = 2$. This weird effect is due to the dimensionality of space. In three dimensions, the mean square fluctuation is finite.

A more general proof of the lack of positional order in $d \leq 2$ that goes beyond the harmonic approximation was by Mermin [86]. In this paper, he first proposed the following criterium for crystallinity:

$$\begin{aligned} \tilde{\rho}(\vec{k}) &= 0 & \text{for } \vec{k} \text{ not a reciprocal lattice vector,} \\ \tilde{\rho}(\vec{k}) &\neq 0 & \text{for at least one non-zero reciprocal lattice vector,} \end{aligned} \quad (2.379)$$

with $\tilde{\rho}(\vec{k})$ the Fourier transform of $\rho(\vec{r})$, in the thermodynamic limit, that is

$$\tilde{\rho}(\vec{k}) = \frac{1}{N} \sum_{i=1}^N e^{i\vec{k}\cdot\vec{r}_i}. \quad (2.380)$$

Using Bogolyubov's identity, Mermin showed that the condition (2.379) cannot be satisfied in $d \leq 2$ since in thermal equilibrium at non-vanishing temperature, for all \vec{k} , $\langle \tilde{\rho}(\vec{k}) \rangle$ is bounded from above by a quantity that vanishes in the thermodynamic limit.

The possibility of a two-dimensional system with constant density (all Fourier modes vanish) being, however, anisotropic over long distances was left open by Peierls and Landau. The actual definition of the orientational order was also given by Mermin in his 1968 paper. Within the harmonic solid model he simply noticed that

$$\langle [\vec{r}(\vec{R} + \vec{a}_1) - \vec{r}(\vec{R})] \cdot [\vec{r}(\vec{R}' + \vec{a}_1) - \vec{r}(\vec{R}')] \rangle \quad (2.381)$$

approaches a_1^2 at long distances $|\vec{R} - \vec{R}'| \rightarrow \infty$, implying that the orientation of the local order is maintained all along the sample. The status of the studies of orientational order in two dimensional systems in the 90s is summarised in [87].

Because the symmetry group of both phases is the same in the thermodynamic limit (QLRO does not result in a macroscopic broken symmetry), it seems that a phase transition is not necessary. However, as we have seen, the loss of order in the low temperature phase is very weak, and samples of macroscopic but finite size are expected to exhibit broken symmetry, so that for all practical purposes there is a symmetry difference between the two phases, and we would expect a phase transition.

2.11.2 Melting scenarii

In $d \geq 3$ melting is a first order phase transition between crystal and liquid (although the details of how this transition occurs are still not fully understood and may depend on the material). In $d = 2$, instead, there is no full consensus yet as to which are the mechanisms for melting and how the passage from solid (with quasi-long-range positional and long-range orientational order) to liquid (with both short-range positional and orientational order) occurs. In the late 70s Halperin & Nelson [88] and Young [89] suggested that the transition can occur in two steps, with an intermediate anisotropic *hexatic phase* with short-range positional and quasi-long-range orientational order. Both transitions, between solid and hexatic on the one hand, and hexatic and liquid on the other, were proposed to be driven by the dissociation of *topological defects*, and therefore be of BKT type:

- In the first stage, at the melting transition T_m , dislocation pairs unbind to form a bond orientationally ordered hexatic liquid.
- In the second stage, at T_i , the disclination pairs which make up the dislocations unbind to form an isotropic liquid.

What are these topological defects? In two dimensions, an isolated *dislocation* is formed by inserting an extra half row of particles into a triangular lattice. Similarly, an isolated *disclination* is formed by inserting (removing) a 60° wedge of material into (from) a triangular lattice, to form a $+1(-1)$ disclination. A $+1$ disclination corresponds to a point

having sevenfold symmetry, while a -1 disclination corresponds to a point of fivefold symmetry. Dislocations and disclinations are considered topological defects because they cannot be eliminated from the lattice without a global rearrangement of particles (inserting or removing a half-row or a 60° wedge of particles).

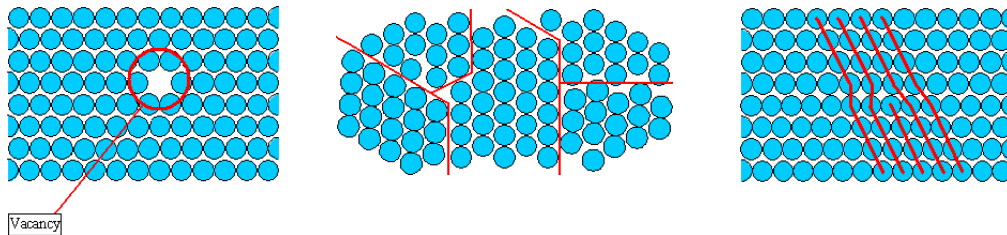


Figure 2.40: A vacancy, a grain boundary between regions with different order and a dislocation in a triangular lattice.

Moreover, within the KTHNY theory, the *finite size scaling* of the order parameters is expected to be as follows. In the solid phase the translational order parameter should decay with system size as $N^{-\eta}$ with $\eta \leq 1/3$. In the hexatic phase the hexatic order parameter should decay with system size as $N^{-\eta_6}$ with $\eta_6 \rightarrow 0$ at the transition with the solid and, according to Nelson & Halperin, $\eta_6 \rightarrow 1/4$ at the transition with the liquid. All these conclusions were derived from an RG analysis of the continuous elastic model of a solid separated into the contribution of the smooth displacements and the one of the defects.

A large number of numerical and experimental attempts to confirm (or not) this picture followed. A summary of the situation at the beginning of the 90s can be found in [87] and close to ten years ago in [90]. Early numerics and experiments faced some difficulty in establishing the existence of the hexatic phase, and suggested instead coexistence between solid and liquid as expected in a single first order phase transition scenario. However, by the turn of the century the existence of the hexatic phase was settled and quite widely accepted (see the references by Maret *et al.* cited below) although evidence for both

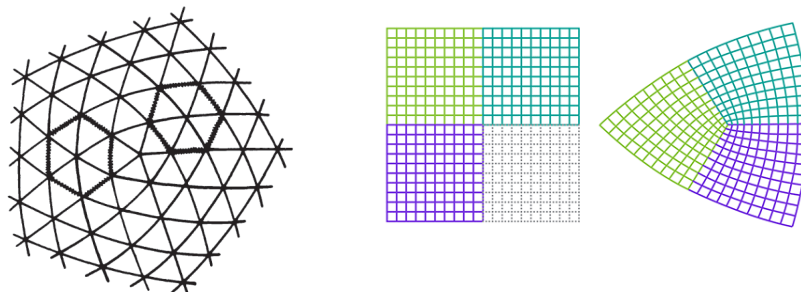


Figure 2.41: Disclination in a triangular and a square lattice.

transitions being of BKT kind remained still elusive.

More recently, Krauth and collaborators [92, 93, 94] came back to this problem with powerful numerical techniques and they suggested that, for sufficiently hard repulsive interactions between disks, the transition between the hexatic and liquid phases is first order. A phenomenon similar to the one put forward by Domany, Schick and Swendsen [78] with a numerical study, and later shown rigorously by van Enter and Shlosman [79] for the $2d$ XY model with a different potential, would then be at work. Namely, that the BKT transition derived with renormalisation group techniques would be preempted by a first order one. This new scenario allows for co-existence of the liquid and hexatic phases in a finite region of the phase diagram. The mechanisms for the transitions could then be the following.

- In the first stage, at T_m , dislocation pairs unbind to form a bond orientationally ordered hexatic phase.
- In the second stage, at T_i , grain boundaries made of strings of alternating five and seven fold defects would percolate across the sample and liquify it.

While real time video microscopy on superparamagnetic colloids interacting via a *soft* r^{-3} potential tend to confirm the KTHNY scenario experimental evidence for the new scenario in a colloidal *hard disks* system was recently given. It seems plausible that the mechanism for melting in $2d$ be non-universal and depend on the interaction potential and other specificities of the systems. Indeed, the numerical simulations prove that for sufficiently soft potential the first order transition is replaced by the conventional BKT one [94]. Moreover, a choice between the two is also made by the *form* of the particles: a dependence of the order of the transition with the number of sides of the constituent polygons was claimed in this paper.

The nature of the second transition, at T_i , remains, therefore, to be understood.

2.12 First order phase transitions

At a first order phase transition the system transits from one phase to another in a discontinuous way. The free energies equalise at the transition, as shown in Fig. 2.42 borrowed from [98]. First order transitions are characterised by a discontinuity in the order parameter and thermodynamic densities, with an associated delta-peak behaviour in the susceptibility. The jump in energy density is associated to *latent heat*.

At a first order phase transition, the correlation length of all phases involved, ξ_a , is strictly finite. There are two (or more, say N_p) co-existing phases in which the order parameter, say O , takes the mean values $\langle O \rangle = O_\alpha$ with $\alpha = 1, \dots, N_p$. For systems sizes, $L \gg \xi_a$, one can expect its probability distribution at the critical point to be

$$P(O) = \mathcal{N}^{-1} \exp \left(-\beta \sum_{\alpha=1}^{N_p} \frac{(O - \langle O \rangle_\alpha)^2}{2\chi_\alpha L^{-d}} \right), \quad (2.382)$$

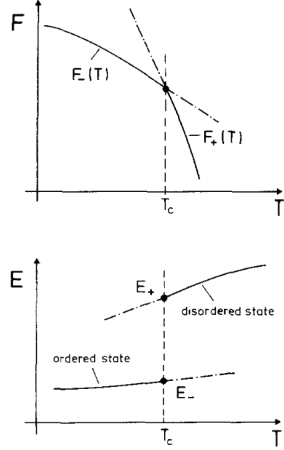


Fig. 1. Schematic plot of the free energy F per lattice site versus temperature T (upper part) and of the internal energy E per lattice site (lower part), for a temperature driven first-order transition T_c . The two branches of the free energy are denoted as $F_-(T)$ {ordered states at low temperatures} and as $F_+(T)$ {disordered states at high temperatures}, respectively. Corresponding energies at T_c are denoted as E_- and E_+ , respectively. Dash-dotted parts of the curves represent metastable states, observable at least in a finite box as considered here

Figure 2.42: Figure from [98].

with the finite volume susceptibility

$$\chi_\alpha = \beta \langle (O - \langle O \rangle_\alpha)^2 \rangle_\alpha L^d \propto L^d. \quad (2.383)$$

For values of the order parameter between the ones of the phases involved, the system is in *co-existence*, or in a *mixed phase*, with a finite portion of it in each of the phases. This is sketched in Fig. 2.43. The weight of this intermediate region is expected to vanish as

$$P(O) \sim \exp[-\sigma 2L^{d-1}] \quad (2.384)$$

with σ the *interface tension* or, in other terms, the energy of each “broken bond”. $P(O)$ is then flat in this range of O . The measured averaged order parameter is

$$\langle O \rangle = \frac{V_1}{V} \langle O \rangle_1 + \frac{V_2}{V} \langle O \rangle_2 \quad (2.385)$$

for a mixed case with two phases, V_1 and V_2 the volumes occupied by the two phases and $\langle O \rangle_1$ and $\langle O \rangle_2$ the averaged values in them.

2.12.1 Stability of ordered phases

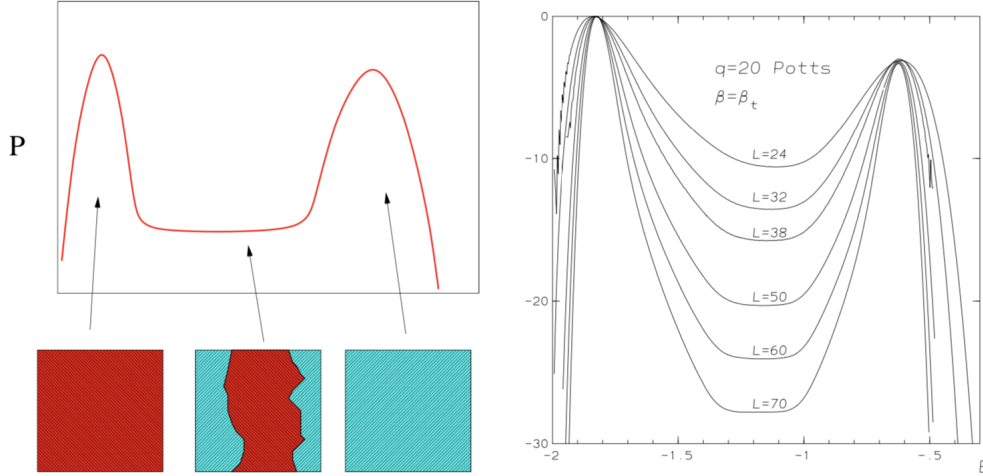


Figure 2.43: Left: Order parameter distribution and sketch of snapshots at a first order phase transition between two phases. Cases falling in the first peak are ordered in one phase, cases falling in the second peak are ordered in the other one, and cases with phase coexistence fall below the rather flat part in between the peaks. Right: Energy distribution of the Potts model with 20 states [97].

The classical nucleation theory (CNT) considers the thermally induced generation of stable phase droplets in the metastable surrounding.

A ferromagnet under a magnetic field

Let us study the stability properties of an equilibrium ferromagnetic phase under an applied external field that tends to destabilise it. If we set $T = 0$ the free-energy is just the energy. In the ferromagnetic case the free-energy cost of a spherical droplet of radius R of the equilibrium phase parallel to the applied field embedded in the dominant one (see Fig. 2.44-left) is

$$\Delta F(R) = -2\Omega_d R^d h m_{\text{eq}} + \Omega_{d-1} R^{d-1} \sigma_0 \quad (2.386)$$

where σ_0 is the interfacial free-energy density (the energy cost of the domain wall) and Ω_d is the volume of a d -dimensional unit sphere. We assume here that the droplet has a regular surface and volume such that they are proportional to R^{d-1} and R^d , respectively. The excess free-energy reaches a maximum

$$\Delta F_c = \frac{(d-1)^{d-1}}{d^d} \frac{\Omega_{d-1}^d}{\Omega_d^{d-1}} \left(\frac{\sigma_0}{2h m_{\text{eq}}} \right)^{d-1} \sigma_0 \quad (2.387)$$

at the critical radius

$$R_c = \frac{(d-1)}{d} \frac{\Omega_{d-1}}{\Omega_d} \frac{\sigma_0}{2h m_{\text{eq}}}, \quad (2.388)$$

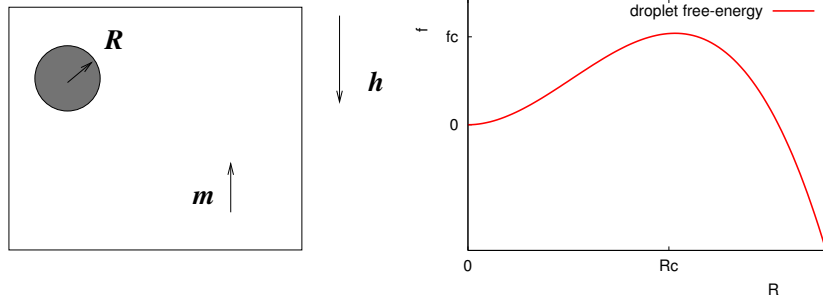


Figure 2.44: Left: the droplet. Right: the free-energy density $f(R)$ of a spherical droplet with radius R .

see Fig. 2.44-right ($h > 0$ and $m_{\text{eq}} > 0$ here, the signs have already been taken into account). The free-energy difference vanishes at

$$\Delta F(R_0) = 0 \quad \Rightarrow \quad R_0 = \frac{\Omega_{d-1}}{\Omega_d} \frac{\sigma_0}{2hm_{\text{eq}}} . \quad (2.389)$$

Several features are to be stressed:

- The barrier vanishes in $d = 1$; indeed, the free-energy is a linear function of R in this case.
- Both R_c and R_0 have the same dependence on hm_{eq}/σ_0 : they monotonically decrease with increasing hm_{eq}/σ_0 vanishing for $hm_{\text{eq}}/\sigma_0 \rightarrow \infty$ and diverging for $hm_{\text{eq}}/\sigma_0 \rightarrow 0$.
- In dynamic terms, the passage above the barrier is done *via thermal activation*; as soon as the system has reached the height of the barrier it rolls on the right side of the ‘potential’ ΔF and the favourable phase nucleates. It is then postulated that the nucleation time is inversely proportional to the probability of generation of the critical droplet, $t_{\text{nuc}}^{-1} \propto P(R_c) \simeq e^{-\beta \Delta F(R_c)}$.
- As long as the critical size R_c is not reached the droplet is not favorable and the system remains positively magnetised.
- In models defined on a lattice, or with anisotropic interactions, the droplets need not be spherical and the particular form they may take has an impact on the results derived above that have to be modified accordingly.

2.12.2 The Potts model

We have already seen the Potts model [95, 96] in the context of percolation theory.

In two dimensions, the Potts models undergo a transition at $\beta_c = \ln(1 + \sqrt{q})$. The transition is of second order if $q \leq 4$, otherwise first order. In 3d the transition is second order only if $q = 2$. The correlation length and latent heat are also known analytically.

The transition is very *weakly first order* if q is small. For example, when $q = 5$ the latent heat is $\mathcal{L} \approx 0.053$, the interface tension $\sigma \approx 0.000199$, the correlation length in the disordered phase $\xi \approx 2512$. (The “natural” magnitude for all of these quantities is 1.) Note that in this case, to see the first order character of the transition one would need to use $L \gg 2512$ which can be hard to achieve numerically. For $q = 20$, the transition is strong: $\mathcal{L} \approx 1.2$, $\sigma \approx 0.18$, $\xi \approx 2.7$.

2.12.3 Finite size effects

At finite L , the thermodynamic quantities (say, the energy) are continuous and rounded instead of discontinuous. The δ -function behaviour of their associated susceptibilities (the specific heat, $C_V = d\langle H \rangle / dT$, for the energy), has only a ‘hump’. One can argue that $C_L^{\max} \sim (E_+ - E_-)^2 L^2 / (4T_c^2)$.

2.13 Summary

This Section contains a (very) rapid summary of what we discussed

2.13.1 First order phase transitions

In a first-order phase transition a state that is stable on one side of the transition, becomes metastable on the other side of it. The order parameter jumps at the transition, for example, from zero in the disordered phase to a non-vanishing value in the ordered one. The correlation length, that is extracted from the correlations of the fluctuations of the order parameter with respect to its average, is always finite.

In common discussions of this kind of transition, the interplay between only two states is considered, each one being the preferred one on the two sides of the transition. But this is not necessarily the case and a competition between various equivalent stable states can also arise. The dynamics of first order phase transitions is driven by nucleation of the new stable phase within the metastable one in which the system is placed initially. During a long period of time the system attempts to nucleate one or more bubbles of the stable phase until some of them reach the critical size and then quickly grow. In the multi-nucleation problem, two possibilities then arise: either one of them rapidly conquers the full sample or many of them touch, get stuck, and a new coarsening process establishes. The latter case is the one that will be of interest in the hexatic-liquid transition, as we will argue below.

2.13.2 Second order phase transitions

In a second-order phase transition a state that is stable on one side of the transition, becomes unstable on the other side of it and, typically, divides continuously into an even number of different stable points, related in pairs by symmetry. The order parameter is continuous at the transition and, for example, it grows from zero in the ordered phase. The correlation length, also extracted from the correlations of the fluctuations of the order parameter with respect to its average, diverges algebraically on both sides of the transition.

When the parameters are taken across the critical value, the system needs to accommodate to the new conditions and it does progressively, by locally ordering domains of each of the possible and equivalent new equilibrium states. The latter process is called coarsening or domain growth and, although it is a very general phenomenon, its details depend on some characteristics of the problem as the conservation laws and the dimension of the order parameter. The symmetry breaking process, whereby one of the equivalent equilibrium states conquers the full sample, is achieved late after the system is taken across the phase transition. Indeed, equilibration takes a time that scales with the system size and diverges in the thermodynamic limit.

2.13.3 Infinite order phase transitions

Berezinskii-Kosterlitz-Thouless (BKT) phase transitions lack an order parameter taking a non-vanishing value on one side of the transition (in the thermodynamic limit) and are not related to spontaneous symmetry breaking. They are transitions of a different kind, driven by the unbinding of topological defects when a critical value of a control parameter (typically temperature over an energy scale) is reached. In the disordered phase the density of free topological defects is finite and the correlation function of the would-be order parameter decays exponentially, with a correlation length that is proportional to the distance between unbound defects. This length diverges exponentially at the transition and remains infinite in the full quasi-long-range ordered phase. Topological defects exist in the ordered phase but they bound in pairs and such localised in space. The divergence of the correlation length implies that the correlations of the would-be order parameter decay algebraically beyond the transition, that the system has quasi long range order and that this full phase behaves as a critical point. In terms of the associated susceptibility, it is finite in the disordered phase and it diverges in the full subcritical phase. Even more so, the transition is characterised by essential singularities in all thermodynamic functions. The reason for this behaviour are (spin or density) wave excitations with a linear dispersion relation at long wave-lengths. The dynamics of such phase transitions is characterised by the growth of the quasi-long-range order and the annihilation of topological defects.

Appendices

2.A Appendices

2.A.1 Polar coordinate system

The polar coordinate system is such that

$$\begin{aligned}\hat{e}_r &= \cos \varphi \hat{e}_x + \sin \varphi \hat{e}_y \\ \hat{e}_\varphi &= -\sin \varphi \hat{e}_x + \cos \varphi \hat{e}_y\end{aligned}\tag{2.A.1}$$

and

$$\hat{e}_\varphi = \hat{e}_z \times \hat{e}_r .\tag{2.A.2}$$

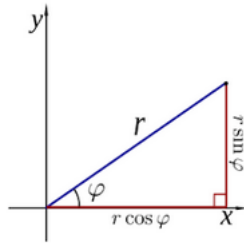


Figure 2.45: Polar coordinates notation convention.

2.A.2 Fourier transform

We define the Fourier transform (FT) of a function $f(\vec{x})$ defined in a volume V as

$$\tilde{f}_{\vec{k}} = V^{-1} \int_V d^d x f(\vec{x}) e^{i\vec{k}\vec{x}}\tag{2.A.1}$$

This implies

$$f(\vec{x}) = \sum_{\vec{k}} \tilde{f}_{\vec{k}} e^{-i\vec{k}\vec{x}}\tag{2.A.2}$$

where the sum runs over all \vec{k} with components k_i satisfying $k_i = 2\pi n_i/L$ with n_i an integer and L the linear size of the volume V .

In the large V limit these equations become

$$\tilde{f}(\vec{k}) = V^{-1} \int_V d^d x f(\vec{x}) e^{-i\vec{k}\vec{x}}\tag{2.A.3}$$

$$\tilde{f}(\vec{x}) = \int_V \frac{d^d k}{(2\pi)^d} f(\vec{k}) e^{i\vec{k}\vec{x}}\tag{2.A.4}$$

The Fourier transform of a real function $f(\vec{x})$ satisfies $\tilde{f}^*(\vec{k}) = \tilde{f}(-\vec{k})$.

2.A.3 The angle correlation

In terms of the Fourier components, the canonical measure is a Gaussian, with a weight that is just a sum over independent modes,

$$P[\{\phi_{\vec{k}}\}] \propto e^{-\frac{K}{V} \sum_{\vec{k}} k^2 |\phi_{\vec{k}}|^2} = e^{-\frac{K}{V} \sum_{\vec{k}} k^2 \phi_{\vec{k}} \phi_{-\vec{k}}} \quad (2.A.1)$$

where we collected in K all the parameters in the Hamiltonian times the inverse temperature β of the Boltzmann weight. We avoid using tilde to distinguish the Fourier transformed from the original fields as the interpretation should be obvious. Each mode is an independent random variable with a Gaussian distribution of zero mean and correlations

$$\langle \phi_{\vec{k}} \phi_{\vec{k}'} \rangle = \frac{V}{K k^2} \delta_{\vec{k}, -\vec{k}'} . \quad (2.A.2)$$

From this expression one can easily compute the averages and correlations in real space. First, $\langle \phi(\vec{r}) \rangle = 0$. Next,

$$\langle \phi(\vec{r}) \phi(\vec{r}') \rangle = \frac{1}{V^2} \sum_{\vec{k}} \sum_{\vec{k}'} e^{i\vec{k} \cdot \vec{r}} e^{i\vec{k}' \cdot \vec{r}'} \langle \phi_{\vec{k}} \phi_{\vec{k}'} \rangle = \frac{1}{VK} \sum_{\vec{k}} \frac{e^{i\vec{k} \cdot (\vec{r} - \vec{r}')}}{k^2} . \quad (2.A.3)$$

In the continuum limit the sum over modes can be replaced by an integral, $\frac{1}{V} \sum_{\vec{k}} \cdots \mapsto \int \frac{d^d k}{(2\pi)^d} \cdots$ and

$$\langle \phi(\vec{r}) \phi(\vec{r}') \rangle = \frac{1}{K} \int \frac{d^d k}{(2\pi)^d} \frac{e^{i\vec{k} \cdot (\vec{r} - \vec{r}')}}{k^2} = -\frac{1}{K} C_d(\vec{r} - \vec{r}') . \quad (2.A.4)$$

We should remember, though, that there is a lower cut-off of the possible wave-vector values (an *infrared* long-distance cutoff) determined by the system size, which is proportional to L^{-1} . There is also a higher (an *ultraviolet* short-distance) cut-off given by the lattice spacing and proportional to a^{-1} . The right-hand-side is the Coulomb potential due to a unit charge at the origin in a d -dimensional space, since it is the solution to

$$\nabla^2 C_d(\vec{r}) = \delta^d(\vec{r}) . \quad (2.A.5)$$

This equation is solved using Gauss' theorem

$$\int_V d^d r \nabla^2 C_d(\vec{r}) = \int_S d\vec{S} \cdot \vec{\nabla} C_d(\vec{r}) = \int_S dS \hat{e}_r \cdot \vec{\nabla} C_d(\vec{r}) = 1 \quad (2.A.6)$$

For a spherically symmetric solution $C_d(\vec{r}) = C_d(r)$ and $\vec{\nabla} C_d(\vec{r}) = dC_d(r)/dr \hat{e}_r$, and a spherical volume V in d dimensions with radius r , the equation becomes

$$1 \propto r^{d-1} \frac{dC_d(r)}{dr} . \quad (2.A.7)$$

From this equation, taking r to be a variable and integrating from a to r , one deduces the long distance behaviour

$$\lim_{r \gg a} C_d(r) \propto \begin{cases} \text{const} & d > 2 \\ \ln(r/a) & d = 2 \\ \frac{r^{2-d} - a^{2-d}}{2-d} & d < 2 \end{cases} \quad (2.A.8)$$

and, therefore, the phase fluctuations

$$\langle [\phi(\vec{r}) - \phi(\vec{0})]^2 \rangle = -\frac{1}{K} [2C_d(0) - 2C_d(r)] \mapsto \frac{2[r^{2-d} - a^{2-d}]}{K(2-d)\Omega_d} \quad (2.A.9)$$

(the subtracted constant has been fixed so that this quantity vanishes at zero distance) one finds that while they are finite for $d > 2$, they diverge for $d \leq 2$, and order is thus destroyed by the spin-waves at sufficiently low dimensions. One can also rewrite the expressions using L as the unit of distance.

2.B Problems

2.B.1 The classical Potts model

The Hamiltonian of the Potts model is

$$H = -J \sum_{\langle ij \rangle} \delta_{s_i s_j} \quad (2.B.10)$$

The spin variables s_i can take q natural values, $s_i = 1, \dots, q$. These are also called colours in the literature and we will call them this way henceforth. The case $q = 2$ is the Ising model. The sum runs over nearest neighbours on a cubic lattice in d dimensions and each pair is counted only once. The coupling is ferromagnetic $J > 0$ and δ_{ab} is the Kronecker delta. We couple the model to a heat bath at temperature T .

1. Generic.

- (a) Describe the ground states.
- (b) Which phases do you expect? Characterise them in terms of typical spin configurations.

2. Mean-field treatment.

- (a) Consider the fully-connected case in which each spin interacts with all the other ones in the sample and each pair is counted once in the sum. Write the Hamiltonian. How should you modify the model to let it have an interesting thermodynamic limit?
- (b) You are going to characterise order in this problem using q order parameters, which you will call x_a with $a = 1, \dots, q$, and take them to be the proportion of sites taking each colour. Which condition do they satisfy?
- (c) Set up the mean-field analysis of this problem writing the free-energy density as a function of the x_a in the $N \gg 1$ limit. You can argue which should be the form of each contribution in the large N limit without making the explicit derivation.
- (d) Supposing that in the low temperature phase the symmetry is broken in favour of the first color, rewrite this free-energy density distinguishing the corresponding order parameter, say x_1 , with respect to the other $q - 1$ ones which you will take to be identical $x_2 = \dots = x_q$.
- (e) Express x_1 as $x_1 = (1/q)[1 + (q - 1)s]$, with s a new parameter and rewrite the free-energy as a function of s .

- (f) If one Taylor expands the free-energy density around $s \sim 0$ keeping up to cubic contributions in powers of s , using $\ln(1+x) = x - \frac{x^2}{2} + \frac{x^3}{3} - \frac{x^4}{4} + \mathcal{O}(x^5)$, one finds

$$\beta[f(s) - f(0)] = \frac{(q-1)}{2q} (q - \beta J) s^2 - \frac{(q-1)(q-2)}{6} s^3 + \mathcal{O}(s^4)$$

What do you conclude about the phase transition in the mean-field Potts model for generic q ?

- (g) Do you expect to find the same behaviour working in the micro-canonical ensemble? Explain.

3. Decimation of the unidimensional Potts model

Consider the Potts model on a $d = 1$ space with periodic boundary conditions.

- Take three nearby sites on the line, labelled $k-1$, k and $k+1$. Perform the partition sum over the central spin s_k (decimation). Establish the recurrence relations for the parameter e^K with $K = \beta J$.
- Which are the fixed points? Determine whether they are stable or unstable.
- Is there a finite temperature phase transition?
- Do you know an argument to show that there is no finite temperature phase transition in this problem without going through this kind of calculation?
- Do you expect a finite temperature phase transition in $d = 2$?

2.B.2 A classical Ising chain with alternating couplings

Take an Ising chain with alternating coupling constants

$$H = -J_1 \sum_{\substack{i \text{ odd} \\ i=1}}^L s_i s_{i+1} - J_2 \sum_{\substack{i \text{ even} \\ i=2}}^L s_i s_{i+1}, \quad (2.B.11)$$

with $J_1 > 0$, $J_2 > 0$, $s_i = \pm 1, 0$, and periodic boundary conditions $s_{L+1} = s_1$. The system is in equilibrium with a bath at inverse temperature β and one defines $K_1 = \beta J_1$ and $K_2 = \beta J_2$. See Fig. 2.46 for a sketch.

- Write the Boltzmann weights of the group of four neighbouring spins, s_1, s_2, s_3, s_4 , with s_1 and s_4 at the borders of this segment of the chain on the one hand, and s_4, s_5, s_6, s_7 , with s_4 and s_7 at the borders of this other segment of the chain on the other hand. (See Fig. 2.46.)

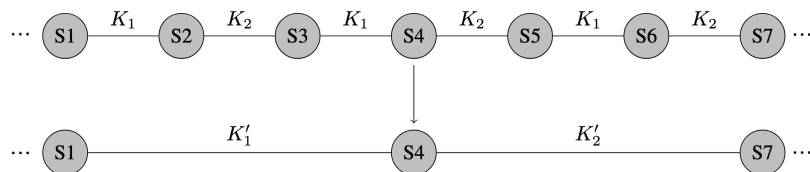


Figure 2.46: The Ising chain with alternating coupling constants, J_1 and J_2 .

2. Write the result of the decimation of the two central spins (s_2 and s_3 on the one hand, and s_5 and s_6 on the other) in the two cases, separately.

You have the choice of working with the exponential representation of the Boltzmann factors (which will lead to relatively ugly expressions and we do not recommend it) or to proceed as in a TD (which will lead to more compact expressions that we will use below) following the steps:

- (a) Represent the exponentials as $e^{K s_i s_j} = A(K)[1 + s_i s_j B(K)]$ with parameters $A(K)$ and $B(K)$ that you have to fix.
 - (b) Rewrite the Boltzmann factors $e^{-\beta H_l}$ and $e^{-\beta H_r}$ in this representation.
 - (c) Sum over the internal spin configurations.
 - (d) Identify the spin-dependent terms and read from them the relation between new and old parameters.
3. You must have derived

$$\begin{aligned}\tanh K'_1 &= (\tanh K_1)^2 \tanh K_2 \\ \tanh K'_2 &= (\tanh K_2)^2 \tanh K_1\end{aligned}$$

in question 2. Which are the fixed points of the recurrence?

4. Which one(s) is(are) stable/attractive and instable/repulsive? Give first an intuitive argument to guess the answer and then prove it (at least sketch the calculation to be done, if you do not have time to do all the calculations).

References

- [1] H. E. Stanley, *Introduction to phase transitions and critical phenomena* (Oxford University Press, New York, 1971).
- [2] R. J. Baxter, *Exactly Solved Models in Statistical Mechanics*, (London: Academic, 1982).
- [3] N. Goldenfeld, *Lectures on phase transitions and the renormalization group* (Addison-Wesley, 1992).
- [4] J. Cardy, *Scaling and renormalization in Statistical Physics*, Cambridge Lecture notes in physics (Cambridge University Press, 1996).
- [5] D. J. Amit, *Field theory, the renormalization group and critical phenomena* (World Scientific, Singapore, 1984).
- [6] G. Parisi, *Statistical field theory* (Addison-Wesley, 1988).
- [7] B. Simon, *Phase Transitions and Collective Phenomena* (Cambridge University Press, 1997).
- [8] I. Herbut, *A modern approach to critical phenomena* (Cambridge University Press, 2006).
- [9] A. M. Tsvelik, *Quantum field theory in condensed matter*, 2nd ed. (Cambridge University Press, 2007).
- [10] M. Kardar, *Statistical Physics of Fields*, (Cambridge University Press, 2007).
- [11] A. J. Berlinsky and A. B. Harris, *Statistical Mechanics: An Introductory Graduate Course*, (Springer, Switzerland, 2019).
- [12] For a historical introduction see G. Jaeger, *The Ehrenfest Classification of Phase Transitions: Introduction and Evolution*, Arch. Hist. Exact Sci. **53**, 51 (1998).
- [13] F. Romá, L. F. Cugliandolo, and G. S. Lozano, *Numerical integration of the stochastic Landau-Lifshitz-Gilbert equation in generic time-discretization schemes*, Phys. Rev. E **90**, 023203 (2014).
- [14] J. E. Mayer and E. Montroll, *Molecular distributions*, J. Chem. Phys. **9**, 2 (1941).
- [15] D. C. Brydges, *A short course on cluster expansions*, in *Critical Phenomena, Random Systems, Gauge Theories*, K. Osterwalder and R. Stora, eds., Les Houches 1984 pp. 129-183 (Elsevier/North Holland, Amsterdam, 1986).

-
- [16] H. A. Kramers and G. H. Wannier, *Statistics of the two-dimensional ferromagnet*, Phys. Rev. **60**, 252 (1941).
 - [17] H. A. Kramers and G. H. Wannier, *Statistics of the two-dimensional ferromagnet Part I*, Phys. Rev. **60**, 252 (1941). *Statistics of the two-dimensional ferromagnet Part II*, Phys. Rev. **60**, 263 (1941).
 - [18] L. Onsager, *Crystal statistics I A two-dimensional model with an order-disorder transition*, Phys. Rev. **65**, 117 (1944).
 - [19] J-M Luck, *Systèmes désordonnés unidimensionnels*, ALEA-Saclay (1992).
 - [20] V. L. Ginzburg, *Some remarks on phase transitions of the 2nd kind and the microscopic theory of ferroelectric materials*, Soviet Physics - Solid State **2**, 1824 (1961).
 - [21] M. Vopsaroiu, K. O'Grady, M. T. Georgieva, P. J. Grundy, and M. J. Thwaites, *Growth Rate Effects in Soft CoFe Films*, IEEE Transactions on magnetics **41**, 3253 (2005).
 - [22] P. Heller and G. B. Benedek, *nuclear magnetic resonance in MnF_4 near a critical point*, Phys. Rev. Lett. **8**, 428 (1962).
 - [23] J. Lipa, C. Edwards, and M. Buckingham, *Precision Measurement of the Specific Heat of CO_2 Near the Critical Point*, Phys. Rev. Lett. **25**, 1086 (1970).
 - [24] A. Jesche, N. Caroca-Canales, H. Rosner, H. Borrmann, A. Ormeci, D. Kasinathan, H. H. Klauss, H. Luetkens, R. Khasanov, A. Amato, A. Hoser, K. Kaneko, C. Krellner, and C. Geibel, *Strong coupling between magnetic and structural order parameters in $SrFe_2As_2$* , Phys. Rev. B **78**, 180504R (2008).
 - [25] C. Domb, *On the theory of cooperative phenomena in crystals*, Adv. Phys. **9**, 145 (1960).
 - [26] R. Mélin, J. C. Anglès d'Auriac, P. Chandra and B. Douçot, *Glassy behaviour in the ferromagnetic Ising model on a Cayley tree*, J. Phys. A: Math. Gen. **29**, 5773 (1996).
 - [27] G. Semerjian, M. Tarzia, and F. Zamponi, *Exact solution of the Bose-Hubbard model on the Bethe lattice*, Phys. Rev. B **80**, 014524 (2009).
 - [28] Y. Khaluf, E. Ferrante, P. Simoens, and C. Huepe, *Scale invariance in natural and artificial collective systems: a review*, J. R. Soc. Interface **14**, 20170662 (2017).
 - [29] F. Portelli, *Fluctuations des grandeurs globales dans les systèmes corrélés*, ENS-Lyon thesis under the advise of P. W. Holdsworth.
 - [30] B. Mandelbrot, *The Fractal Geometry of Nature* (W. H. Freeman, 1982).

-
- [31] A-L Barabasi, H. E. Stanley, *Fractal concepts in surface growth*, (Cambridge University Press, 1995).
- [32] B. Hu, *Introduction to real-space renormalization group methods in critical and chaotic phenomena*, Phys. Rep. **91**, 233 (1982).
- [33] H. J. Maris and L. P. Kadanoff, *Teaching the renormalization group*, Am. J. Phys. **46**, 652 (1977).
- [34] M. E. Fisher, in *Critical Phenomena*, Proc. 51st Enrico Fermi Summer School, Varena, edited by M. S. Green (Academic Press, N.Y., 1972).
- [35] E. Brézin, *An investigation of finite size scaling*, Journal de Physique **43**, 15 (1982).
- [36] A. Corral, R. Garcia-Millan, and F. Font-Clos, *Exact Derivation of a Finite-Size Scaling Law and Corrections to Scaling in the Geometric Galton-Watson Process*, PlosOne **11**, e0161586 (2016).
- [37] E. Ibarra-García-Padilla, F. J. Poveda-Cuevas, and C. G. Malanche-Flores, *The Hobbyhorse of Magnetic Systems: The Ising Model*, arXiv:1606.05800
- [38] A. Sandvik, in *ICTP School in Computational Condensed Matter Physics: From Atomistic Simulations to Universal Model Hamiltonians*, Trieste, Italia, 2015.
- [39] D. P. Landau, *Finite-size behavior of the Ising square lattice*, Phys. Rev. B **13**, 2997 (1976).
- [40] K. Binder, *Finite size scaling analysis of ising model block distribution functions*, Zeitschrift für Physik B: Cond. Matter **43** 119-140 (1981).
- [41] K. Binder, *Critical Properties from Monte Carlo Coarse Graining and Renormalization*, Phys. Rev. Lett. **47**, 693-696 (1981).
- [42] K. Binder and D. P. Landau, *Finite-size scaling at first- order phase transitions*, Phys. Rev. B **30**, 1477 (1984).
- [43] G. Palma and D. Zambrano, *Cluster Algorithm Renormalization Group Study of Universal Fluctuations in the 2D Ising Model*,
- [44] A. Wipf, *Statistical Approach to Quantum Field Theory An Introduction*, Lecture Notes in Physics **864** (Springer Verlag, 2013).
- [45] P. W. Kasteleyn and C. M. Fortuin, J. Phys. Soc. Jpn. (Suppl.) **26** , 11 (1969). C. M. Fortuin and P. W. Kasteleyn, Physica (Amsterdam) **57**, 536 (1972).
- [46] T. Blanchard, L. F. Cugliandolo, and M. Picco, *A morphological study of cluster dynamics between critical points*, J. Stat. Mech. **2012** P05026 (2012).

-
- [47] R. H. Swendsen and J. S. Wang, Phys. Rev. Lett. **58**, 86 (1987).
- [48] T. Blanchard, L. F. Cugliandolo, M. Picco, and A. Tartaglia, *Critical percolation in the dynamics of the 2d ferromagnetic Ising model*, J. Stat. Mech. 113201 (2017).
- [49] A. L. Efros, *Physics and geometry of disorder: percolation theory*, (Mir Publishers, Mockba, 1986)
- [50] D. Stauffer and A. Aharony, *Introduction To Percolation Theory*, (Taylor and Francis, London, 1994)
- [51] *Percolation theory*, unpublished (2002).
- [52] A. A. Saberi, Phys. Rep. **578**, 1 (2015).
- [53] T. T. Kantzas, K. D. O’Neil and O. A. Semenikhin, Electrochim. Acta **53**, 1225 (2007).
- [54] M. E. J. Newman, R. M. Ziff, *A fast Monte Carlo algorithm for site or bond percolation*, Phys. Rev. E **64**, 016706 (2001).
- [55] P. W. Kasteleyn and C. M. Fortuin, J. Phys. Soc. Japan **26** (Suppl.), 11 (1969).
- [56] C. M. Fortuin and P. W. Kasteleyn, Physica **57** 536 (1972).
- [57] N. D. Mermin, *Absence of Ordering in Certain Classical Systems*, J. Math. Phys. **8**, 1061 (1967).
- [58] N. D. Mermin and H. Wagner, *Absence of ferromagnetism or antiferromagnetism in one- or two-dimensional isotropic Heisenberg models*, Phys. Rev. Lett. **17**, 1133 (1966).
- [59] O. Mc Bryan and T. Spencer, *On the decay of correlation functions in $SO(n)$ -symmetric ferromagnets*, Comm. Math. Phys. **53**, 299 (1977).
- [60] S. Friedli and Y. Velenik, *Statistical Mechanics of Lattice Systems: A Concrete Mathematical Introduction*, (Cambridge University Press, 2017).
- [61] S. Coleman and E. J. Weinberg, *Radiative corrections as the origin of spontaneous symmetry breaking*, Phys. Rev. D **8**, 1888 (1973).
- [62] P. C. Hohenberg, *Existence of long-range order in one and two dimensions*, Phys. Rev. **158**, 383 (1967).

- [63] P. Archambault, S. T. Bramwell, J.-Y. Fortin, P. W. C. Holdsworth, S. Peysson, J.-F. Pinton, *Universal magnetic fluctuations in the two-dimensional XY model*, J. App. Phys. **83**, 7234 (1998)
S. T. Bramwell, P. W. C. Holdsworth, and J.-F. Pinton, *Universality of rare fluctuations in turbulence and critical phenomena*, Nature **396**, 552 (1998).
S. T. Bramwell, K. Christensen, J.-Y. Fortin, P. C. W. Holdsworth, H. J. Jensen, S. Lise, J. López, M. Nicodemi, J.-F. Pinton, and M. Sellitto, *Universal Fluctuations in Correlated Systems*, Phys. Rev. Lett. **84**, 3744 (2000).
- [64] H. E. Stanley and T. A. Kaplan, *Possibility of a Phase Transition for the Two-Dimensional Heisenberg Model*, Phys. Rev. Lett. **17**, 913 (1966).
- [65] M. A. Moore, *Additional Evidence for a Phase Transition in the Plane-Rotator and Classical Heisenberg Models for Two-Dimensional Lattices*, Phys. Rev. Lett. **23**, 861 (1969).
- [66] D. Mukamel, *Statistical mechanics of systems with long range interactions*, in *Long range interacting systems* Les Houches IX, T. Dauxois, S. Ruffo and L. F. Cugliandolo eds., (Oxford University Press, 2010).
- [67] J. M. Kosterlitz and D. J. Thouless, *Long range order and metastability in two dimensional solids and superfluids*, J. Phys. C: Solid State Phys. **5**, L124 (1972).
- [68] J. M. Kosterlitz and D. J. Thouless, *Ordering, metastability and phase transitions in two-dimensional systems*, J. Phys. C: Solid State Phys. **6**, 1181 (1973).
- [69] J. M. Kosterlitz, *The critical properties of the two-dimensional XY model*, J. Phys. C: Solid State Phys. **7**, 1046 (1974).
- [70] Very nice computer program demonstrations can be found here: <https://quantumtheory.physik.unibas.ch/people/bruder/Semesterprojekte2007/p6/index.html#x1-30002>, A. Käser, T. Maier, and T. Rautenkranz (2007).
- [71] Several animation in YouTube show the dynamics of the 2d XY model; see *e.g.* <https://www.youtube.com/watch?v=VpRBf0nc-pg> by S. Burton.
- [72] R. E. Peierls, *Über die statistischen Grundlagen der Elektronentheorie der Metalle*, Helv. Phys. Acta **7**, 24 (1934).
- [73] R. E. Peierls, *Surprises in Theoretical Physics* (Princeton University Press, 1979) and refs. therein.
- [74] P. Chaikin and T. Lubensky, *Principles of Condensed Matter Physics*, (Cambridge University Press, 1995).

-
- [75] Y. Komura and Y. Okabe, *Large-Scale Monte Carlo Simulation of Two-Dimensional Classical XY Model Using Multiple GPUs*, J. Phys. Soc. Japan **81**, 113001 (2012).
- [76] M. Hasenbusch, *The Binder Cumulant at the Kosterlitz-Thouless Transition*, J. Stat. Mech P08003 (2008)
- [77] G. M. Wysin, A. R. Pereira, I. A. Marques, S. A. Leonel and P. Z. Coura, *Extinction of BKT transition by nonmagnetic disorder in planar-symmetry spin models*, Phys. Rev. B **72**, 094418 (2005).
- [78] E. Domany, M. Schick and Swendsen, *First-order transition in an XY model with nearest-neighbor interactions*, Phys. Rev. Lett. **52**, 1535 (1984).
- [79] A. C. D. Van Enter and S. B. Shlosman, *First-order transitions for n -vector models in two and more dimensions: Rigorous proof*, Phys. Rev. Lett. **89**, 285702 (2002).
- [80] L. D. Landau, *On the theory of phase transitions i.*, Phys. Z. Sowjet **11**, 26 (1937).
- [81] L. D. Landau, *On the theory of phase transitions ii.*, Phys. Z. Sowjet **11**, 545 (1937).
- [82] R. E. Peierls, *Bemerkungen über umwandlungstemperaturen*, Helv. Phys. Acta Supp. II, **7**, 91 (1934).
- [83] N. W. Ashcroft and N. D. Mermin *Solid State Physics*, Ch. 22, Classical Theory of the Harmonic Crystal (Harcourt College Publisher, Forth Worth., 1976).
- [84] B. J. Alder and T. E. Wainwright, *Phase Transition in Elastic Disks*, Phys. Rev. **127**, 359 (1962).
- [85] N. N. Bogoliubov, Phys. Abhandl. S. U **6**, 113 (1962).
- [86] N. D. Mermin, *Crystalline order in two dimensions*, Phys. Rev. **176**, 250 (1968).
- [87] *Bond-Orientational Order in Condensed Matter Systems*, K. J. Strandburg ed. (Springer-Verlag, Heidelberg, 1992).
- [88] D. R. Nelson and B. I. Halperin, *Dislocation-mediated melting in two dimensions*, Phys. Rev. B **19**, 2457 (1979).
- [89] A. P. Young, *Melting and the vector Coulomb gas in two dimensions*, Phys. Rev. B **19**, 1855 (1979).
- [90] U. Gasser, *Crystallization in three- and two-dimensional colloidal suspensions*, J. Phys.: Cond. Matt. **21**, 203101 (2009).
- [91] E. Bernard and W. Krauth and D. B. Wilson, *Event-chain Monte Carlo algorithms for hard-sphere systems*, Phys. Rev. E **80**, 056704, (2009).

-
- [92] E. Bernard and W. Krauth, *Two-Step Melting in Two Dimensions: First-Order Liquid-Hexatic Transition*, Phys. Rev. Lett. **107**, 155704, (2011).
- [93] M. Engel, J. A. Anderson, S. C. Glotzer, M. Isobe, E. P. Bernard and W. Krauth, *Hard-disk equation of state: First-order liquid-hexatic transition in two dimensions with three simulation methods*, Phys. Rev. E **87**, 042134 (2013).
- [94] S. Kapfer and W. Krauth, *Two-Dimensional Melting: From Liquid-Hexatic Coexistence to Continuous Transitions*, Phys. Rev. Lett. **114**, 035702 (2015).
- [95] R. B. Potts, *Some generalized order-disorder transformations*, Proc. Cambridge Philos. Soc. **48**, 106 (1952).
- [96] F. Y. Wu, *The Potts model*, Rev. Mod. Phys. **54**, 235 (1982).
- [97] A. Billoire, T. Neuhaus and B. Berg, *A Determination of Interface Free Energies*, Nucl. Phys. B **413**, 795 (1994).
- [98] K. Vollmayr, J. D. Reger, M. Schencher, and K. Binder, *Finite size effects at thermally-driven first order phase transitions: a phenomenological theory of the order parameter distribution*, Z. Phys. B **91**, 113 (1993).